# Phanerozoic paleoenvironmental and paleoclimatic evolution in Svalbard

Aleksandra Smyrak-Sikora<sup>1,2</sup>, Peter Betlem<sup>3</sup>, Victoria S. Engelschiøn<sup>4</sup>, William J. Foster<sup>5</sup>, Sten-Andreas Grundvåg<sup>6</sup>, Mads E. Jelby<sup>7</sup>, Morgan T. Jones<sup>8,9</sup>, Grace E. Shephard<sup>10,11</sup>, Kasia K. Śliwińska<sup>12</sup>, Madeleine L. Vickers<sup>8</sup>, Valentin Zuchuat<sup>13,14</sup>, Lars Eivind Augland<sup>9</sup>, Jan Inge Faleide<sup>9</sup>, Jennifer M. Galloway<sup>15</sup>, William Helland-Hansen<sup>7</sup>, Maria A. Jensen<sup>2</sup>, Erik P. Johannessen<sup>16</sup>, Maayke Koevoets<sup>17</sup>, Denise Kulhanek<sup>18</sup>, Gareth S. Lord<sup>19</sup>, Tereza Mosociova<sup>2,9</sup>, Snorre Olaussen<sup>2</sup>, Sverre Planke<sup>9,20</sup>, Gregory D. Price<sup>21</sup>, Lars Stemmerik<sup>12</sup>, and Kim Senger<sup>2</sup>

**Correspondence:** Aleksandra Smyrak-Sikora (aleksandra.a.smyrak-sikora@ntnu.no)

Received: 11 December 2024 – Discussion started: 14 January 2025 Revised: 14 May 2025 – Accepted: 27 May 2025 – Published:

Abstract. Sedimentary rocks can provide information about the Earth paleoenvironment and are studied extensively to understand the causes and consequences of global climate changes in deep time. They facilitate long-time perspectives that constrain climate models and provide analogues for how Earth systems may respond to, and recover from, intervals of profound environmental change, including projected anthro-

pogenic change. The Norwegian Svalbard archipelago offers an extensive Phanerozoic stratigraphic record that reflects the geological evolution of the northern flanks of continental assemblages that include Laurentia, Eurasia, and Pangea. Svalbard's Phanerozoic sedimentary and paleoclimatic archive is controlled largely by Svalbard's overall northward platetectonic motion from equatorial to high latitudes but also

<sup>&</sup>lt;sup>1</sup>Department of Geosciences, Norwegian University of Science and Technology (NTNU), Trondheim 7031, Norway

<sup>&</sup>lt;sup>2</sup>Department of Arctic Geology, The University Centre in Svalbard (UNIS), Longyearbyen 9171, Norway

<sup>&</sup>lt;sup>3</sup>Norwegian Geotechnical Institute (NGI), Oslo 0806, Norway

<sup>&</sup>lt;sup>4</sup>Natural History Museum, University of Oslo, Oslo 0562, Norway

<sup>&</sup>lt;sup>5</sup>Department of Earth System Science, University of Hamburg, 20146 Hamburg, Germany

<sup>&</sup>lt;sup>6</sup>Department of Geosciences, The Arctic University of Norway, Tromsø 9019, Norway

<sup>&</sup>lt;sup>7</sup>Department of Geoscience, Aarhus University, 8000 Aarhus C, Denmark

<sup>&</sup>lt;sup>8</sup>Department of Ecology, Environment and Geoscience (EMG), Umeå University, Umeå, Sweden EDI

<sup>&</sup>lt;sup>9</sup>Department of Geosciences, University of Oslo, Oslo 0315, Norway

<sup>&</sup>lt;sup>10</sup>Centre for Planetary Habitability (PHAB), University of Oslo, Oslo 0315, Norway

<sup>&</sup>lt;sup>11</sup>Research School of Earth Sciences, Australian National University, Acton, Canberra, Australia

<sup>&</sup>lt;sup>12</sup>Department of Geo-energy and Storage, The Geological Survey of Denmark and Greenland (GEUS), Copenhagen 1350, Denmark

<sup>&</sup>lt;sup>13</sup>Mineral Resources, CSIRO, Australia

<sup>&</sup>lt;sup>14</sup>Geological Institute, RWTH-Aachen University, 52062 Aachen, Germany

<sup>&</sup>lt;sup>15</sup>Geological Survey of Canada (GSC)/Commission géologique du Canada, Calgary, AB, Canada

<sup>&</sup>lt;sup>16</sup>EP Skolithos, Sisikveien 36, 4022 Stavanger, Norway

<sup>&</sup>lt;sup>17</sup>Geological Survey of the Netherlands (TNO), Utrecht 3584 CB, the Netherlands

<sup>&</sup>lt;sup>18</sup>Institute of Geosciences, Kiel University, 24118 Kiel, Germany

<sup>&</sup>lt;sup>19</sup>Equinor, Bergen, Norway

<sup>&</sup>lt;sup>20</sup>Volcanic Basin Energy Petroleum Research AS (VBER), Oslo

<sup>&</sup>lt;sup>21</sup>School of Geography, Earth and Environmental Sciences, University of Plymouth, Plymouth, Devon, PL4 8AA, United Kingdom

by regional to local formation of topography and basins in response to long-term plate reorganization, as well as the near- and far-field influence of large igneous province activity on the tectono-stratigraphic and paleoclimatic develop-5 ment. Various sedimentary and geochemical proxies, such as bentonite beds and carbon isotope excursions associated with the far-reaching environmental effects of the Siberian Traps, the High Arctic Large Igneous Province, and the North Atlantic Igneous Province, are present in Svalbard's near com-10 plete geological record. As such, Svalbard is unique in that these and numerous other global environmental perturbations are recorded within a relatively restricted study area, with most of the key events preserved and recorded in easily accessible drill cores and well-exposed outcrop sections. Here 15 we review deep-time paleoenvironmental and paleoclimate research in Svalbard by summarizing 148 peer-reviewed scientific articles. The review builds on the well-established tectono-stratigraphic and lithostratigraphic framework, as well as state-of-the art environmental reconstructions, to pro-20 vide insights into the Earth system during the Phanerozoic northward drift of Svalbard and the many major biotic crises in the geological past. We focus on globally significant events including (i) the expansion of Devonian vegetation, (ii) the Carboniferous-Permian response to icehouse conditions dur-25 ing the Late Paleozoic Ice Age (LPIA), (iii) the End-Permian Mass Extinction (EPME) and the subsequent Triassic recovery, the (iv) Carnian Pluvial Episode, (v) Jurassic-Early Cretaceous climate perturbations including the Volgian Isotopic Carbon Excursion (VOICE) and the Aptian Ocean Anoxic 30 Event 1a (OAE1a), and (vi) the Paleocene-Eocene Thermal Maximum (PETM). We present and synthesize existing core and outcrop data that preserve biological and geochemical proxies and climate-sensitive sedimentary facies that reflect environmental change in terrestrial and marine settings. Fi-35 nally, we discuss the Phanerozoic climate recorded in Svalbard and its role in providing high-latitude calibration points for several global paleoclimate events to provide a higherlatitude perspective to complement the dominance of midand low-latitude locations and datasets in the literature.

#### 40 1 Introduction

The recent Intergovernmental Panel on Climate Change report (IPCC; Pörtner et al., 2022) and the Intergovernmental Science-Policy Platform on Biodiversity and Ecosystem Services (Watson et al., 2019) highlight the challenges humanity is facing due to ongoing and projected climate change. Human–environment interactions have accelerated dramatically through the industrial revolution, and the human species is now considered to be a dominant geological force on the planet (Seibold, 1990; Stewart, 2016). The rate of change the planet is experiencing is unprecedented for at least the last 66 Myr (Zeebe et al., 2016), which could lead to a biodi-

versity crisis of similar amplitude to the crises experienced during previous hyperthermals throughout the Phanerozoic. However, it is still uncertain when ecological tipping points, at which an ecosystem can no longer cope with environmental change, will be reached. It is thus critical to understand and define the trajectories and pace of ecological change that is the result of a major climate perturbation.

Studying episodes of past climate change, as recorded in the geological record, can provide insights into the response of Earth system processes to climate perturbations. Deeptime paleoclimatology, here considered to be pre-Quaternary (i.e., older than 2.58 Ma; all absolute ages refer to the International Stratigraphic Chart 2023/09), in its broadest sense refers to deciphering how and why the climate changed in 65 the past and the consequences of those changes for life on Earth. Throughout the pre-Quaternary Phanerozoic (ca. 538.8 to 2.58 Ma), mass extinctions or smaller-scale biodiversity crises occurred repeatedly, often in response to rapid climate change (Fig. 1.; e.g., Bond and Grasby, 2017; Kemp 70 et al., 2015). Understanding past climate trends and episodes of major environmental perturbations will better constrain our understanding of the causes and consequences of future change (e.g., Soreghan, 2004; Jansen et al., 2007). Many proxies exist to constrain past paleoenvironmental and climatic settings, grouped into biological, chemical, and geophysical, including climate-sensitive sedimentary facies. Different proxies are suitable for quantifying various paleoclimatic signals, including volcanic activity, atmospheric gas concentration, land/sea temperature, seasonality, precipita- 80 tion, and ocean oxygenation.

Significant perturbations to global climate are often related to relatively short-lived catastrophic events (from minutes to 1-2 Myr), including meteorite impacts, volcanic and kimberlite eruptions, the emplacement of large igneous provinces 85 (LIPs; Wignall, 2001; Bryan and Ernst, 2008; Green et al., 2022), and the biogeochemical cascades that these events cause. For example, these events disturb Earth's biosphere by causing extreme changes in temperature, precipitation, wildfire frequency, sea level, oxygen level, and saturation states of biologically important elements in the ocean (e.g., Larson and Erba, 1999; Weissert and Erba, 2004; Hönisch et al., 2012); release of deleterious substances such as mercury (e.g., Grasby et al., 2011; Sanei et al., 2012; Galloway and Lindström, 2023); and trophic knock-on effects, affecting both the atmosphere and marine realms (Jenkyns, 2010). LIP volcanism in particular directly perturbs the climate system via release of gasses directly to the atmosphere, including SO<sub>2</sub>, CH<sub>4</sub>, and CO<sub>2</sub>, as well as HCl, halocarbons, and Hg. LIP emplacements are in turn often associated with 100 global environmental changes, including mass extinctions and smaller-scale biotic crises such as oceanic anoxic events (OAEs; Schlanger and Jenkyns, 1976; Grasby et al., 2011; Bond et al., 2014; Ernst and Youbi, 2017; Jones et al., 2016; Svensen et al., 2019; Grasby and Bond, 2023). LIPs, by def- 105 inition (Bryan and Ernst, 2008), involve significant igneous

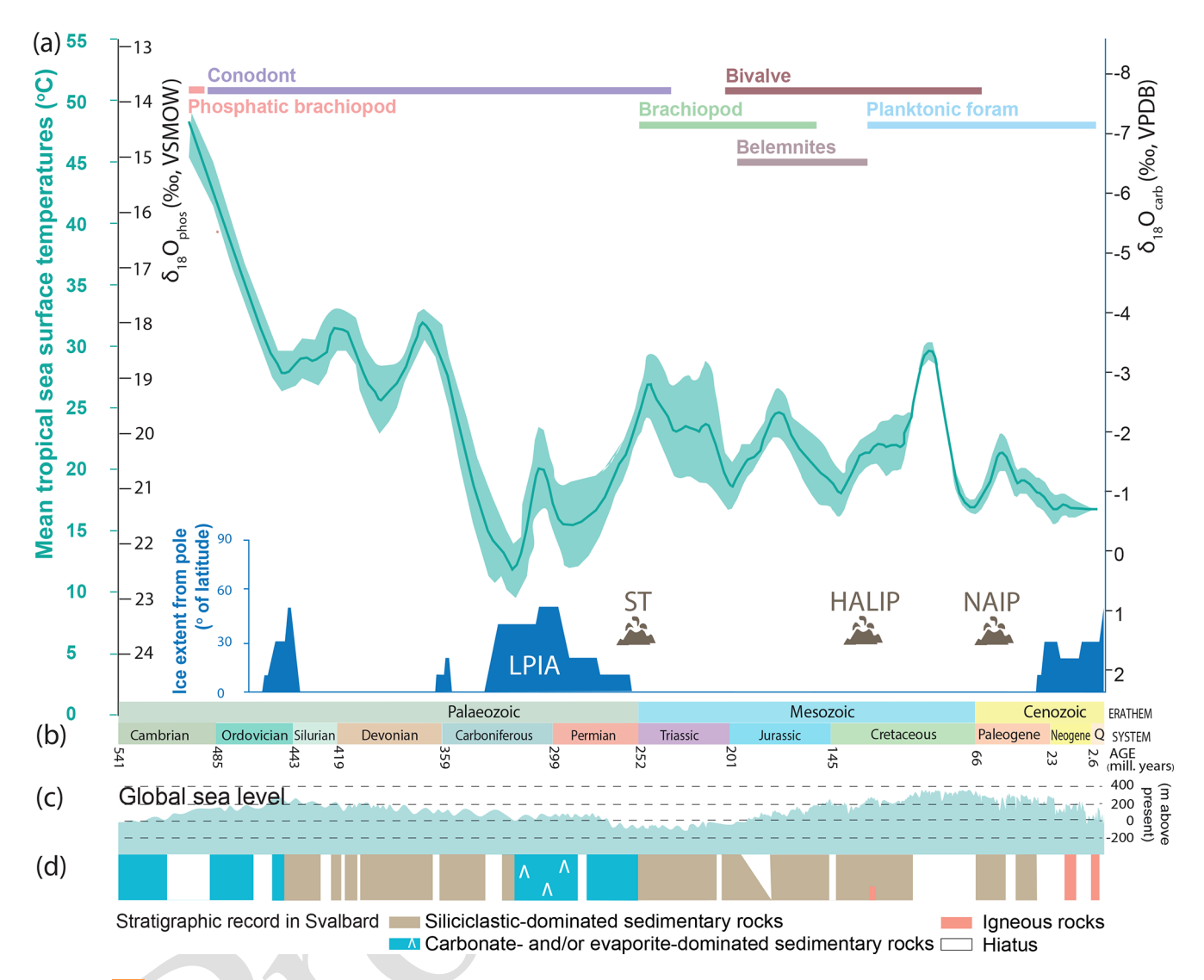


Figure 1. ISIThe stratigraphic record of Svalbard in a global deep-time climate context. (a) Global data coverage including mean tropical sea surface temperatures per Myr marked as a green curve, with shaded area 95 % confidence intervals, based on oxygen isotopes from phosphatic and carbonate fossils from Scotese et al. (2021), after Song et al. (2019). The scale of  $\delta^{18}O_{Phos}$  (black axis on the left) represents phosphatic fossils (phosphatic brachiopod, conodont, and fish). The scale of  $\delta^{18}O_{Carb}$  (black axis on the right) represents carbonate fossils (belemnite, bivalve, brachiopod, planktonic foraminifera). The ice extent from pole, marked in blue, after Macdonald (2020), LPIA – Late Paleozoic Ice Age; major LIPs recorded in Svalbard: ST – Siberian Traps, HALIP – High Arctic Large Igneous Province, NAIP – North Atlantic Igneous Province, (b) Phanerozoic timescale, (c) sea-level curve (after Dallmann, 2015, based on work of the International Commission on Stratigraphy), and (d) overview of the geological record of Svalbard (modified from Dallmann, 2015).

volumes of igneous material ( $> 0.1 \times 10^6 \, \mathrm{km^3}$ ) emplaced or erupted over large areas ( $> 0.1 \times 10^6 \, \mathrm{km^2}$ ) in an intraplate setting and within a short duration (1–5 Myr pulse for  $> 75 \, \%$  of the volume, 50 Myr maximum lifespan), although some 5 igneous activity broadly accepted as LIPs has protracted histories (e.g., the High Arctic Large Igneous Province, HALIP; Dockman et al., 2018; Heyn et al., 2024).

Svalbard is a Norwegian archipelago comprising all islands between 74–81° N and 15–35° E, including the largest island of Spitsbergen (Fig. 2). Extensive numbers of geological data have been acquired from outcrops and drill cores

across Svalbard. This data collection was largely triggered by the importance of Svalbard as an equivalent to the sedimentary successions in the offshore areas of the Norwegian Barents Sea (Steel and Worsley, 1984; Olaussen et al., 2025, and references therein). The stratigraphic succession in Svalbard is very extensive (Fig. 1d) with distinctive shifts in deposition over time, indicating a genetic link between deposition and paleolatitudinal position (Fig. 3), as initially identified by Steel and Worsley (1984). Svalbard's Phanerozoic paleonvironmental evolution is largely controlled by two main factors: (1) the northward tectonic motion of Svalbard from

equatorial to polar latitudes (Fig. 3) and (2) the influence of proximal and distant LIPs (Fig. 1). Many of the regional to global-scale events can be directly studied on sedimentary rock exposures of Svalbard, notably the vertically tilted Festningen section in western Spitsbergen (e.g., Grasby et al., 2015b; Vickers et al., 2019a, 2023; Senger et al., 2022). These and other events have also been recorded in drill cores collected for coal exploration, research purposes, and CO<sub>2</sub> storage in central Spitsbergen (e.g., Dypvik et al., 2011; Midtkandal et al., 2016; Grundvåg et al., 2017; Olaussen et al., 2019; Senger et al., 2019; Zuchuat et al., 2020; Jelby et al., 2025).

The Arctic has warmed twice to nearly 4 times as fast as the rest of the globe in recent decades (Rantanen et al., 2022). 15 This phenomenon, known as polar amplification, is largely due to oceanographic and atmospheric feedback processes (e.g., Screen and Simmonds, 2010). Polar amplification is evident in the geological past as extreme climates that are inconsistent with temperature distributions predicted by cur-20 rent models (Evans et al., 2018; Price et al., 2020). Since the Cretaceous, Svalbard has occupied an Arctic position, following its earlier location within more northerly boreal zones of the paleocontinents. Due to the current position of Svalbard and its paleogeographic history, the nearly contin-25 uous Phanerozoic record on Svalbard provides an ideal site to study polar amplification and, prior to the Cretaceous, to elucidate the effects of the breakup of supercontinents and subsequent northward plate tectonic movement (Fig. 3).

Currently, there are no compilations of paleoclimate and 30 paleoenvironmental research from Svalbard addressing the pre-Quaternary Phanerozoic depositional record that is available. As a first, this study synthesizes the stratigraphic record covered by drill core material and high-quality outcrops with reliable geochronological constraints. This contribution also 35 provides an overview of the range of proxies used to reconstruct Syalbard's paleoenvironmental evolution. Owing to its own unique tectonostratigraphic evolution, we do not include the successions exposed on Bjørnøya (the southernmost island of the Svalbard archipelago) in this review (see papers 40 by Worsley et al., 2001; Grundvåg et al., 2023; Janocha et al., 2024, for details on this succession). To provide a framework for the review of Svalbard's deep-time climate history, the five-step paleoclimate classification of Zhang et al. (2016) was used, which recognizes five major climates. These are as 45 follows: A - Tropical, B - Dry, C - Temperate, D - Continental, and E - Polar. This division enables the deep-time climate classification estimated primarily from climatically sensitive deposits and paleontological evidence supplemented by geochemical proxies including isotope data. We systematically 50 compile published literature (n = 148) of relevance to deeptime paleoclimate and paleoenvironments in Svalbard. The synthesized data proxies (e.g., total organic carbon (TOC),  $\delta^{18}$ O, and  $\delta^{13}$ C) reflect environmental changes in terrestrial and marine ecosystems that are presented in the broader con-55 text of pan-hemispherical and global climate events. The overall evolution of the paleoclimate preserved in the geological record of Svalbard is discussed and compared with the paleo-position of Svalbard and global average temperature trends.

60

#### 2 Tectonic and stratigraphic development

The sedimentary successions preserved in Svalbard record a changing climate controlled to a large degree by the paleolatitude of Svalbard along with global climatic transitions (e.g., Steel and Worsley, 1984). Since the start of the Paleozoic, Svalbard gradually drifted from near-equatorial lati- 65 tudes to its present position at 74-81° N (Fig. 3; Scotese et al., 1979; Torsvik et al., 2002; Torsvik and Cocks, 2019). Svalbard's lower Paleozoic geological record expresses its affinity to Laurentia. Broadly speaking, Svalbard was part of the Laurasian or Eurasian plates during its post-Devonian 70 history. The overall northward motion from an equatorial position in the Devonian and early Carboniferous to its present polar location during the Late Cretaceous (Fig. 3) was a response to absolute plate movement and relates to the breakup of the supercontinent Pangea near the end of the Jurassic. The LIPs with documented influence on the depositional record in Svalbard (Fig. 3) include the Siberian Traps, implicated as the causal factor of the End-Permian Mass Extinction (EPME; ca. 252 Ma; Reichow et al., 2009; Burgess et al., 2017); the High Arctic Large Igneous Province 80 (HALIP) that influenced paleoenvironments of Svalbard and much of the circum-Arctic area during the Early Cretaceous (Midtkandal et al., 2016; Vickers et al., 2019a; Galloway et al., 2022, 2023; Galloway and Lindström, 2023); and the North Atlantic Igneous Province (NAIP), associated with 85 the opening of the North Atlantic and the warming of the Paleocene-Eocene Thermal Maximum (PETM; started ca. 56 Ma; Charles et al., 2011).

#### 2.1 Paleozoic (Cambrian to Permian ca. 538-252 Ma)

The early Paleozoic succession of the Oslobreen Group (Fig. 4) preserved in northeastern Svalbard (Fig. 2) was deposited on the northern margin of Laurentia in a post-rift to a passive margin setting (Fig. 3; Smelror et al., 2024). Later, the Caledonian Orogeny started with the closure of the Iapetus Ocean and subsequent collision of Laurentia and Baltica in the Early Ordovician–Early Devonian (ca. 485–410 Ma; Barentsian Caledonides in Gee et al., 2006, 2008; Gee and Teben'kov, 2004; Harland et al., 1974). Caledonian deformation, metamorphism, and late crustal magmatism impacted mainly western and central-northern Svalbard, leaving the northeastern parts of the archipelago practically undeformed (Johansson et al., 2004, 2005; Smelror et al., 2024).

The syn- to post-Caledonian, Upper Silurian (Pridoli?) to Upper Devonian (Frasnian) Old Red Sandstone (ORS) succession (ca. 423–372 Ma) represented by the Siktefjellet, Red 105 Bay, and Andrée Land groups (Fig. 4; Friend et al., 1997;

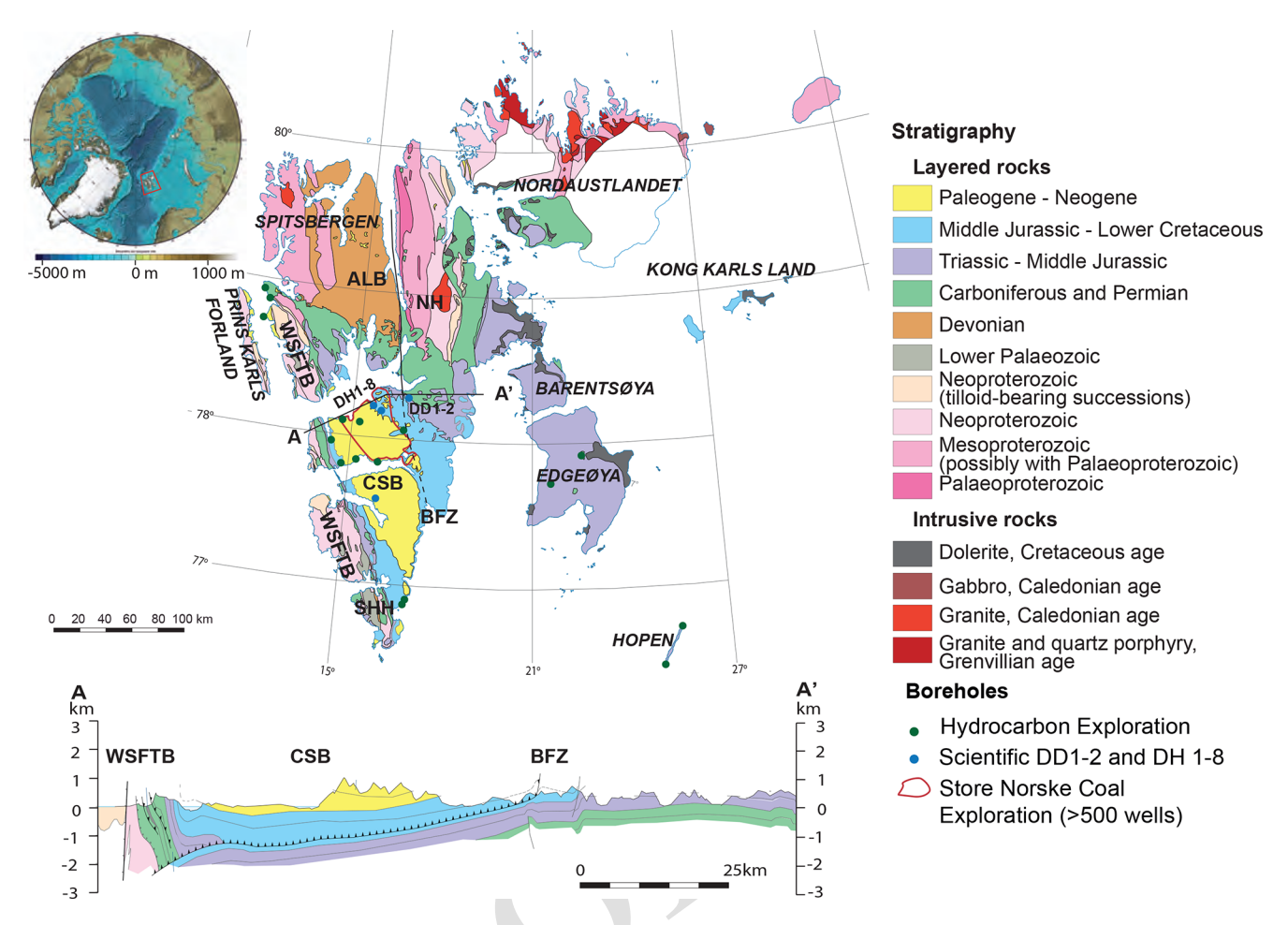


**Figure 2.** Geological map of Svalbard and a regional cross-section illustrating the major structural elements of central Spitsbergen and spatial coverage of industrial and research boreholes of relevance to deep time paleoclimatic studies. Upper left: International Bathymetric Chart of the Arctic Ocean (IBCAO; Jakobsson et al., 2012[152]). Geological Map of Svalbard and cross-section (A–A'; bottom) from Dallmann (2015). Location of boreholes from Senger et al. (2019). NH – Nordfjorden High, SHH – Sørkapp Hornsund High, ALB – Andrée Land Basin, BFZ – Billefjorden Fault Zone, WSFTB – West Spitsbergen Fold and Thrust Belt. CSB – Central Spitsbergen Basin.

Blomeier et al., 2003a, b) is preserved in post-orogen collapse basins located in the central part of northern Spitsbergen (Fig. 2; Piepjohn et al., 2000; Blomeier et al., 2003a, b; Braathen et al., 2018; Smelror et al., 2024). Significant deformation of the ORS succession subsequently took place during the Late Devonian compressional Svalbardian Event that is correlated with Ellesmerian Orogeny in Arctic Canada (McCann, 2000; Piepjohn, 2000; Bergh et al., 2011; Piepjohn and Dallmann, 2014; Piepjohn and von Gosen, 2018; Beranek et al., 2020).

The Tournaisian (?) – Viséan (ca. 359–330 Ma) continental coal-bearing deposits of the Billefjorden Group are widespread across Spitsbergen (Fig. 2) and unconformably overlie the deformed Devonian and pre-Caledonian succession (Piepjohn et al., 2000). The thickness of the Billefjorden Group reaches up to 250 m in central Spitsbergen (Cutbill and Challinor, 1965; Gjelberg and Steel, 1981) and 40–100 m in northeastern Spitsbergen (Lauritzen and Worsley, 1975;

Scheibner et al., 2012). The thickness along the west coast of Spitsbergen is uncertain due to younger deformation and 20 repetition of the succession. The Billefjorden Group is unconformably overlain by the Serpukhovian (upper Mississipian) to Artinskian (Cisuralian) mixed siliciclastic-carbonateevaporite deposits of the Gipsdalen Group (ca. 331–284 Ma). The lower Gipsdalen Group consists of syn-tectonic units 25 filling up rift basins, the Billefjorden, Lomfjorden, St Jonsfiorden, and Inner Hornsund troughs, developed along north south-striking long-lived lineaments formed in response to regional-scale extension (Fig. 4; Holliday and Cutbill, 1972; Gjelberg and Steel, 1981; Johannessen and Steel, 1992; 30 Faleide et al., 2008; Braathen et al., 2012). The thickest (> 1.5 km) and best-preserved basin fill occurs in the Billefjorden Trough, while corresponding succession is missing on the structural highs (Fig. 2; Cutbill and Challinor 1965; Johannessen and Steel, 1992; Braathen et al., 2012; 35 Smyrak-Sikora et al., 2018, 2021). The syn-rift units of the

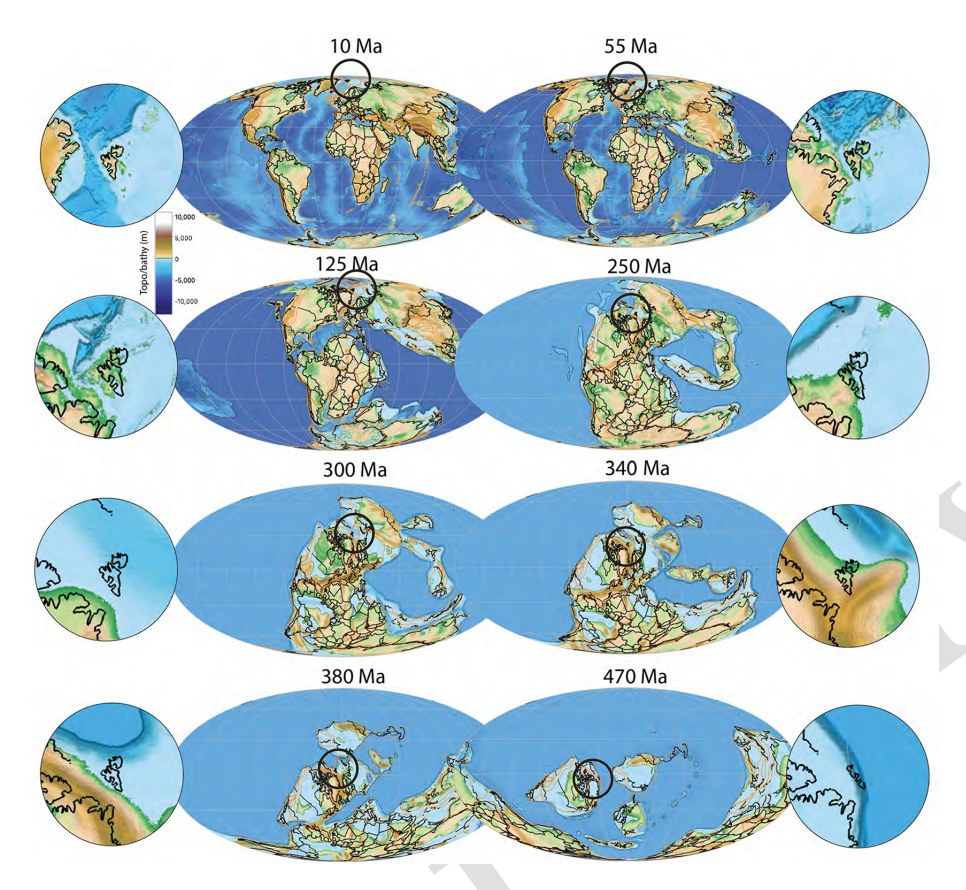


**Figure 3.** Global paleogeography (PaleoDEMs) from Scotese and Wright (2018), redrawn via export from GPlates (v2.5 Müller et al., 2018) for selected time steps. Terrane boundaries in orange and political boundaries and present-day coastlines in black. Yellow dashed ring in the global Mollweide projections identifies the approximate location of Svalbard at the selected time periods with zoom in shown to the side of global maps. As this is a global model there may be discrepancies from regional Svalbard paleogeography whereby the reader is directed to Dallmann (2015) for regional resolution.

lower Gipsdalen Group were subsequently overlain by up to 500 m thick warm-water carbonate platform deposits of the upper Gipsdalen Group (Hüneke et al., 2001; Blomeier et al., 2011; Ahlborn and Stemmerik 2015; Sorento et al., 5 2020). The Gipsdalen Group is overlain by upper Artinskian (Cisuralian) to Changhsingian (Lopingian) cool-water carbonate and spiculitic platform sediments of the Tempelfjorden Group (ca. 284 (?)-252 Ma). The thickness of the Tempelfjorden Group varies across Spitsbergen from 6 to 460 m 10 (Blomeier et al., 2013; Uchman et al., 2016; Matysik et al., 2018), including complete absence of Permian deposits on the Sørkapp-Hornsund High, where Carboniferous fluvial deposits are unconformably overlain by Lower Triassic continental conglomerates (Zuchuat, 2014). These thickness 15 variations indicate ongoing uplift of the Nordfjorden High and the Sørkapp-Hornsund High that can be linked with the late Permian rift event along the western Barents shelf margin (Faleide et al., 2008; Olaussen et al., 2025).

#### 2.2 Mesozoic

In the Early to Middle Triassic (ca. 252–237 Ma), Syalbard 20 was part of a shallow shelf that experienced significant subsidence and which was filled with up to 700 m of sediments sourced from west and east (the Sassendalen Group; Fig. 4; Mørk et al., 1982, 1999a; Wesenlund et al., 2022b; Bjerager et al., 2023). By the end of the Middle Triassic (ca. 237 Ma), 25 deltaic systems sourced in the Uralides and the Fennoscandian Shield reached and probably traversed Svalbard (Riis et al., 2008; Glørstad-Clark et al., 2010; Høy and Lundschien, 2011; Anell et al., 2013; Klausen et al., 2017, 2019; Gilmullina et al., 2022). Towards the latest Triassic and Early Jurassic, subsidence rates gradually decreased and sometimes even became negative, as expressed by condensed units with a 20 m thick, shallow-marine and continental sandstoneshale unit of Rhaethian (latest Triassic; ca. 208-201 Ma) to Bathonian (?) age (Middle Jurassic; ca. 168–165 Ma), truncated by several subaerial unconformities (Drachev, 2016; Faleide et al., 2018; Olaussen et al., 2018; Rismyhr et al., 2018; Müller et al., 2019). This Upper Triassic deltaic and

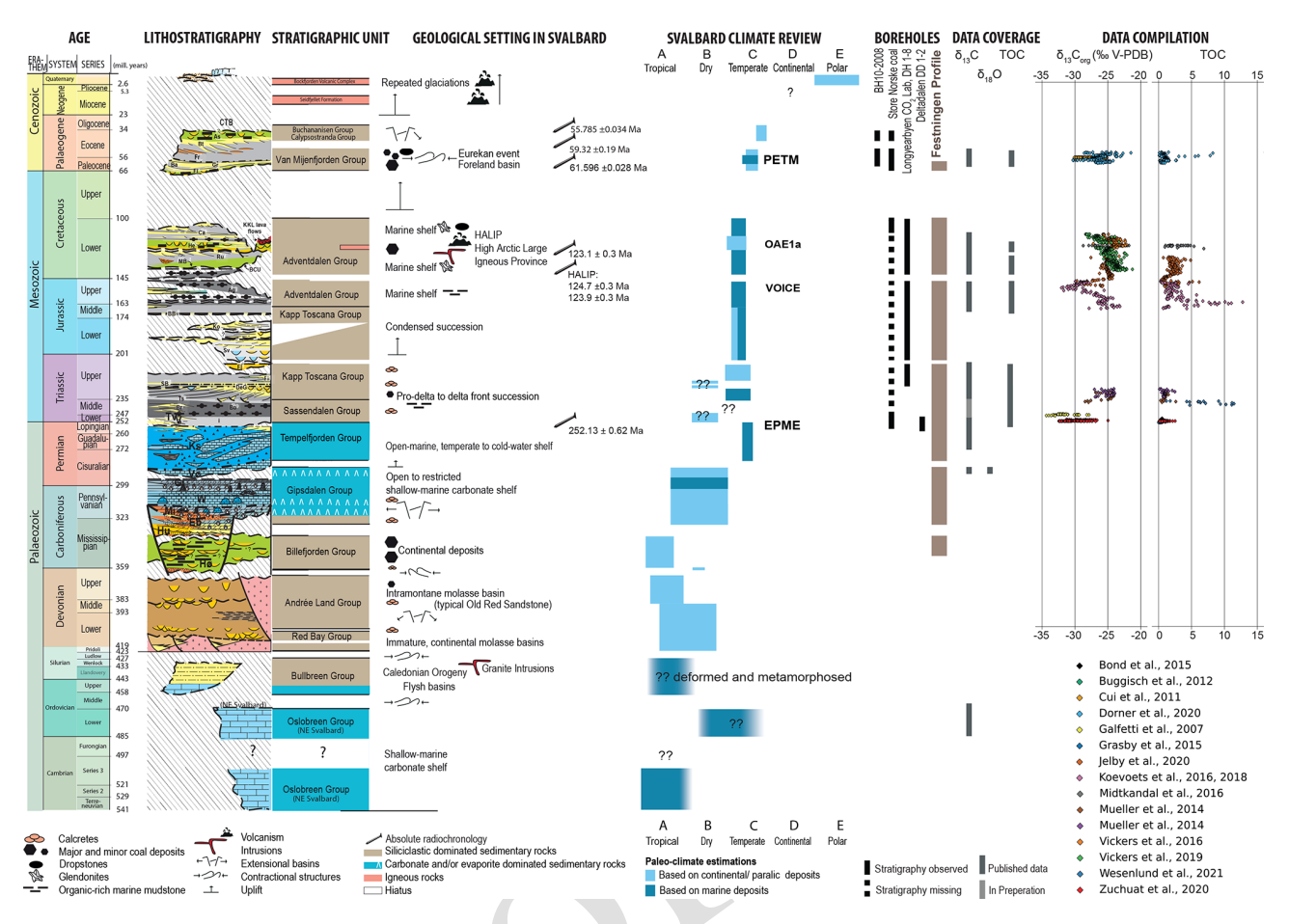


Figure 4. Stratigraphic column and climate summary of Svalbard highlighting the nearly continuous sedimentary record from the Devonian to the Neogene. The stratigraphic coverage of research boreholes is indicated. Post-Devonian lithostratigraphic column after Olaussen et al. (2025). Climate zones from Zhang et al. (2016). The climate indicators used to construct the plot are summed up in Table S1. Illustration of data coverage is based on Gruszczyński et al. (1989), Mii et al. (1997), Wignall et al. (1998, 2016), Galfetti et al. (2007), Cui et al. (2011), Buggisch et al. (2012), Mueller et al. (2014), Bond et al. (2015), Grasby et al. (2015a), Koevoets et al. (2016), Midtkandal et al. (2016), Vickers et al. (2016, 2019a, 2023), Hammer et al. (2019), Doerner et al. (2020), Jelby et al. (2020b), Zuchuat et al. (2020), Wesenlund et al. (2021), Blattmann et al. (2024), and Leu et al. (2024). Carbon isotope values ( $\delta^{13}C_{org}$ ) and total organic carbon (TOC) plotted from published datasets with extended stratigraphic coverage. Only data with sufficient thickness records were used. Stratigraphic age is based on a proxy conversion from sediment thickness to time. All data are publicly accessible upon publication via the Zenodo repository (Supplement 2<sup>TSS</sup>).

Upper Triassic to Middle Jurassic condensed section belongs to the Kapp Toscana Group. Subsidence rates increased again during the Late Jurassic (ca. 161–145 Ma), which led to the deposition of organic-rich marine strata of the lower Advent-5 dalen Group (e.g., Koevoets et al., 2016, 2019).

The upper Middle and Upper Jurassic/lowermost Cretaceous succession preserved in Svalbard consists of the Agardhfjellet Formation, and the Lower Cretaceous succession is represented by the Rurikfjellet, Helvetiafjellet, and Carolinefjellet formations, all assigned to the Adventdalen Group (Fig. 4). These marine to continental units reflect increased subsidence with uplift in the north and northwest that formed a continental, siliciclastic platform. This uplift is related to emplacement of the HALIP across the Arctic, includ-

ing Svalbard, Franz Josef Land, the New Siberian Islands, the Barents Shelf, Sverdrup Basin, northern Greenland, and the Alpha-Mendeleev Ridge, via both subaerial eruptive and intrusive magmatism (Maher, 2001; Estrada and Henjes-Kunst, 2013; Senger et al., 2014a; Evenchick et al., 2015; Polteau et al., 2016; Davis et al., 2017; Dockman et al., 2018; Naber et al., 2021; Bédard et al., 2021; Galloway et al., 2022). HALIP magmatism is thought to be derived from the arrival of a thermally elevated mantle plume that caused large volumes of mafic rocks including sills, dikes, lavas, and pyroclastic material (Maher, 2001; Senger et al., 2014a, b; Buchan and Ernst, 2018; Bédard et al., 2021; Naber et al., 2021; Heyn et al., 2024). Robust U–Pb dating points to a short magmatic pulse affecting Svalbard at ca. 124.5 Ma (Corfu et al., 2013).

However, in the adjacent Sverdrup Basin (Arctic Canada), multiple magma emplacement episodes have been identified, with pulses peaking at  $122 \pm 2 \,\mathrm{Ma}$ , at  $95 \pm 4 \,\mathrm{Ma}$ , and at  $81 \pm 4$  Ma (Jens et al., 2015 Kingsbury et al., 2018; <sup>5</sup> Davis et al., 2017; Dockman et al., 2018; Bédard et al., 2021; Dummann et al., 2024). In Spitsbergen, the HALIP activity triggered southward tilting of the platform, which resulted in progradation of a sand-rich fluviodeltaic system towards the south (Steel and Worsley, 1984; Gjelberg and Steel, 1995; 10 Worsley, 2008; Midtkandal and Nystuen, 2009; Grundvåg and Olaussen, 2017; Grundvåg et al., 2017). The extent of the uplifted and eroded area increased during the Late Cretaceous (ca. 100-66 Ma) to the whole of Svalbard, which resulted in the upper middle Albian deposits (uppermost Lower 15 Cretaceous; ca. 113-100 Ma; Hurum et al., 2016a; Hurum et al., 2016b) being unconformably overlain by Paleocene strata (Jochmann et al., 2020; Helland-Hansen and Grundvåg, 2021).

#### 2.3 Cenozoic

20 The mid-Paleocene saw the recommencement of sediment deposition in Svalbard after a  $\sim 60\,\mathrm{Myr}$  hiatus in response to large-scale regional changes in plate tectonic configurations (Fig. 3). The base of the Paleocene strata in Svalbard has been dated to 61.8 Ma (Jones et al., 2017), close 25 to the Danian-Selandian boundary (ca. 61.6 Ma). This age is contemporaneous with several changes around the Greenland microplate, including increased rifting between Greenland and Eurasia in the proto-Northeast Atlantic region (Abdelmalak et al., 2023), the first pulse of North At-30 lantic Igneous Province (NAIP) volcanism (Storey et al., 2007a), a change from carbonate- to siliciclastic-dominated sediments in the North Sea (Clemmensen and Thomasen, 2005), widespread shear deformation along eastern Greenland (Guarnieri, 2015), and an increase in the rate of seafloor 35 spreading in the Labrador Sea (Roest and Srivastava, 1989; Oakey and Chalmers, 2012). The combination of seafloor spreading in the Labrador Sea and rifting along the mid-Norwegian margin instigated compression between Greenland and Svalbard, which evolved into a dextral transpres-40 sional regime as rifting transitioned to seafloor spreading in the NE Atlantic by 55 Ma (Storey et al., 2007b). This period was also coincident with the rifting and breakup of the Eurasia Basin to the north of Svalbard. The dextral transpression along the Greenland-Svalbard margin caused lo-45 calized crustal shortening and the formation of the West Spitsbergen Fold and Thrust Belt, WSFTB (Fig. 2; Harland, 1995), linked to the Eurekan deformation (ca. 63–35 Ma) and plate reorganization in the North Atlantic (Dallmann et al., 1993; Braathen et al., 1995, 1999; Maher et al., 1995; 50 Bergh et al., 1997; Gee and Teben'kov, 2004; Faleide et al., 2008; Leever et al., 2011; Blinova et al., 2013; Piepjohn et al., 2015, 2016; Gion et al., 2017). A north-south- trending foreland basin, known as the Central Spitsbergen Basin (CSB) or the Central Tertiary Basin (CTB) in older literature, formed east of the WSFTB and was filled with over 1.9 km thick Paleocene to Eocene (Oligocene?) deposits of the Van Mijenfjorden Group (Fig. 4; Steel et al., 1981, 1985; Helland-Hansen, 1990; Müller and Spielhagen, 1990; Bruhn and Steel, 2003; Jochmann et al., 2020; Helland-Hansen and Grundvåg, 2021). During the Paleocene–Eocene transition (ca. 56 Ma), a passive margin started to develop to the north of Svalbard as a result of the opening of the Eurasia Basin. Finally, an Oligocene (ca. 34–23 Ma) transtensional rift phase eventually gave way to the formation of a passive margin west of Spitsbergen (Faleide et al., 2008; Lasabuda et al., 65 2018; Haaland et al., 2024).

The transpressional deformation related to the WSFTB was followed by NW-SE transtensional rifting that formed a series of grabens along the western Svalbard margin (Steel et al., 1985; Blinova et al., 2009; Kleinspehn and Teyssier, 2016; Kristoffersen et al., 2020; Haaland et al., 2024). The Forlandsundet Graben, one of the grabens cropping out between the islands of Prins Karls Forland and Spitsbergen (Fig. 2) contains between 1000-3000 m of Eocene to potentially Oligocene strata (Gabrielsen et al., 1992; Schaaf et 75 al., 2021). The final separation between Greenland and the Barents Shelf margin eventually led to the opening of the Fram Strait. A shallow and narrow gateway was initially established around 20 Ma (Jokat and Herter, 2016; Fyhn and Hopper, 2025), and the transition from a restricted to fully 80 ventilated Arctic Ocean took place around 17.5 Ma (Jakobsson et al., 2007). The establishment of a deep-water connection through the Fram Strait is currently debated, with suggested ages of 13.7 Ma (Jakobsson et al., 2007), 10 Ma (e.g., Kristoffersen and Husebye, 1985; Kristoffersen, 1990), and 5 Ma (Lawver et al., 1990). During these times, Svalbard and the rest of the Barents Shelf margin experienced several changes in motion relative to the adjacent Greenland plate.

The present archipelago configuration of Svalbard with respect to the otherwise submerged setting of the Barents Shelf is thought to be a consequence of a combination of uplift during the Late Cretaceous, Paleocene–Eocene Eurekan deformation, and ongoing Holocene (last 11.7 kyr) isostatic rebound (Dimakis et al., 1998 (Worsley, 2008; Henriksen et al., 2011a, b; Dörr et al., 2013; Lasabuda et al., 2021). This uplift and exposed nature of Svalbard has resulted in the present-day exhumation of the metamorphic succession along the northern and western coasts of Svalbard and the younger sedimentary cover as described above (Fig. 3).

3 Data 100

Paleoclimate research in Svalbard has traditionally relied on the exceptionally exposed and vegetation-free outcrops, typical of the present Arctic landscape. For the last 2 decades, research drilling across Svalbard has increasingly been utilized and provides drill core material which can be repur-

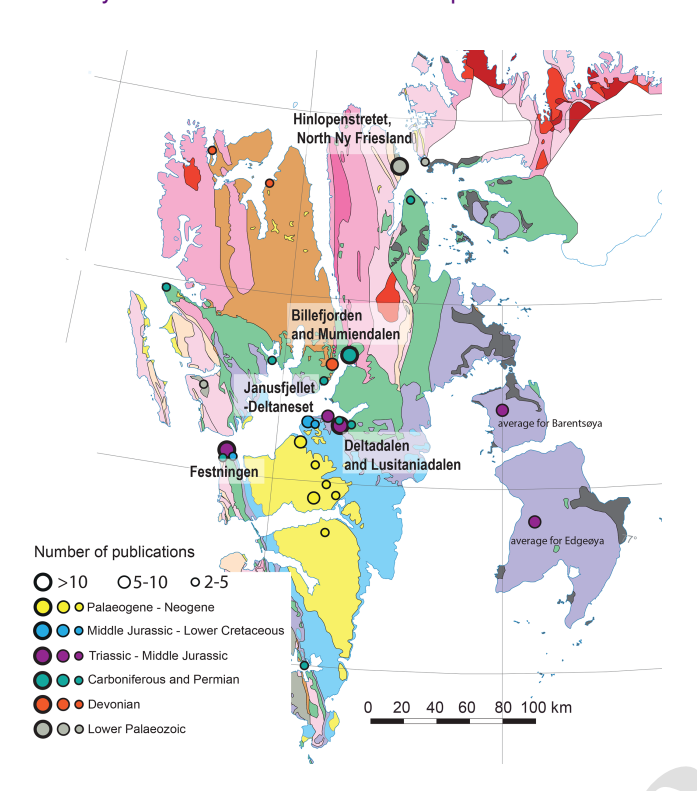


**Figure 5.** Location of data presented in the reviewed articles summed up in Table S3 highlighting the most studied sections in Svalbard. The size of a circle corresponds to the number of publications addressing deep-time paleoclimate proxies. See Fig. 2 for the legend of the geological map.

posed for high-resolution paleoenvironmental and paleoclimate research.

#### 3.1 Key stratigraphic sections

Figure 5 shows the geographic distribution of the primary study sites referenced in the 148 key publications summed up in Tables 1 and 2 (listed with more details in Table S3 in the Supplement). Many of these articles are centered on important sites with good chronological and lithological constraints. Most of the outcrops are also covered by high-resolution digital outcrop models freely available through the Svalbox database (Betlem et al., 2023), facilitating data integration. Four of the localities are represented by 10 or more publications and are described below.

#### 3.1.1 Festningen

15 The Festningen section in western Spitsbergen offers a nearly complete stratigraphic section spanning the Mississippian (ca. 359 Ma) to the Paleocene (Fig. 6). The ∼7 km long section is easily accessible along the shoreline, with nearly vertical sedimentary layers due to Eurekan deformation. Festningen is an important regional stratigraphic profile and routinely targeted by geologists (Hoel and Orvin 1937; Steel et

al., 1978; Mørk et al.,1982; Nagy and Berge, 2008; Midtkandal and Nystuen, 2009; Grundvåg et al., 2019), including those interested in deep-time paleoclimate (e.g., Bond et al., 2015; Grasby et al., 2016a; Vickers et al., 2023). Mørk and Grundvåg (2020) offer a geological guidebook for the section, whereas Senger et al. (2022) provided an open-access digital outcrop model (DOM) of the 5 km long part of the protected section. The high-resolution (7 mm pixel resolution) DOM is suitable for planning additional sampling and quantitative structural and sedimentological analyses and integrating existing paleoclimatic research (Fig. 6).

#### 3.1.2 Janusfjellet-Deltaneset

The Janusfjellet section in central Spitsbergen exposes an Upper Triassic to Paleocene siliciclastic-dominated succession that has been extensively studied as part of the Longyearbyen CO<sub>2</sub> lab project (Olaussen et al., 2019). The succession includes both the Upper Triassic-Middle Jurassic sandstone reservoirs of the Kapp Toscana Group as well as the overlying Upper Jurassic-Lower Cretaceous Advent- 40 dalen Group. The Agardhfjellet Formation, the lowermost part of the Adventdalen Group, has also been extensively studied as one of the richest marine reptile sites in the world, yielding 60 specimens so far (Hurum et al., 2012; Delsett et al., 2016), along with an abundant seep fauna (Hryniewicz 45 et al., 2015). The outcropping section dips gently at about 3° to the southwest and exposes the same stratigraphy as in the fully cored boreholes in Adventdalen (Olaussen et al., 2019). As an excellent analog to the Longyearbyen CO<sub>2</sub> lab reservoir–caprock system, the outcrops have been systematically studied with focus on sedimentology (Rismyhr et al., 2018; Jelby et al., 2020a), fault and fracture characterization (Ogata et al., 2014a, b; Mulrooney et al., 2018; Betlem et al., 2024; Rizzo et al., 2024), sandstone injectites (Ogata et al., 2023), and paleoclimatic signals (Koevoets et al., 2018; Jelby 55 et al., 2020b).

#### 3.1.3 Sassendalen

Sassendalen is a key region for understanding the Permian—Triassic transition and evolution of Svalbard, and within Sassendalen there are many key sections for defining different aspects of the lithostratigraphic framework of central Spitsbergen (e.g., Mørk et al., 1999a, b). It is also a notable area to study global ecosystem recovery after the End-Permian Mass Extinction (see Hurum et al., 2018; Kear et al., 2023). Deltadalen and Lusitaniadalen are two valleys on the western side of Sassendalen that excellently expose the Permian Kapp Starostin to Botneheia formations. In addition, there is the more eastern Fulmardalen (Hammer et al., 2019; Hansen et al., 2024). The Deltadalen outcrop is directly next to the Deltadalen research boreholes, where deposits of the EPME and Permian—Triassic boundary were cored (Zuchuat et al., 2020). As such, it provides borehole—outcrop corre-

Key, selected boreho	Key, selected boreholes with significant core or cutting material.	cutting material.				
Borehole(s)	Penetrated strata	Penetrated strata (age and formation)	Depth (meters)	Drill core availability	Complementary datasets	Key reference
	Youngest	Oldest				
Gipsdalen (DD-1-DD-8)	Pennsylvanian Ebbadalen Fm	Precambrian Basement	91.9–210.5	Berlin-Spandau and Uni Oslo	Technical reports	Senger et al. (2019).
Deltadalen (DD-1 and DD-2)	Lower Triassic Vikinghøgda Fm	Lopingian Kapp Starostin Fm	92.9–99.3	Oslo	Reports	Zuchuat et al. (2020), Schobben et al. (2020), Rodríguez-Tovar et al. (2021)
Tromsøbreen II	Lower Cretaceous Carolinefjellet Fm	Pennsylvanian (?) Minkinfjellet Fm (?)	2337	5 cores, in Lund	Reports	Senger et al. (2019).
Reindalspasset	Lower Cretaceous Carolinefjellet Fm	Mississippian, Billefjorden Gr	2315	Cuttings, in Endalen Svalbard	Reports	Senger et al. (2019).
UNIS CO <sub>2</sub> lab (DH-1–DH-8)	Lower Cretaceous Carolinefjellet Fm	Upper triassic De Geerdalen Fm	down to 969.7	Longyearbyen	Reports, wireline logs, publications	Corfu et al. (2013), Midtkandal et al. (2016), Polteau et al. (2016), Olaussen et al. (2019), Senger et al. (2024).
SNSK boreholes, including core BH9/05	Eocene Frysjaodden Fm	Metamorphic basement	numerous	Endalen	Reports	Cui et al. (2011), Dypvik et al. (2011), Charles et al. (2011), Nagy et al. (2013), Jones et al. (2019).
Sysselmannbreen (BH2008-10)	Eocene (?) Oligocene (?) Aspelintoppen Fm	Late Paleocene Basilika Fm	1085	Endalen, Equinor lab (Bergen)	Reports	Johannessen et al. (2011), Doerner et al. (2020).
Key outcrop sections (> 10 publications)	(> 10 publications)					
Outcrop sections	Penetrated strata (age and formation)	Penetrated strata (age and formation)	Extent	Key reference(s)		
	Youngest	Oldest				
Hinlopenstretet, North Ny Friesland	Ordovician	Cambrian	around 10 km	Hansen and Holmer (2010), Stouge et al. (2012), Lehnert et al. (2013), Abay et al. (2022).	10), Stouge et al. (2012) ay et al. (2022).	ÿ
Billefjorden	Lower Permian	Upper Devonian	over 20 km of composite sections	Cutbill and Challinor (1965), Gjelberg and Steel (1981), Ahlborn and Stemmerik (2015), Berry and Marshall (20 Davies et al. (2021), Smyrak-Sikora et al. (2021).	965), Gjelberg and Stee (2015), Berry and Mar yrak-Sikora et al. (2021	Steel (1981), Marshall (2015), 2021).
Festningen	Paleogene Firkanten Fm	Carboniferous	5–6 km	Hoel and Orvin (1937), Steel et al. (1978), Mørk et al. (19 Nasy and Berse (2008), Midtkandal and Nystuen (2009).	Steel et al. (1978), Mørl Midtkandal and Nystue	Mørk et al. (1982), vstuen (2009).
	A DEPOSIT A LIA	Billefjorden Gr		Grasby et al. (2015a), Grundvåg et al. (201 Senger et al. (2022), Vickers et al. (2023).	rundvåg et al. (2019), N kers et al. (2023).	19), Mørk and Grundvåg (2020),
Deltadalen and Lusitaniadalen	Lower Triassic Vikinghøgda Fm	Lopingian Kapp Starostin Fm	around 7 km	Dagis and Korcinskaja (1987) ISSA, Mørk et al. (1999a, b), Foster et al. (2017), Zuchuat et al. (2020)	1987) <mark>1186</mark> , Mørk et al. ( nuat et al. (2020)	1999a, b),
Deltaneset- Janusfjellet	Lower Cretaceous Carolinefjellet Formation 187		around 7 km	Hurum et al. (2018), Rismyhr et al. (2018) Olaussen et al. (2019), Koevoets et al. (201	myhr et al. (2018), .oevoets et al. (2018), J	, 18), Jelby et al. (2020a, b).

Stratigraphic intervals		Silurian	Cambro- Devonian	Carboniferous– Permian	Permian– Triassic boundary	Triassic	Jurassic- Cretaceous	Paleogene
N of	N of papers	10	11	27	22	30	30	18
articles	boreholes	0	0	0	3	2	10	9
	outcrops	10	11	27	21	30	27	11
Proxies	Biological indicators	8	8	15	14	22	24	10
and data	Climate-sensitive facies	3	7	18	2	2	3	9
	Carbon isotopes $\delta^{13}$ C	2	2	8	8	6	13	6
	Oxygen isotopes $\delta^{18}$ O	1	1	4	0	0	4	1
	TOC/Rock-Eval	2	2	1	3	6	7	6
	Mercury, Hg	0	0	0	2	1	1	1

Table 2. Summary of proxies based on Table S3, which reviews 148 selected papers. The dataset is plotted in Fig. 13.

lation, with the benefit of facilitating detailed sedimentological studies and high-resolution sampling away from the boreholes. In addition, a well-exposed section of Permian— Triassic transition crops out along Lusitaniadalen located around 5 km northwest from Deltadalen and has been the focus of multiple studies directly focused on the Permian— Triassic boundary (e.g., Mørk et al., 1999a, b; Foster et al., 2017a; Rauzi et al., 2024).

#### 3.1.4 Hinlopenstretet, North Ny Friesland

The Ny Friesland section in northeastern Spitsbergen is exposed along the south coast of the Hinlopen Strait (Fig. 2) and consists of a ~ 1 km thick Terreneuvian–Middle Ordovician carbonaceous succession of the Oslobreen Group (ca. 539–458 Ma; Hansen and Holmer, 2010; Stouge et al., 2012; Lehnert et al., 2013; Abay et al., 2022; Smelror et al., 2024). This succession, consisting of siliciclastic shoreline facies at the base, passing up to a shallow-marine carbonate platform deposits, belongs to the North Atlantic/Arctic warm-water carbonate platform formed on eastern Laurentia (McKerrow et al., 1992; Stouge et al., 2012).

#### 3.1.5 Billefjorden and Munindalen

The inner part of Billefjorden exposes the Billefjorden Fault Zone, where the Devonian Old Red Sandstone (ORS) deposits on the west, several kilometers thick, are faulted against the several metamorphic and sedimentary successions in the east. These include pre-Devonian metamorphic basement, up to 250 m of Mississippian units and over 2 km of Pennsylvanian to Permian deposits (Braathen et al., 2012; Smyrak-Sikora et al., 2018, 2021). In Munindalen, the lower-most Upper Devonian deposits of the Andrée Land Group expose plant fossils that represent terrestrialization and evolution of one of the oldest forests in the world (Berry and Marshall, 2015; Davies et al., 2021). The fossil Devonian forests units are locally unconformably overlaid by the Mississip-35 pian siliciclastics with coal seams belonging to the Bille-

fjorden Group (Cutbill and Challinor, 1965; Gjelberg and Steel, 1981). Up the section, the Gipsdalen Group consists of the syn-rift and post-rift mixed siliciclastic-carbonate–evaporite units (Holliday and Cutbill, 1972; Gjelberg and Steel, 1981; Johannessen and Steel, 1992; Stemmerik, 2000; 40 2008; Blomeier et al., 2011; Ahlborn and Stemmerik, 2015; Sorento et al., 2020; Smyrak-Sikora et al., 2018, 2021).

#### 3.2 Drill cores

Table 1 summarizes the drill cores presently available from Svalbard. The cores are mostly from coal exploration by Store Norske Spitsbergen Kulkompani (SNSK) and CO<sub>2</sub> storage research drilling in Adventdalen by The University Centre in Svalbard (UNIS) (Olaussen et al., 2019; Senger et al., 2025). In addition, stratigraphic research boreholes, including the Sysselmannbreen (Johannessen et al., 2011) and Deltadalen (Zuchuat et al., 2020) boreholes, are given. Limited core material from past petroleum exploration efforts is known to exist (18 boreholes were drilled from 1960 to 1994; see review by Senger et al., 2019), but these have, hitherto, not been used in any paleoclimate investigations. Nonetheless, the associated wireline data from these wells are important calibration points for regional correlation of outcrops and onshore seismic reflection data.

#### 3.2.1 Coal drilling

Exploration coal drilling focused on Paleocene stratigraphy of the Van Mijenfjorden Group in the Central Spitsbergen Basin (CSB) and Mississippian coal-rich strata of the Billefjorden Group near Pyramiden. Lower Cretaceous and Eocene coal-bearing strata were targeted in minor campaigns. Cores from the Russian/Soviet coal mining company Trust Arktikugol, including sites near Barentsburg, Colesdalen, and Pyramiden, are not available and likely lost as evidenced by defunct core sheds scattered around Svalbard. However, reports from these drill cores (Verba, 2013) have been used locally to constrain surface geological mapping, 70

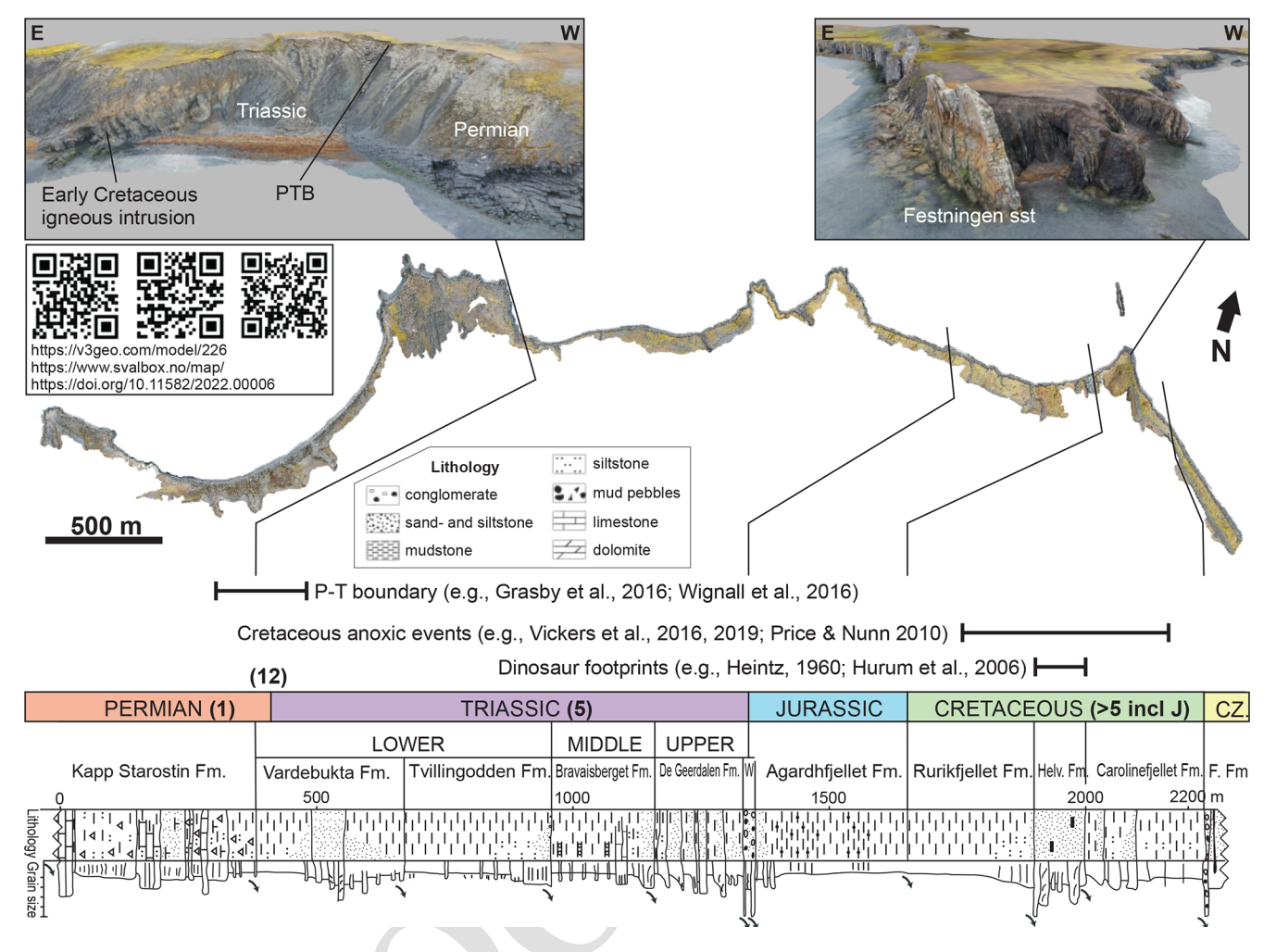


**Figure 6.** Stratigraphic column of the best-preserved part of the Festningen section, from Mørk and Grundvåg (2020), tied to the digital model of the entire Festningen section as presented in Senger et al. (2022). The inset images of the Permian–Triassic boundary and the Festningen sandstone illustrate screenshots of the digital outcrop model that is accessible online and freely available for download by following the QR codes and URLs. Paleoclimate-related research conducted on the section is highlighted for key events. These include amongst others the End-Permian Mass Extinction and the subsequent recovery phase (e.g., Wignall et al., 1998; Grasby et al., 2016a), as well as several Cretaceous cooling events, anoxic events, and their associated deposits (Price and Nunn, 2010; Vickers et al., 2016, 2019a; Grundvåg et al., 2019). Abbreviations: CZ = Cenozoic, W = Wilhelmøya Subgroup, Helv. Fm = Helvetiafjellet Fm, F. Fm = Firkanten Fm. The QR codes provide direct access to the digital model. Figure modified after Senger et al. (2022).

such as in Mimerdalen (Piepjohn and Dallmann, 2014) and in the Billefjorden Trough (Smyrak-Sikora et al., 2021). The Norwegian coal mining company SNSK stores most of its cores in Endalen near Longyearbyen, with drill dates ranging from the late 1960s to 2014, the last year of Norwegian coal exploration. These cores were investigated in several paleoclimate-related studies, particularly across the PETM and North Atlantic Igneous Province (NAIP)-related ash deposits (Table 1; Dypvik et al., 2011; Jones et al., 2019).

#### 10 3.2.2 Longyearbyen CO<sub>2</sub> lab, DH-1 to DH-8

Eight boreholes were fully cored near Longyearbyen from 2007 to 2013 to characterize a potential CO<sub>2</sub> storage site

(Braathen et al., 2012; Olaussen et al., 2019; Senger et al., 2025). Four of the boreholes reach the planned Upper Triassic units of the Kapp Toscana Group target storage unit at 670–700 m, while the other boreholes focus on the cap rock and overburden succession of the Adventdalen Group. The full coring across the shale-dominated cap rocks provides important constraints on the stratigraphy of the Jurassic-Cretaceous strata (Koevoets et al., 2016; Midtkandal et al., 2016; Jelby et al., 2020a, b; Śliwińska et al., 2020) and also contributed to refining the global geological timescale (Zhang et al., 2021b). Senger et al. (2025) provide a full overview of the datasets generated by the project including a live database of the resulting publications, including those focusing on deep-time paleoclimate.

#### 3.2.3 Sysselmannbreen, BH10-2008

The BH10-2008 (also known as Sysselmannbreen) research borehole was drilled and fully cored in 2008 to recover a full section of the Eocene–Oligocene (?) clinoform succession of the Van Mijenfjorden Group in the CSB (Johannessen et al., 2011). The 1085 m long core was split, with one half stored in a container in Endalen, outside of Longyearbyen, and the other half stored in Equinor's laboratory in Bergen (Doerner et al., 2020).

#### 10 3.2.4 Deltadalen, DD-1 and DD-2

The most recent research drilling in Svalbard was conducted in 2014 at Deltadalen specifically to target the uppermost Permian part of the Tempelfjorden Group and Lower Triassic succession of the Sassendalen Group, with a specific interest in the EPME and its aftermath (Zuchuat et al., 2020). The two ca. 100 m deep boreholes were drilled and fully cored. The drill cores are stored at the University of Oslo.

#### 4 Deep-time paleoclimate in Svalbard

4.1 Early Paleozoic (Cambrian, Ordovician, Silurian, 538.8–419.2 Ma)

### 4.1.1 Cambrian to Middle Ordovician – the Great Ordovician Biodiversification Event

The early Paleozoic registered two of the greatest evolutionary events in the history of life: the Cambrian Explosion <sup>25</sup> (ca. 540–510 Ma) and the Great Ordovician Biodiversification Event (GOBE; ca. 497–445 Ma; Webby et al., 2004; Servais and Harper, 2018). This upper Furongian to Upper Ordovician diversification event is linked to cooling of previously very warm tropical oceans (Webby et al., 2004; Servais <sup>30</sup> and Harper, 2018).

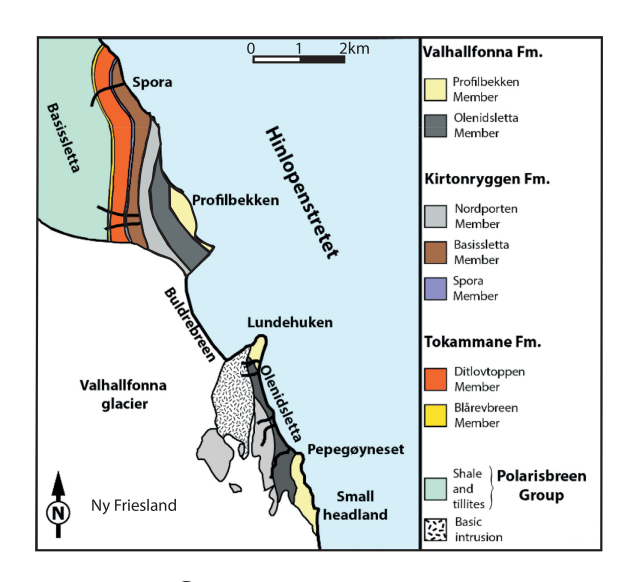
During the Cambrian and Ordovician, Svalbard was in a near-equatorial position (Torsvik et al., 2012; Fig. 3). The Terreneuvian to Middle Ordovician Oslobreen Group (Fig. 4) strata preserved in Svalbard formed on a large carbonate 35 platform along the northern margin of Laurentia, also exposed in the Northeast Greenland Basin and eastern North Greenland Basin (Stouge et al., 2012; Fig. 2). The mildly deformed, 1-1.2 km thick sandstones, fossiliferous limestone, and dolomite are preserved in northeastern Spitsber-40 gen (Fig. 7; Harland and Wilson, 1956; Oslobreen Series in Gobbett and Wilson, 1960; Fortey and Bruton, 1973; Stouge et al., 2011; 2012; Dallmann, 2015). The succession is potentially interrupted by a  $\sim$  15 Myr hiatus spanning over the Series 2, Miaolingian, Furongian, and possibly the earliest 45 Ordovician (Fortey and Bruton, 1973; Smelror et al., 2024), although the lack of dateable fossils might affect this interpretation (Smelror et al., 2024). The Oslobreen Group shows surprisingly low maximum burial temperatures (Bergström, 1980; Abay et al., 2022) and eastward increasing tectonothermal influence linked to the Caledonian Orogeny (Johansson et al., 2004). The trilobites and fauna generally show a Pacific and Laurentian affinity (Fortey and Bruton, 1973; Hansen and Holmer, 2010; Stouge et al., 2012).

In Ny Friesland, the Terreneuvian microbial laminated limestone/dolomite rocks contain centimeter-scale erratic 55 chert nodules. The Lower to Middle Ordovician (ca. 485-458 Ma) carbonates were deposited in a paleotropical marine shelf setting experiencing episodes of water column redox stratification (Lee et al., 2019). Stouge (2012) also interprets the Tremadocian (Lower Ordovician; ca. 485–478 Ma) environment in Svalbard and Greenland as a typical tropical shelf. Occurrence of oolite beds interbedded with domed stromatolites throughout the Tremadocian on Ny Friesland and adjacent islands (Kröger et al., 2017) is consistent with a peritidal tropical carbonate factory. Uchman and Hanken (2024 recognize that carbonates of the uppermost part of Terreneuvian and the Cambrian Series 2 contain pseudomorphs after evaporites. Hansen and Holmer (2010) identify strong ties of Lower and Middle Ordovician brachiopods to faunas in North America and Greenland at the generic 70 level. Hansen and Holmer (2010) also discuss the transition from low-diversity brachiopod fauna in the Tremadocian and early Floian (Early Ordovician; ca. 478-470 Ma), followed by an abrupt diversification event in the late Floian and into the Middle Ordovician. The hypersaline conditions, 75 however, mask the expected record of the Great Ordovician Biodiversification Event (Uchman and Hanken, 2024). Bulk  $\delta^{13}$ C<sub>org</sub> values recorded from the Lower Ordovician to lowermost Middle Ordovician succession in Svalbard range from -29 to -32% with an average of -30.4% (Fig. 7; Lee et 80 al., 2019). This is close to the average  $\delta^{13}C_{org}$  of  $-29.4\,\%$ for global marine organic matter for this time interval (e.g., Hayes et al., 1999, Edwards and Saltzman, 2016). The Middle Ordovician part of the succession represents an overall deepening, transgressive sequence (Kröger et al., 2017; Lee 85 et al., 2019). The *Olenidae* Trilobite faunas in the lower and upper Olenidsletta Member indicate periods of redox stratification in deep-water, low-oxygen conditions (Lee at al., 2019). Kröger et al. (2017) suggest that the gradual transition to deeper deposits with more shale and local siltstone 90 and glauconitic horizons accompanied by increased burrowing and fossiliferous, cherty mud-wackestone, and skeletal grainstone is evidence of general climate cooling in the transition to the Middle Ordovician (i.e., the incipient phase of Ordovician cooling). Despite changing to colder sea floor conditions, tropical carbonate production continued in an inner carbonate ramp, while a cold-water carbonate factory prevailed in the outer ramp (Smelror et al., 2024).

### 4.2 Late Paleozoic (Devonian, Carboniferous, Permian, 419.2–251.9 Ma)

100

The Devonian, Carboniferous, and Permian periods record the only complete greenhouse to icehouse to greenhouse cy-



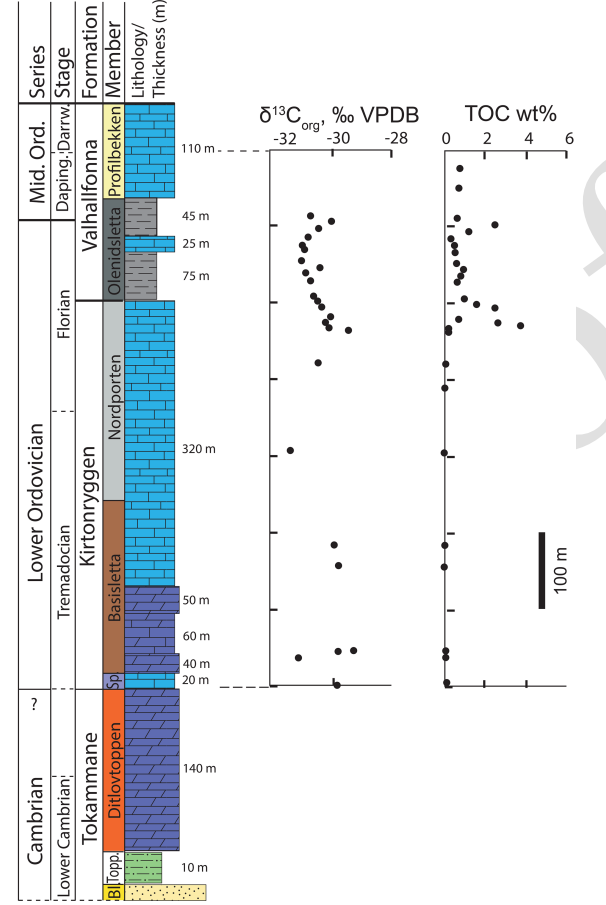


**Figure 7.** Stratigraphic section of the Cambrian and Ordovician Oslobreen Group succession in Ny Friesland, northern Spitsbergen (see Fig. 5 for location) after Fortey and Bruton (1973), Harland (1997), Stouge et al. (2012), Lehnert et al. (2013), Lee et al. (2019) and Abay et al. (2022). Bulk organic carbon isotopes ( $\delta^{13}C_{org}$ ; in ‰VPDB); total organic carbon (TOC; in weight percent); Bl. – Blårevbreen Member; Topp. – Topiggane Member; Sp. – Spora Member.

cle (LPIA) on a vegetated Earth (cf. Isbell et al., 2008). In Svalbard, the relatively complete Devonian to Permian sedimentary succession, which encompasses the Old Red Sandstone, Billefjorden, Gipsdalen, and Tempelfjorden groups (Fig. 4), provides an opportunity to study responses of the tropical and near-tropical depositional systems with the terrestrial and shallow-marine settings to the LPIA glaciations. Svalbard occupied a near equatorial position for most of the Devonian and Carboniferous and from the Permian started northwards drift (Fig. 3; Torsvik and Cocks, 2019).

#### Devonian: Old Red Sandstone, terrestrialization, and first forest

The advent of terrestrial vascular plants in the latest Silurian earliest Devonian influenced weathering processes and soil formation and strongly impacted the CO<sub>2</sub> cycle and global climate (Berner, 1993, 2005; Gensel, 2008, and references therein; Kenrick et al., 2012). The impact of vascular plants can be observed in Svalbard in the Uppermost Silurian to Upper Devonian Old Red Sandstone succession (Friend et al., 1997; Blomeier et al., 2003a, b). This > 8 km thick succession is restricted to extensional collapse basins formed in pure extensional (Piepjohn and Dallmann, 2014) or, more likely, transfersional settings (Braathen et al., 2018). The Andrée Land Basin exposed in central-north Spitsbergen was filled mainly by a terrestrial succession, with 25 marginal-marine conditions recorded in the northernmost part (Blomeier et al., 2003a). It notably includes red and gray-green fluvial, alluvial, lacustrine, and coastal sedimentary strata arranged into fining-upward units, with abundant plant material (Friend, 1965; Moody-Stuart, 1966; Blomeier et al., 2003a, b; Piepjohn and Dallmann 2014). The succession recorded indications of long-term climatic variability, such as shifts in paleosols from calcretes and vertisols to coal and preservation of in situ tropical forests (Berry and Marshall, 2015). The biological evidence of environmental conditions recorded in the Old Red Sandstone come from plant fossils (Berry, 2005; Berry and Marshall 2015; Davies et al., 2021), palynomorphs (Vigran, 1964; Allen, 1965, 1967; Friend et al., 1997), vegetation-induced sedimentary structures (Davies et al., 2021), and scarce marine-influenced 40 fauna including ostracods and bivalves (e.g., Friend, 1961; Worsley, 1972). Bulk geochemistry along with extraction and biomarker analysis of Middle Devonian coal indicates a terrestrial plant origin with high liptinite content (Vogt, 1941; Blumenberg et al., 2018). The flora evolved over time from 45 diminutive plants in the Middle Devonian to the first in situ forests of *lycopsids* and *archaeopterids* in the early Frasnian (Late Devonian; ca. 383–372 Ma; Berry and Marshall, 2015; Davies et al., 2021). Based on sedimentological and biological evidence for highly variable seasonal discharge and scarcity of thick calcretes, Davies et al. (2021) suggested that the precipitation regime in the Devonian was tropical and monsoonal and that the stratigraphic partitioning into red

bed and gray-green strata attests to long-term fluctuations in drainage and oxidizing conditions.

#### 4.2.2 Carboniferous to Cisuralian: Late Paleozoic Ice Age (LPIA)

5 The Late Paleozoic Ice Age (LPIA) is one of the most important climatic events of the Phanerozoic that significantly influenced climate and depositional systems on Earth (Gastaldo et al., 1996; Montañez et al., 2007; Isbell et al., 2008). The LPIA is the closest analog to present climate 10 conditions, characterized by discrete periods of glaciations separated by warm interglacials (Montañez and Poulsen, 2013). The LPIA glaciations started in the latest Devonian ca. 362 Ma, extended throughout the Carboniferous), and lasted at least until ca. 285 Ma during the middle 15 of the Artinskian (Cisuralian), potentially extending until ca. 260 Ma around the Guadalupian-Lopingian transition in the more Alpine settings in eastern Gondwana (Montañez and Poulsen, 2013; Rosa and Isbell, 2021). During this time, Svalbard drifted from a tropical position into the north-20 ern subtropical warm arid zone (Fig. 2; e.g., Torsvik and Cocks, 2019).

The early stage of the LPIA coincided with deposition of the Mississippian Billefjorden Group. This succession unconformably overlies the folded Paleo-Neoproterozoic and 25 Devonian successions. The terrestrial deposition occurred on broad floodplains and included abundant coal seams deposited under the humid tropical climate (Fig. 4; Gjelberg and Steel, 1981; Fairchild et al., 1982; Steel and Worsley, 1984; Lopes et al., 2019). The coal-bearing succession 30 reaches up to 55 m thickness in eastern Spitsbergen (Scheibner et al., 2012) and 350 m in central Spitsbergen (Gjelberg and Steel, 1981; see borehole SLE 116 in Smyrak-Sikora et al., 2021). Over 1200 m of cumulative thickness is reported along the west and south parts of Spitsbergen 35 (Gjelberg and Steel, 1981), where this succession is repeated several times due to the Paleocene and Eocene WSFTB (Maher et al., 1995; Braathen and Bergh, 1995; Fig. 10 in Horota et al., 2022). The fluvio-lacustrine coal deposits were commercially mined in Pyramiden from 1910 to 1998. The 40 coal is characterized by relatively heavy  $\delta^{13}$ C values, a low gammacerane index and high Pr/Ph ratios, distinctive from the Pennsylvanian coals associated with evaporites (Nicolaisen, 2019). Based on spores and plant fossils, Scheibner et al. (2012) suggested that the Billefjorden Group strata were 45 deposited in a humid climate, in accordance with a paleogeographic position 10–15° N (Fig. 3).

The shift from humid tropical to warm, arid to semiarid depositional environments occurred during the late Serpukhovian (Mississippian) at the boundary between the <sup>50</sup> Billefjorden and Gipsdalen groups (Fig. 4; Holliday and Cutbill, 1972; Gjelberg and Steel, 1981; Johannessen and Steel, 1992) and coincides with the initiation of regional-scale rifting in Svalbard and the Barents Shelf (Nøttvedt et al., 1993; Faleide et al., 2008; Braathen et al., 2012; Smyrak-Sikora et al., 2018, 2021). The following mixed siliciclastic-evaporitecarbonate succession of the lower Gipsdalen Group was deposited during the Pennsylvanian in an array of north-southstriking rift basins (Gjelberg and Steel 1981; Smyrak-Sikora et al., 2021). The shift from the Billefjorden Group to the Gipsdalen Group is abrupt across most of Svalbard, and the 60 boundary likely represents a period of non-deposition or erosion, especially on the structural highs. Contrastingly, in the inner part of one of the Billefjorden Trough, the transition is more gradual and occurs in a fluvial succession where the only changes recorded in the meandering river system is 65 the shift from humid to arid-climate soil profiles (Olaussen et al., 2023). This change in climate setting does not correspond to recognized northward drift of Svalbard (Torsvik and Cocks, 2019), and the reasons for this change are poorly understood. The Billefjorden Trough began as a continental rift basin followed by the opening of a connection to the ocean in the Bashkirian, which made the preposition sensitive to glacio-eustatic sea-level variations (Smyrak-Sikora et al., 2018, 2021).

The impact of the LPIA glaciations and deglaciations is 75 most readily recognized in the Bashkirian (Mississippian; onset ca. 323 Ma) to Sakmarian (Cisuralian; ca. 293-290 Ma) part of Gipsdalen Group, namely the paralic to marine syn- to post-rift succession comprising the upper Ebbadalen to Gipshuken formations (Fig. 8). Glacio-eustatic sea-level varia- 80 tions related to LPIA significantly impacted sedimentation in shallow shelf and coastal environments. Episodes of sealevel lowstands are represented by terrestrial siliciclastics, gypsum strata that precipitated in salinas and sabkhas, karst, and exposure surfaces which are interbedded with restricted to open-marine carbonate deposits formed during the sealevel highstands (Stemmerik, 2000, 2008; Ahlborn and Stemmerik, 2015; Sorento et al., 2020; Smyrak-Sikora et al., 2021). The number of cycles in the Bashkirian to Sakmarian part of the Gipsdalen Group exceeds 130 cycles (Ahlborn 90 and Stemmerik, 2015; Sorento et al., 2020; Smyrak-Sikora et al., 2021); however, the lack of good stratigraphic control limits cyclostratigraphic constraints. The LPIA in Svalbard is manifested also by Asselian (peak icehouse) atmospheric dust load estimated to be higher than the Moscovian (moder-95 ate icehouse; Oordt et al., 2020). This is consistent with the record from the Russian Platform that shows a  $\delta^{18}O$  maximum during the glacial maximum in the Asselian (Grossman et al., 2008). The Asselian to Artinskian ca. 2.5 % decrease in  $\delta^{18}$ O in the Southern Urals is attributed to a ca. 4–7 °C <sub>100</sub> increase in temperature and is used as evidence for glacial retreat (Korte et al., 2005). This is in line with the presence of a major Sakmarian deglaciation event across the western Barents Shelf and Svalbard resulting in regional deepening of the carbonate platforms and a temporary stop of glacio- 105 eustatic cyclic deposition (Stemmerik, 2008; Ahlborn and Stemmerik, 2015; Sorento et al., 2020).

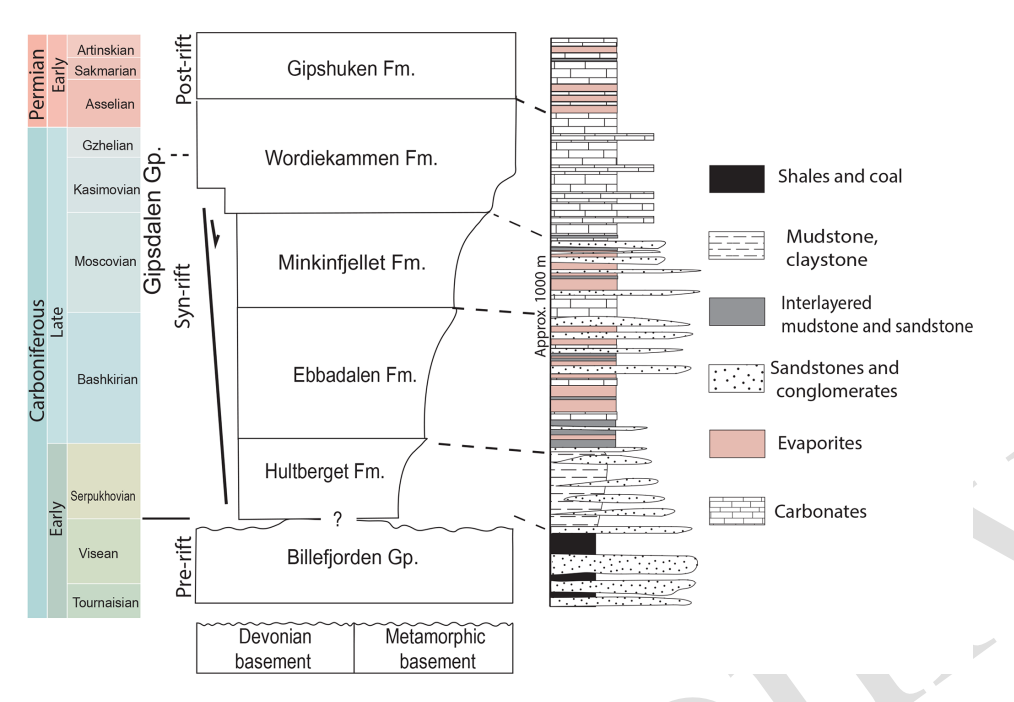


**Figure 8.** Carboniferous stratigraphy and simplified lithological profile demonstrating a shift from humid–tropical climate during deposition of the coal-bearing Billefjorden Group to the semi-arid to arid climate of the Gipsdalen Group seen as a change of climate-sensitive facies from coal-bearing units to red siliciclastics, evaporites, and warm-water carbonates. Modified from Braathen et al. (2012) and Smyrak-Sikora et al. (2021).

#### 4.2.3 Late Permian: cold-water carbonate platform

A transition from warm-water carbonate-evaporite deposition to the temperate to cool-water mixed siliceouscarbonate ramp occurred in the upper Artinskian (Cisuralian; 5 ca. 285 Ma) and corresponds to the transition from the Gipsdalen Group to the Tempelfjorden Group (Ezaki et al., 1994; Stemmerik, 2000, 2008; Hüneke et al., 2001; Stemmerik and Worsley, 2005; Blomeier et al., 2009, 2013; Buggisch et al., 2012; Dustira et al., 2013; Sorento et al., 2020; Olaussen et 10 al., 2025). The transition is attributed to the continued northern drift of Svalbard and closure of the Uralian seaway to the warmer Tethys to the southeast (Stemmerik, 2008) and was likely also the result of a deepening of the entire shelf (Blomeier et al., 2013). For the remainder of the Permian, 15 cool- to cold-water conditions prevailed along the northwestern margin of Pangea, leading to the deposition of a ca. 460 m thick succession dominated by spiculitic chert and cool-water carbonates (Cutbill and Challinor 1965; Blomeier et al., 2013; Uchman et al., 2016; Matysik et al., 2018).

Extensive oxygen isotopic data have been derived from brachiopods from the Artinskian–Changhingian (middle Cisuralian to Lopingian; ca. 285–252 Ma) Kapp Starostin Formation (e.g., Gruszczynski et al., 1989 [152]; Mii et al., 1997; Korte et al., 2005; Nielsen et al., 2013). However, the high variability in the isotopic data from these Permian brachiopods (e.g., Gruszczynski et al., 1989; Korte et al., 2005) is inconsistent with the marine habitat of

these taxa (Grossman et al., 2008). Diagenetic alteration accounts for the low  $\delta^{18}$ O values of most samples (Mii et al., 1997). To exclude diagenetically altered brachiopods, 30 many researchers have used geochemistry and petrography (e.g., Mii et al., 1997) and targeted the best-preserved parts of shells. Excluding these potentially altered values, brachiopod  $\delta^{18}$ O values are generally -2% to -7% for the Kungurian–Wuchiapingian (upper Cisuralian-Lopingian; ca. 35 283-254 Ma) interval of the Kapp Starostin Formation (Mii et al., 1997). The Guadalupian–Lopingian  $\delta^{13}$ C maximum of 7.5% represents the highest spiriferid brachiopod  $\delta^{13}$ C values in the Phanerozoic (Gruszczynski et al., 1989; Mii et al., 1997) and may reflect changes in global storage of organic 40 carbon (Mii et al., 1997). Matysik et al. (2018) investigated the multistage diagenesis of the Kapp Starostin Formation, at medium burial depths with deep-burial overprinting.

#### 4.2.4 Capitanian crisis

Within the Kapp Starostin Formation, it has also been proposed that a less severe middle Permian (Capitanian) mass extinction is recorded (Bond et al., 2015). This Capitanian crisis is thought to be indicated by a negative  $\delta^{13}C_{org}$  isotope excursion, a lithofacies change (i.e., the loss of carbonate beds), and a drop in species richness (Grasby and Beauchamp, 2009; Beauchamp and Grasby, 2012; Bond et al., 2015). In addition, these changes have been correlated to similar changes in the Sverdrup Basin, Arctic Canada (Bond

et al., 2020). These changes are also associated with redox proxies (pyrite framboids, Th/U and V/Al), suggesting the development of anoxic conditions, and the loss of carbonates from the Kapp Starostin Formation was interpreted to be the 5 consequence of ocean acidification, leading to a sustained interval of a shallow lysocline and calcite compensation depth (CCD) (Beauchamp and Grasby, 2012; Grasby et al., 2015a), making this transition consistent with other hyperthermal events. The timing of these changes is also consistent with 10 the changes observed at tropical paleolatitudes (Sun et al., 2012; Wignall et al., 2012 (S10), suggesting that the Capitanian crisis was a global event. However, the interpretation that the Capitanian crisis is recorded in the Kapp Starostin Formation is disputed, owing to the lack of biostratigraphi-15 cal data confirming the rocks are of Capitanian age (Shen et al., 2005 Lee et al., 2022). A reanalysis of the same sections using brachiopod data suggested that this event is not the Capitanian crisis but instead a faunal turnover that occurred during the Kungurian (Lee et al., 2022), where shoal-20 ing of the lysocline and CCD is also observed in the Sverdrup basin (Beauchamp and Grasby, 2012). Moreover, based on the "lysocline-ocean acidification" model, the development of shallow lysocline and calcite compensation depth is interpreted to have persisted for millions of years (Beauchamp 25 and Grasby, 2012), although the large carbonate buffering capacity of ocean water suggests that ocean acidification is unlikely to persist for such long intervals of time (Hönisch et al., 2012; Cui et al., 2015). It, therefore, remains equivocal as to whether the Kapp Starostin Formation records the 30 Capitanian Crisis.

 Mesozoic (Triassic, Jurassic, Cretaceous, 252.2–66 Ma)

#### 4.3.1 The Permian-Triassic transition

The End-Permian Mass Extinction Event (EPME) at ca. 35 252 Ma (Burgess et al., 2014) was the most catastrophic extinction event of the Phanerozoic, which decimated 75 % of terrestrial species (Hochuli et al., 2010) and 81 % of marine species (Stanley, 2016). This extinction is associated with a marked and continuous global negative carbon isotope ex-40 cursion (CIE; Korte and Kozur, 2010), along with an oxygen isotope anomaly (e.g., Sun et al., 2012). The cause(s) of the EPME is debated; both a bolide impact and the emplacement and eruptions of the Siberian Traps LIP are implicated as causal mechanisms (Svensen et al., 2009, 2018; Grasby et 45 al., 2011; Sanei et al., 2012; Ogden and Sleep, 2012; Ivanov et al., 2013; Burgess and Bowring, 2015; Sanson Barrera, 2016; Wu et al., 2021). Even though the intrusive and extrusive character of the Siberian Traps LIP is generally accepted as the extinction trigger that led to the cascading en-50 vironmental changes, it is not fully understood which environmental changes led to the collapse of terrestrial and marine ecosystems (e.g., Hochuli et al., 2010; Korte and Kozur, 2010; Black et al., 2014; Grasby et al., 2015b; Joachimski et al., 2020; Scotese et al., 2021; Wu et al., 2021; Galloway and Lindström, 2023a).

In Svalbard, the mass extinction event is expressed differently compared to equatorial Tethyan carbonate successions. In west and central Spitsbergen, the pre-extinction interval belongs to the uppermost part of the Kapp Starostin Formation, which is usually devoid of any skeletal fossil 60 material (Fig. 9; Bond et al., 2015; Grasby et al., 2015a; Lee et al., 2022). The only exception is the poorly preserved lingulid brachiopod species documented (e.g., Gobbet, 1963 and rare impressions of large brachiopods, bryozoans, and bivalves so far, making it virtually impossible to robustly reconstruct diversity dynamics during this important interval (Uchman et al., 2016; Foster et al., 2022). The Permian Kapp Starostin Formation is, therefore, poorly age-constrained, and no index fossils of Changhsingian (preextinction) age have yet been identified. Based on sedimentological evidence as well as on the nature of the sharp negative  $\delta^{13}C_{org}$  excursion, the upper part of the Kapp Starostin and the overlying Triassic Sassendalen Group (separated in the Vardebukta Formation in the west and Vikinghødga Formation in the east) have been interpreted to represent continuous deposition across the Permian-Triassic boundary (Wignall et al., 1998; Schobben et al., 2020; Zuchuat et al., 2020). This transition is also associated with the abrupt disappearance of cemented, highly bioturbated, spiculite- and chert-bearing mudstones and sandstones, conformably overlain by easily 80 weathered, usually laminated, scarcely bioturbated, silicapoor mudstones (e.g., Mørk et al., 1993, 1999a, b; Uchman et al., 2016; Rodríguez-Tovar et al., 2021). The EPME has, therefore, been interpreted as a progressive phase of extinction starting at the base of the Vardebukta Formation in west 85 Spitsbergen (Wignall et al., 1998; Grasby et al., 2015a) and a horizon ~ 1.6 m into the Vikinghøgda Formation in central Spitsbergen (Mørk et al., 1999b; Nabbefeld et al., 2010). Grasby et al. (2015b), based on mercury anomalies and shifts in carbon isotopes, interpret EPME as a progressive extinction event indicating prolonged volcanic activity and environmental stress preceding the extinction event.

The post-extinction sediments, which in Svalbard are assigned to the Lower Triassic Vardebukta and Vikinghøgda formations, yield a scarce and low-diversity ichnoassemblage (Wignall et al., 1998; Uchman et al., 2016; Rodríguez-Tovar et al., 2021), as well as abundant macrofossils, including key Triassic index fossils (ammonoids and conodonts), which have been useful in inferring the timing of the extinction and the recovery. From the base of both formations, a diverse assemblage of ammonoids have been recorded including *Otoceras boreale*, *Glyptophiceras nielseni*, *Ophiceras spathi*, *O*. cf. *compressum*, *O*. cf. *kochi*, *O*. cf. *poulseni*, *Paravishnuites paradigma*, and *P. oxynotus* (Mørk et al., 1999b), which occur ca. 6 m above the base of the Vikinghøgda Formation (Nakrem et al., 2008) and 2.5 m into the Vardebukta Formation (Alistair McGowan, per-

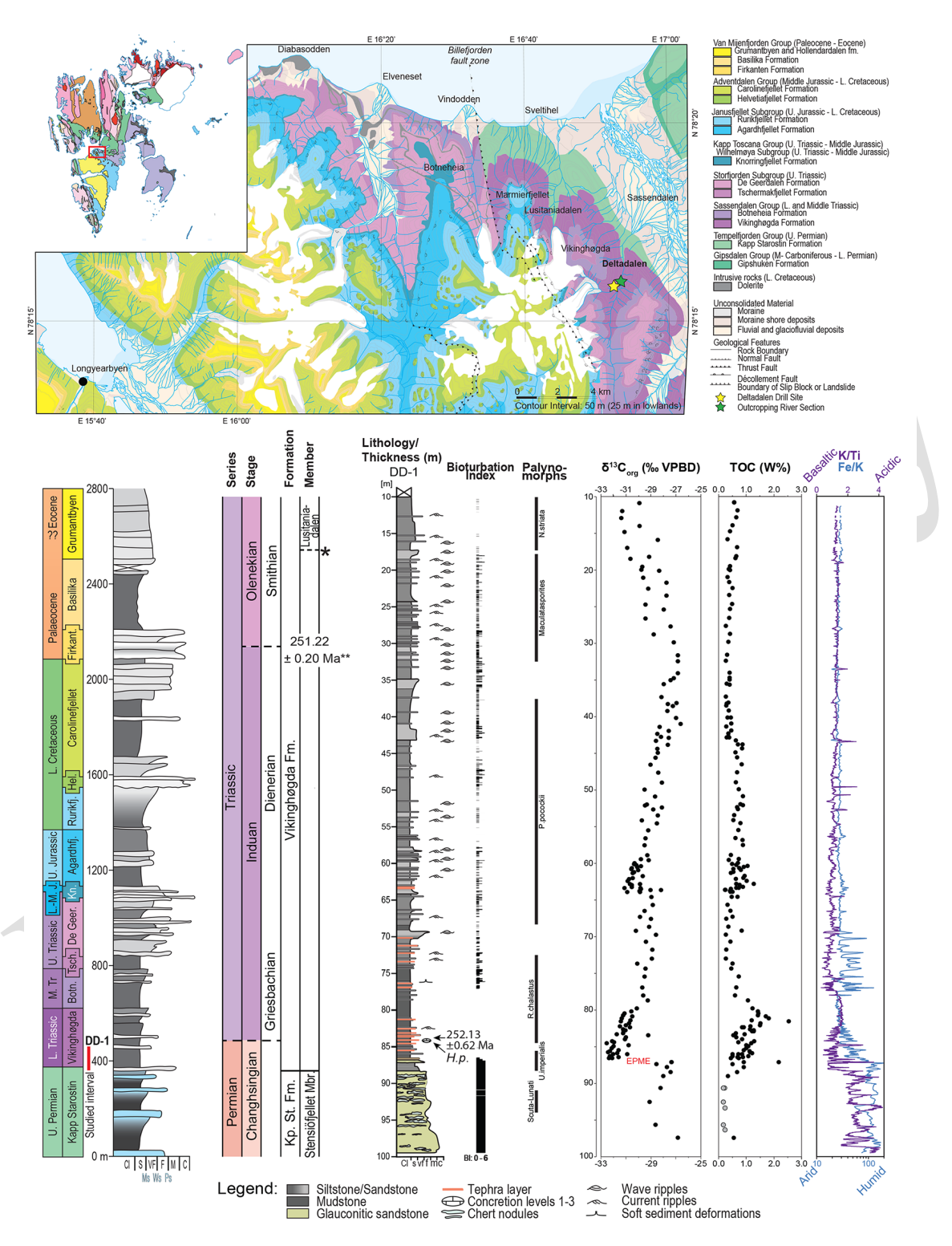


**Figure 9.** Top: geological map of central Spitsbergen highlighting the drill site (yellow star) and the adjacent Deltadalen river section (green star; geological map adapted from Major et al., 1992). Overview of the sedimentary section illustrating the lithostratigraphic formations in central Spitsbergen after Dallmann et al. (1999), Mørk et al. (1999b), Midtkandal et al. (2008), Nagy and Berge (2008), Dypvik et al. (2011), Blomeier et al. (2013), Lord et al. (2014 ISIA), Koevoets et al. (2016), and Smelror and Larssen (2016 ISIA). Bottom: the Permian–Triassic boundary as it appears in the Deltadalen DD-1 drill core. Modified after Zuchuat et al. (2020). EMPE – End-Permian Mass Extinction Event; Kp. St. Fm. – Kapp Starostin Formation; Mbr. – member; Fm – formation; H.p – *Hindeodus parvus*; \* – member boundary after Mørk et al. (1999b); \*\* Induan–Olenekian boundary age after Burgess et al. (2014).

sonal communication, November 2015). Mørk et al. (1999b), Nakrem et al. (2008), and Zuchuat et al. (2020) also described conodonts from the base of the Vikinghøgda Formation, which suggests that the interpreted extinction horizon 5 in Svalbard is time-equivalent with the onset of the mass extinction at the Global Stratotype Section and Point (GSSP) in Meishan, China, and the Permian-Triassic boundary occurs 4.1 m into the Vikinghøgda Formation. This record is similar to other high-latitude clastic Permian-Triassic successions in 10 Jameson Land, Greenland (Twitchett et al., 2001); the Sverdrup Basin in Canada (Henderson and Baud, 1997); and the South Verkhoyansk region, Russia (Biakov et al., 2016). Furthermore, in South Verkhoyansk, the Changhsingian sandstones record bivalve communities with large Intomodesma 15 species that suddenly go extinct at the base of the Otoceras concavum ammonoid zone (Biakov et al., 2016), coincident with the change in bioturbation record in Svalbard (Uchman et al., 2016; Rodríguez-Tovar et al., 2021).

Numerous geochemical and sedimentological studies have 20 investigated the environmental changes recorded in Svalbard associated with the EPME. The negative  $\delta^{13}C_{org}$  and  $\delta^{13}C_{carb}$ isotope excursions, which occur just prior to the Permian-Triassic boundary, reflect a rapid influx of isotopically light carbon into the atmosphere, while the influx of heavy met-25 als and the presence of abundant tephra layers, including one just above the first appearance datum (FAD) of Hindeodus parvus and dated at  $252.13 \pm 0.62 \,\mathrm{Ma}$  (Fig. 9; Zuchuat et al., 2020), are in good agreement with the tephra beds from the Induan GSSP section in Meishan (Burgess et al., 2014) 30 that have been inferred to link the Siberian Traps LIP and the mass extinction in Svalbard (Gruszczynski et al., 1989; Grasby et al., 2015b; Zuchuat et al., 2020). The reduced iron (Fe) / potassium (K) elemental ratio that accompanied the extinction horizon in the Vikinghøgda Formation seems 35 to suggest that the tropical atmospheric circulation (Hadley Cell) could have expanded towards the poles, associated with an increased aridity in the hinterland of the basin (Zuchuat et al., 2020) developed within overall and mega-monsoonal Triassic climate (e.g., Hu et al., 2023). Redox proxies, including 40 lipid biomarkers (Summons et al., 2022), Fe and P speciation (Schobben et al., 2020), trace-metal data (Grasby et al., 2015b; Uchman et al., 2016; Wignall et al., 2016; Zuchuat et al., 2020), and pyrite framboid sizes (Dustira et al., 2013; Wignall et al., 2016), also suggest that the mass extinction 45 is associated with the expansion of oxygen minimum zones in the ocean, bringing anoxic and euxinic conditions into shallow-marine settings, as well as subsequent pulses of redox changes throughout the Early Triassic (Rodríguez-Tovar et al., 2021). Isotopic signatures of lipid biomarkers suggest 50 frequent phytoplankton blooms, and phosphorus speciation data indicate an increase in nutrient supply and the remobilization of biologically available P as a consequence of the mass-extinction event initiating feedback that further developed anoxic conditions (Nabbefeld et al., 2010; Schobben et

55 al., 2020).

Thermal stress and ocean acidification are also widely considered as key factors in the EPME, with global average temperature increases reaching 7 °C (Kidder and Worsley, 2004; Svensen et al., 2009; Sun et al., 2012; Stordal et al., 2017; Burger et al., 2019), potentially as much as 9–12 °C 60 (Joachimski et al., 2012, 2020; Schobben et al., 2014; Chen et al., 2016). In Svalbard, there are currently no published geochemical investigations of the environmental changes associated with this hyperthermal event, but the presence of warm-water taxa such as red algae (Wignall et al., 1998), the conodont genus Clarkina (Nakrem et al., 2008), and both ostracod and radiolarian species that were equatorial during the Changhsingian (Foster et al., 2023) suggests that higher paleolatitudinal settings were unusually warm following the mass extinction. The cessation of carbonate rocks combined with 70 the loss of carbonate secreting taxa near the top of the Kapp Starostin and across the Boreal Realm also provided an alternative hypothesis that ocean acidification developed and persisted for an unexpected long duration in the Late Permian (Beauchamp and Grasby, 2012; Grasby et al., 2015a). This 75 hypothesis, however, requires the persistence of undersaturated conditions for millions of years, which is inconsistent with some Earth system models that suggest that ocean acidification events cannot persist for this length of time (e.g., Hönisch et al., 2012). In addition, the lack of dissolution and 80 repair marks on well-preserved mollusks from the extinction aftermath have also been interpreted to suggest that ocean acidification was not severe enough to have impacted skeletal calcification in the Boreal realm, at least at the onset of the Triassic (Foster et al., 2022). Furthermore, based on a metaanalysis of modern calcifying organisms, Leung et al. (2022) suggested that ocean acidification alone may not be a major driver of biodiversity loss as previously thought, with multiple other factors affecting the vulnerability of marine organisms to ocean acidification. More research is, therefore, 90 required to understand the role of thermal stress and ocean acidification in high-latitude marine extinctions.

The impact of the EMPE on terrestrial ecosystems can also be investigated from Svalbard's marine successions. The Permian to Triassic palynological record of Svalbard 95 and the Barents Shelf has been intensely investigated (e.g., Mangerud and Konieczny, 1993), in part due to their utility for petroleum exploration (e.g., Vigran et al., 2014). A spore spike demise of gymnosperms, malformed spores and pollen, a drop in abundance of acritarchs, and compound 100 specific isotopes of algal and land-plant-derived biomarkers all coincide with the mass extinction event, suggesting nearsynchroneity between effects in marine and terrestrial realms (Stemmerik et al., 2001; Nabbefeld et al., 2010; Uchman et al., 2016). The presence of Permian plant taxa, including ma- 105 jor Paleozoic plant groups in the Lower Triassic successions of Svalbard and the Barents Shelf, however, has led to some authors interpreting that the EMPE only had a minor impact on plant communities (Hochuli et al., 2010; Vigran et al., 2014). Aberrant pollen and spores reported from the Barents 110 Sea and elsewhere have been suggested to be a consequence of severe atmospheric pollution and increased UVA-B radiation due to emissions from emplacement of the Siberian Traps (Black et al., 2014; Hochuli et al., 2017; Galloway and 5 Lindström, 2023a, and references therein).

#### 4.3.2 Early Triassic ecosystem recovery

The post-EPME survival and recovery of marine organisms recorded from Svalbard and the Boreal realm was relatively fast compared to equatorial locations (Twitchett and Barras, 10 2004). Within the early Griesbachian H. parvus conodont zone in central Spitsbergen (Lusitaniadalen and Deltadalen), a diverse assemblage of macro and microfossils have been recorded, including the only documented silicified marine assemblage of the Early Triassic (Foster et al., 2017b), the 15 oldest record of post-extinction silica-excreting organisms globally (radiolarians and siliceous sponges; Foster et al., 2023), and the presence of an ecological complex assemblage of trace fossils (Nabbefeld et al., 2010; Rodríguez-Tovar et al., 2021). In addition, across Svalbard, the Lower 20 Triassic succession preserved many groups, including bryozoans (Nakrem and Mørk, 1991), algae (Wignall et al., 1998), conodonts (Nakrem et al., 2008), bivalves and gastropods (Buchan et al., 1965; Tozer and Parker, 1968; Foster, 2015; Foster et al., 2017b), ammonoids (see Nakrem et 25 al., 2008), ostracods (Olempska and Błaszyk, 1996), echinoderms (Salamon et al., 2015), and trace fossils (Wignall et al., 1998). Whilst sedimentation-rate calculations suggest marine ecosystems only required ca. 150 kyr to recover from the mass extinction (Rodríguez-Tovar et al., 2021), based on 30 index conodonts, there is a distinctive pulse of environmental and ecological recovery in the Dienerian (Hatleberg and Clark, 1984; Wignall et al., 1998; Mørk and Worsley, 2006; Salamon et al., 2015).

The Lower Triassic succession of Svalbard is also fun-35 damental for understanding the evolution and radiation of marine vertebrates following the Permian-Triassic transition. The Triassic succession of Svalbard has long been well known for four described vertebrate fossil horizons (in stratigraphic order): the Fish Niveau, Grippia Niveau, Lower 40 Saurian Niveau, and Upper Saurian Niveau (Wiman, 1910, 1928). These bone beds correspond to the Lusitaniadalen (the Fish Niveau) and Vendomdalen (the Grippa and Lower Saurian Niveau) members of the Vikinghøgda Formation that span the Smithian-Spathian transition (Lower Triassic; ca. 45 249.2 Ma), and the Ladinian-age (Middle Triassic; ca. 242– 237 Ma) Blanknuten Member of the Botneheia Formation (the Upper Saurian Niveau; Maxwell and Kear, 2013; Hurum et al., 2018). Recent work on Early and Middle Triassic ecosystems in Svalbard reveals an exceptionally rapid diver-50 sification among marine vertebrates andichthyosaurs likely evolved prior to the EPME (Kear et al., 2023). The bone beds reveal a much more complex food web than previously thought (Hurum et al., 2014, 2018; Bratvold, 2016; Delsett et al., 2017; Ekeheien et al., 2018; Engelschiøn et al., 2018; Økland et al., 2018; Roberts et al., 2022; Kear et al., 2023), suggesting that the Boreal Sea served as a climatic refuge after the EPME (Kear et al., 2023; Foster et al., 2023).

It has been hypothesized that the recovery from the EPME was delayed due to subsequent crises throughout the Early Triassic (Payne et al., 2004; Ware et al., 2011; Song et al., 60 2012; Foster et al., 2017b; Zuchuat et al., 2020; Wu et al., 2021), despite the degree of ichnofacies diversity and intensity reached pre-extinction level in ca. 150 Kyr (Rodríguez-Tovar et al., 2021). The first crisis occurring after the EPME is the "late Dienerian biotic crisis" (late Early Triassic; ca. 65 251 Ma), which is recognized by a negative CIE in the Vikinghøgda Formation in Deltadalen, central Spitsbergen, where it is sandwiched between two thin tephra layers. This benthic crisis was associated with dysoxic conditions in the water column and the seafloor (Zuchuat et al., 2020) and was first documented from the Tethyan with the Werfen Formation, northern Italy (Hofmann et al., 2015; Foster et al., 2017a), as well as from subtropical latitudes along the Panthalassic margin (Ware et al., 2011; Hofmann et al., 2011, 2014). The palynological record from Greenland suggests 75 that this CIE coincides with a more significant turnover in plant communities than at the End-Permian Mass Extinction (Hochuli et al., 2017). This indicates that the late Dienerian Crisis might have been of global significance. The presence of the two tephra horizons directly above and below the neg- 80 ative CIE of the late Dienerian biotic crisis suggests a volcanic trigger for the event, but the exact nature of this potential biotic crisis in Svalbard and globally requires additional research.

The most prevalent of the biotic crises in the Triassic is 85 the Smithian-Spathian transition, which is associated with a negative CIE greater than at the EPME (Payne et al., 2004; Grasby et al., 2013, 2016b) followed by prominent positive C isotope excursion (e.g., Galfetti et al., 2007). In Svalbard, the Smithian-Spathian transition is recorded as a regression 90 and subsequent transgression, with numerous fossiliferous horizons (e.g., Hoel and Orvin, 1937; Buchan et al., 1965; Tozer, 1967; Weitschat and Lehmann, 1978 [1515]; Mørk et al., 1999b; Foster, 2015; Hammer et al., 2019; Hansen et al., 2024; Leu et al., 2024). While the Smithian-Spathian 95 transition has received considerably less attention than the Permian-Triassic transition, recent research has highlighted the multi-factor nature of this event on the dynamic of the C and P cycles in the Arctic (Hammer et al., 2019; Blattmann et al., 2024). Nevertheless, many outstanding questions remain 100 unanswered, both globally and on Svalbard:

- What was the timing of the event?
- What caused the CIE?
- What environmental changes are associated with the CIE?

- How were terrestrial and marine ecosystems impacted by the event?

At the Festningen section, Hg concentrations and Hg/TOC both show a noticeable spike in the Tvillingodden 5 Formation of the Sassendalen Group, which have been associated with Hg loading associated with increased activity from the Siberian Traps (Grasby et al., 2016b). This peak has also been correlated with Hg loading recorded at the Smithian-Spathian boundary at Smith Creek, Arctic Canada, 10 even though the Smithian-Spathian boundary is associated with a carbon isotope peak at most sections globally. In the equivalent Vikinghøgda Formation at the Wallenbergfjellet section, however, the Smithian–Spathian boundary (the top of the Wasatchites tardus ammonoid zone) is associated 15 with a positive CIE (Galfetti et al., 2007; Hammer et al., 2019), and the Hg loading occurred prior to the Smithian— Spathian boundary in the middle to late Smithian (Hammer et al., 2019). This is consistent with the Festningen section, which suggests the Hg loading occurred synchronously dur-20 ing the Smithian (Grasby et al., 2016a). At the Kongressfjellet and Vikinghøgda sections, just above the base of the Vendomdalen Member of the Vikinghøgda Formation, a significant shift in the palynological record is recorded (Mørk et al., 1999b; Galfetti et al., 2007). This Smithian-Spathian 25 turnover is also recorded in the shallow cores drilled at the Svalis Dome, central Barents Sea (Hochuli and Vigran, 2010 TS16). This turnover in the palynological record has been associated with the re-establishment of diverse woody gymnosperm ecosystems, marking a recovery signal from 30 both the Permian-Triassic climate crisis and a "late Smithian Thermal Maximum". This is supported by the synchronous recovery in the latitudinal diversity gradient of ammonoids (Brayard et al., 2009 1817) and the recovery of equatorial benthic marine communities (Twitchett and Wignall, 1996 TS18; 35 Chen et al., 2011; Pietsch and Bottjer, 2014; Hofmann et al., 2014, 2015; Foster et al., 2015, 2017a, 2018, 2023a). The Smithian-Spathian transition, therefore, appears to be marked by a late Smithian Thermal Maximum and a subsequent Smithian-Spathian boundary cooling and associated 40 biotic recovery in Svalbard and pan-Arctic.

# 4.3.3 Middle to Late Triassic: organic-rich mudstones rich in phosphate

The Middle Triassic succession is dominated by organic-rich mudstone to siltstones of the Anisian–Ladinian (Mid<sup>45</sup> dle Triassic; ca. 247–237 Ma) Botneheia and Brevaisberget formations of the upper Sassendalen Group (Mørk and Bjorøy, 1984; Krajewski, 2008, 2013; Grasby et al., 2015b, 2020; Wesenlund et al., 2021; Knies et al., 2022). The upper Blanknuten Member of the Botneheia Formation (Ladinian) reaches 12 wt % TOC, and certain stratigraphic intervals, particularly in the underlying Muen Member (Anisian), contain abundant phosphorite nodules (e.g., Krajewski, 2013; We-

senlund et al., 2021, 2022; Engelschiøn et al., 2023). In the Anisian, nutrient saturated runoff from continental areas, particularly associated with the approaching delta system from 55 the southeast (see next section), coupled with upwelling of nutrient-rich waters from the Panthalassic Ocean, resulted in extensive algal blooms and the formation of oxygen minimum zones, which promoted dysoxia and anoxia and preservation of organic matter and precipitation of phosphate (Kra- 60 jewski, 2013; Vigran et al., 2014; Wesenlund et al., 2022; Engelschiøn et al., 2023). Repeated transgression-regression events, influenced by the emerging delta system, likely contributed to fossil-preservation potential of the Middle Triassic strata as the relatively shallow offshore environment was 65 temporarily punctuated by anoxic events (Mørk et al., 1989; Krajewski, 2013; Engelschiøn et al., 2023). Fossil preservation has also occurred by complete barium sulfate (barite) pseudomorphing, possibly by sulfate remobilization from the organic-rich shales (Engelschiøn et al., 2023). Moreover, the 70 high TOC values in the Ladinian Blanknuten Member suggest deposition under euxinic conditions, possibly governed by restricted water circulation due to shallowing of the basin, as well as water-mass stratification caused by the increasing influx of riverine waters into the marine basin (Wesenlund et 75 al., 2022).

### 4.3.4 Late Triassic: the Carnian Pluvial Episode and the world's largest delta plain

The Carnian Pluvial Episode spanning the Julian 2 and Tuvalian 1 substages of the Carnian (CPE, ca. 233 Ma) marks a period of worldwide documented increased rainfall and associated biotic changes that occurred within an overall global monsoonal system dominating the Triassic climate of Pangea (Simms and Ruffell, 1989; Breda et al., 2009; Preto et al., 2010; Dal Corso et al., 2018; Hu et al., 2023). The CPE was 85 first recognized as concomitant to global carbonate platform environment perturbations, associated with an increased terrigenous input into sedimentary basins (Dal Corso et al., 2018) and the rapid diversification of dinosaurs (Benton et al., 2018). The CPE is also associated with several isotope 90 perturbations in terrestrial and marine C and Hg records, which potentially reflects multiple pulses of volcanic activity of the Wrangellia LIP (Dal Corso et al., 2018; Jin et al., 2023). Analyses of palynological assemblages, chemical weathering indices,  $\delta^{18}$ O apatite records, and redoxsensitive elements suggest that the CPE was characterized by an extremely humid climate (e.g., Roghi, 2004; Baranyi et al., 2019), warm temperatures (Rigo and Joachimski, 2010; Rigo et al., 2012 Sup et al., 2016), and widespread marine dysoxia and anoxia (Soua, 2014; Sun et al., 2016; 100 Tomimatsu et al., 2022). Shallow-water carbonate production switched as a result of climatic variations and eustatic sea-level fall (Jin et al., 2020), which impacted both the marine and the continental biosphere, with high extinction rates in ammonoids and conodonts (Rigo et al., 2007; Dal Corso et 105

al., 2022); rapid extinction of terrestrial tetrapods; and a subsequent diversification of dinosaurs (Bernardi et al., 2018), mammals (Benton et al., 2018), scleractinian corals (Stanley, 2003), calcareous dinoflagellates, and plants (e.g., Dal Corso et al., 2022).

While the CPE is well documented in the Tethyan Realm (Dal Corso et al., 2018), evidence from the Boreal Realm remains limited. In Svalbard, preliminary palynological evidence from the Kapp Toscana Group in central Spitsber-10 gen integrated with organic carbon isotope and paleomagnetic constraints indicates warming during the late Julian-1 (Mueller et al., 2016; Paterson et al., 2016) and suggest wetter conditions starting from the Julian-2, which occurs in the lower part of the De Geerdalen Formation (Mueller et al., <sub>15</sub> 2016). In addition, the detailed study of paleosols in the De Geerdalen Formation above the CPE seems to indicate the transition from humid (coal) to warm arid (caliche) climate settings (Lord et al., 2017, 2022), which might be caused by oscillations within the Triassic mega-monsoonal system 20 (e.g., Preto et al., 2010). Nevertheless, the precise location of the CPE in Svalbard's stratigraphy remains uncertain, and increased research can help understand the exact triggering mechanism of these climate perturbations.

# 4.3.5 Jurassic-Cretaceous: a greenhouse with cold snaps

The Jurassic and Cretaceous saw some of the warmest back-

ground global temperatures of the Phanerozoic (Jenkyns et al., 2012) and collapse of the mega-monsoonal climate prevailing in the Triassic (Sellwood and Valdes, 2008). Per-30 manent polar ice caps were not present, although evidence for episodic cooling and the growth and decay of small, ephemeral polar ice caps has been presented (e.g., Price, 1999; Miller et al., 2005; Grasby et al., 2017b; Alley et al., 2020) accompanied by rafting ice (Frakes and Francis, 1988). Oxygen isotope records of Jurassic and Early Cretaceous from Svalbard have been derived largely from belemnites (e.g., Ditchfield, 1997; Price and Nunn, 2010; Hammer et al., 2011), and an extensive dataset has been derived from Kong Karls Land (Ditchfield, 1997). The usefulness of 40 these data, however, is hampered by low-resolution biostratigraphic age constraints and pervasive diagenesis. Nonetheless, some well-preserved belemnites were identified, and oxygen isotope data from Hammer et al. (2011) from the upper Agardhfjellet Formation (Volgian-Ryzanian, which ap-45 proximately correlates with late Tithonian to early Berriasian, Late Jurassic-Early Cretaceous; ca. 149-140 Ma) and Price and Nunn (2010) from the Hauterivian (Early Cretaceous; ca. 133-126 Ma) part of the Rurikfjellet Formation of Festningen (see Jelby et al., 2020b for a discussion of the age constraints) show  $\delta^{18}$ O values ranging from -3.0% to 0.8% VPDB. The belemnite data from Kong Karls Land (spanning the Aalenian to Valanginian; Middle Jurassic to Early Cretaceous; ca. 175–132 Ma) give  $\delta^{18}$ O values of -0.7% to 1.2% VPDB. These data argue for cooling and warming episodes at these high paleolatitudes and may indicate high seasonality and/or high-frequency climatic variability, although the absolute temperatures they represent are hard to interpret. Common practice would be to assume that the seawater  $\delta^{18}$ O was -1% SMOW (i.e., that of an ice-free world) and use either the equation for molluscan 60 calcite (Anderson and Arthur, 1983) or experimentally derived synthetic calcite (Kim and O'Neil, 1997) to calculate the precipitation temperature of the calcite. However, Price and Nunn (2010) used the presence of glendonites in certain horizons to independently assess paleotemperature of those 65 intervals and back-calculated the  $\delta^{18}O_{sw}$ . This suggested that the seawater  $\delta^{18}$ O was much lower than the global average (i.e., heavily meteorically influenced), which is supported by the depositional setting (ranging from marine to terrestrial delta plain). Furthermore, recent work using clumped isotope thermometry on belemnites suggests that the equations of Kim and O'Neil (1997) or Anderson and Arthur (1983) are not suitable for belemnite calcite, and rather, the temperature equations of Kele et al. (2015) or Daëron et al. (2019) should be used (Price and Passey, 2013; Wierzbowski et al., 2018; 75 Bajnai et al., 2020; Price et al., 2020; Vickers et al., 2019b, 2020, 2021). Using the latter results in warmer estimated temperatures than previously thought, even if one assumes a meteorically influenced  $\delta^{18}O_{sw}$  of -2.5% SMOW. For example, the belemnite data from Kong Karls Land suggest 80 temperatures closer to 12–20 °C rather than the 8–13 °C originally postulated by Ditchfield (1997). The belemnites from Festningen may indicate a temperature range of around 13-30 °C rather than the 9–25 °C originally suggested by Price and Nunn (2010) and Hammer et al. (2011).

# Jurassic-Cretaceous boundary and the Volgian Isotopic Carbon Excursion (VOICE)

The global carbon isotope ( $\delta^{13}$ C) signal of the Upper Jurassic and Jurassic-Cretaceous (J-K, ca. 145 Ma) boundary as recognized in Tethyan, Atlantic, and Pacific sections is generally characterized by a steady decline. This decline has been attributed to progressive deceleration of the carbon cycle due to the development of more oligotrophic oceanic conditions and reduced marine primary production (Weissert and Channell, 1989; Weissert et al., 1998; Weissert and Erba, 2004; Tremolada et al., 2006; Price et al., 2016). In Svalbard, however, the upper Kimmeridgian-middle Volgian succession displays a prominent negative CIE termed the "Volgian Isotopic Carbon Excursion" or "VOICE" by Hammer et al. (2012). The VOICE is of much greater magnitude than the entirety of 100 the long-lived decline of the lower-latitude records (Fig. 11; Morgans-Bell et al., 2001; Price and Rogov, 2009; Žák et al., 2011; Hammer et al., 2012; Zakharov et al., 2014; Koevoets et al., 2016, 2018; Galloway et al., 2020; Jelby et al., 2020b). This recently recognized carbon isotope marker of Boreal 105 sections (observed across Svalbard, northern Siberia, Arctic Canada, the Russian Platform, and possibly the southern UK; Galloway et al., 2020; Jelby et al., 2020b, and references therein) and newly discovered occurrences in the Neuquén Basin of Argentina (Capelli et al., 2021; Weger et al., 2022) and possibly in the eastern Tethys (Fallatah et al., 2024) and western Tethys (Celestino et al., 2017) is characterized by a relatively abrupt negative excursion ( $\leq$  6.4% in Svalbard) in  $\delta^{13}C_{org}$  values. This excursion is followed by a positive trend in  $\delta^{13}C_{org}$  values through the upper Volgian–Ryzanian and across the J-K boundary (Price and Rogov, 2009; Hammer et al., 2012; Dzyuba et al., 2013; Zakharov et al., 2014; Koevoets et al., 2016; Galloway et al., 2020; Jelby et al., 2020b; Vickers et al., 2023).

In Svalbard, the VOICE is documented in both drill core 15 (DH-2, central Spitsbergen) and outcrop sections (e.g., Myklegardfjellet, eastern coast of Spitsbergen; Festningen, western Spitsbergen) and falls within the paper-shale-dominated Oppdalssåta and Slottsmøya members of the Agardhfjellet Formation (Koevoets et al., 2016, 2019; Jelby et al., 20 2020b; Vickers et al., 2023). The VOICE and positive recovery across the J-K boundary were originally considered unique to the Boreal realm, as a result of decoupling from the global carbon reservoir during the Late Jurassic. Galloway et al. (2020) and Jelby et al. (2020b) attributed this Boreally 25 limited CIE to restricted oceanographic connectivity between the shallow epeiric seas of the high northern latitudes and open oceans, associated with water-mass stratification and increased continental runoff (Park et al., 2024) due to an eustatic sea-level lowstand. As a result, basinal depletion of <sup>13</sup>C 30 resulted from oxidation of terrestrial organic matter, or input of isotopically light CO<sub>2</sub> by respiration of marine organisms, and/or riverine dissolved inorganic carbon (DIC) (Patterson and Walter, 1994; Holmden et al., 1998). However, the recent discovery of the VOICE in the Southern Hemisphere (Ro-35 driguez Blanco et al., 2022; Capelli et al., 2022 Weger et al., 2022), albeit with diachroneity seen also in the Arctic (e.g., Rogov, 2021; Rogov et al., 2023), which may reflect poor age control or a latitudinal climate gradient, indicates that the excursion is not limited to high northern latitudes. 40 Weger et al. (2022) suggested that the VOICE was driven by changes in the input of terrestrially derived organic matter, controlled by relative sea-level change and climate, although this hypothesis is refuted by Fallatah et al. (2024) and Galloway et al. (2024) because the VOICE may be present in a 45 restricted setting in the Tethys (Fallatah et al., 2024) and because there is a lack of consistent changes in organic matter type (as indicted by OI and HI) and indices of weather and grain size across the VOICE in the Sverdrup and Barents Sea basin material (Galloway et al., 2024).

<sup>50</sup> Collectively, the VOICE is ascribed variously to restricted circulation (Galloway et al., 2020; Jelby et al., 2020b; Śliwińska, et al., 2020; Fallatah et al., 2024), precipitation of authigenic carbonate in reducing conditions (Dalseg et al., 2016; Rodriguez Blanco et al., 2022), or variations in <sup>55</sup> the input of terrestrially derived organic matter that is in

turn a manifestation of relative sea-level change and climate (Capelli et al., 2021; Weger et al., 2022). However, none of these models alone can explain the contemporaneous enrichment of Ag in Arctic basins (Galloway et al., 2024), and alternatives must be considered. An interval of silver (Ag) 60 enrichment occurs across the VOICE in the Sverdrup Basin (Canadian Arctic, 3–6 times higher than average shale) and at Festningen (6 times higher than average shale). Silver is similarly enriched in black shales of Jurassic and Cretaceous age in the Barents Sea, Norwegian Shelf, and West Siberia Basin (Lipinski et al., 2003; Zanin et al., 2016). The relationship of Ag to organic matter, S, Fe, and redox-sensitive trace elements in the strata from Canada and Festningen suggests that an extra-basinal source of Ag to seawater during the Volgian existed and that the source was enhanced hy- 70 drothermal flux in the proto-Amerasia basin during rift climax, with sufficient circulation to transport high-Ag seawater to surrounding shelves (Svalbard) and within and to extensional basins (Sverdrup Basin). Europium (Eu) values show an anomaly (Eu/Eu\* > 1) during the VOICE in both 75 the Canadian strata and the strata at Festningen, suggesting the presence of hydrothermal fluids. It is possible that the negative carbon isotopic signature of the VOICE is, in part, associated with the putative hydrothermal systems hypothesized to have caused Ag enrichment. Nearly all negative carbon isotope excursions in the geological record, but so far not the VOICE, are interpreted to reflect episodes of massive carbon release. Its global manifestation could therefore be the result of widespread rifting and outgassing of large quantities of CO<sub>2</sub> (see Brune et al., 2017) associated with the breakup of Pangea (Galloway et al., 2024).

#### Valanginian Weissert Event

The Weissert Event is a prominent global carbon cycle perturbation which occurred in the Early Cretaceous (ca. 133 Ma). It is expressed in carbon isotope records (Lini et al., 1992; Price et al., 2016) and is manifested in Arctic Canada (Galloway et al., 2020) and Svalbard (Jelby et al., 2020b; Vickers et al., 2023) (Fig. 11). The isotope event consists of a globally recognized positive CIE of a significant magnitude (2%o-5%o), which is widely documented 95 in marine carbonates, fossil shell material, terrestrial plants, and organic matter (e.g., Lini et al., 1992; Gröcke et al., 2005; Aguirre-Urreta et al., 2008; Price et al., 2016; Galloway et al., 2020; Jelby et al., 2020b; Vickers et al., 2023; Fallatah et al., 2024). Regional to global climate cooling in 100 the Valanginian (Early Cretaceous; ca. 140-133 Ma) is well documented (e.g., Pucéat et al., 2003; Weissert and Erba, 2004; McArthur et al., 2007; Bodin et al., 2015; Meissner et al., 2015; Grasby et al., 2017b), although the timing, magnitude, and extent of this cooling are debated (e.g., van de 105 Schootbrugge et al., 2000; McArthur et al., 2007), as is the mechanism for the CIE. Paleoclimatic reconstructions using biomarkers indicate a ~3 °C global surface cooling across

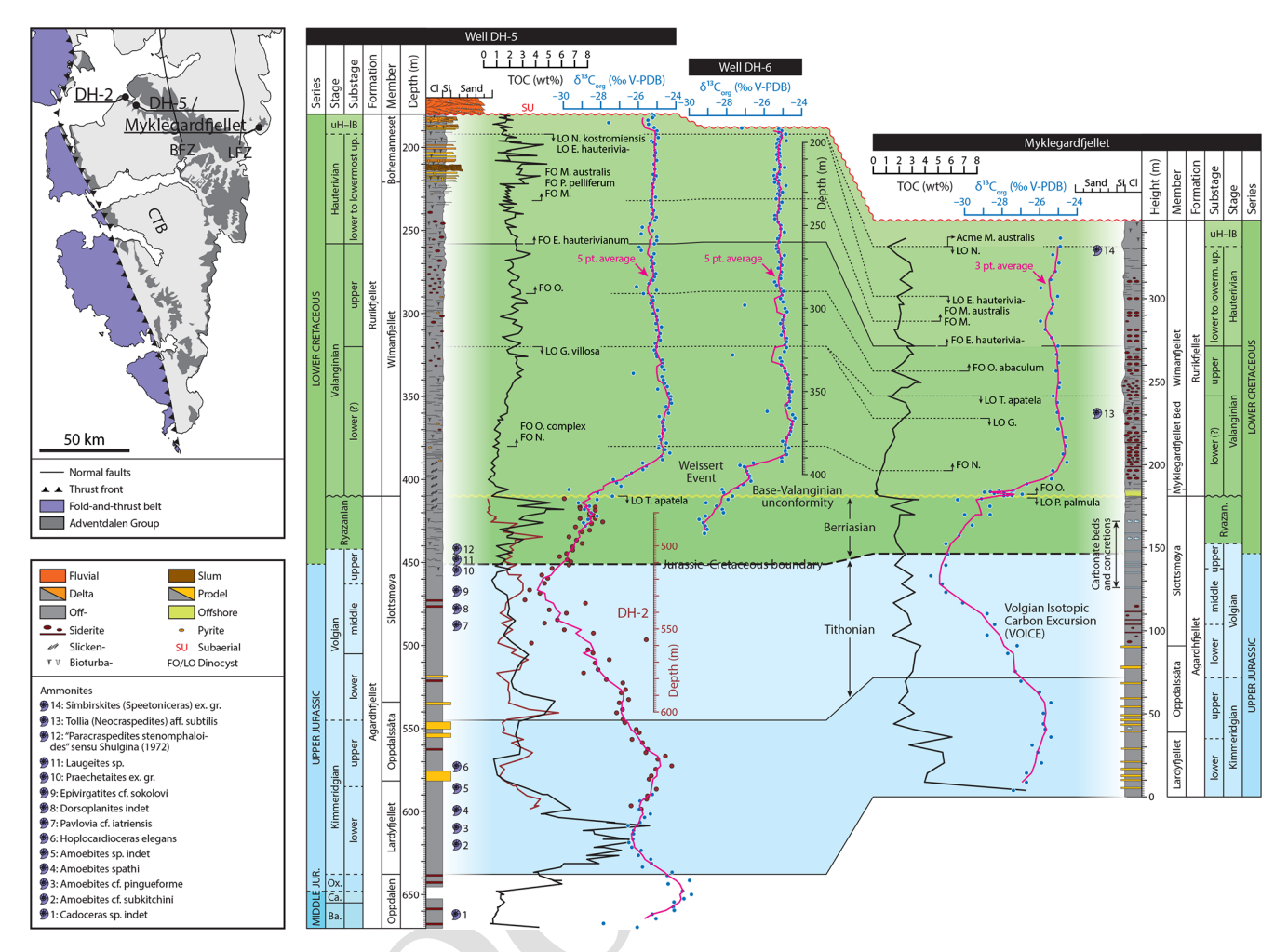


Figure 10. Correlation of organic stable carbon isotope ( $\delta^{13}C_{org}$ ) stratigraphy between the cored wells DH-2, DH-5, and DH-6 and the Myklegardfjellet outcrop section, calibrated by total organic carbon (TOC) trends, and dinocyst and ammonite biostratigraphy (compiled and modified from Jelby et al. 2020b, 2025, and Koevoets et al., 2016, 2018). The boundary between the Agardhfjellet and Rurikfjellet formations (conforming to a base-Valanginian unconformity and demarcated by a marked drop in TOC values) is used as a correlation datum. Note the clear expression of the Weissert Event and "Volgian Isotopic Carbon Excursion" (VOICE) in the different sections. uH-IB, upper Hauterivian-lower Barremian. For details on the dinocyst bio-events, the reader is referred to Jelby et al. (2020b, 2025) and Śliwińska et al. (2020).

the event (Cavalheiro et al., 2021), and glacial deposits from the Eromanga Basin (Australia) suggest the transient development of a small southern polar ice cap (Alley et al., 2020), whereas stable oxygen isotope records show mixed signals,  $_{5}$  with rising  $\delta^{18}O_{belemnite}$  values suggesting cooling in the Boreal Realm from the late Valanginian to early Hauterivian (Podlaha et al., 1998; McArthur et al., 2004; Price and Mutterlose, 2004; Bodin et al., 2015; Meissner et al., 2015), with little change in Tethyan records (e.g., van de Schootbrugge 10 et al., 2000; McArthur et al., 2007).

In the Arctic (including Svalbard), the widespread occurrence of glendonites around the Weissert Event interval (from the Berriasian to Hauterivian; Grasby et al., 2017b; Vickers et al., 2019a; Galloway et al., 2020; Jelby et al., 2025) has 15 led to speculation of the cooling being decoupled from the CIE (e.g., Rogov et al., 2017), although this may partially be an artifact of age uncertainties for the Arctic successions (e.g., Vickers et al., 2019a; Jelby et al., 2020b, 2025). It may also suggest that episodic cooling punctuated the background warmth throughout the Early Cretaceous. The emplacement 20 of the Paraná-Etendeka LIP is broadly coincident with the Weissert Event CIE (Fig. 11), although uncertainties surrounding the exact relative timings have led to much debate around the causal mechanism for the event (e.g., Weissert et al., 1998; Weissert and Erba, 2004; Duchamp-Alphonse 25 et al., 2007; Dodd et al., 2015; Rocha et al., 2020; Gomes and Vasconcelos, 2021). Recently, it has been shown that the peak of Paraná-Etendeka activity coincided with the onset of the Weissert Event (Martinez et al., 2023), supporting a volcanic trigger for this CIE.

30

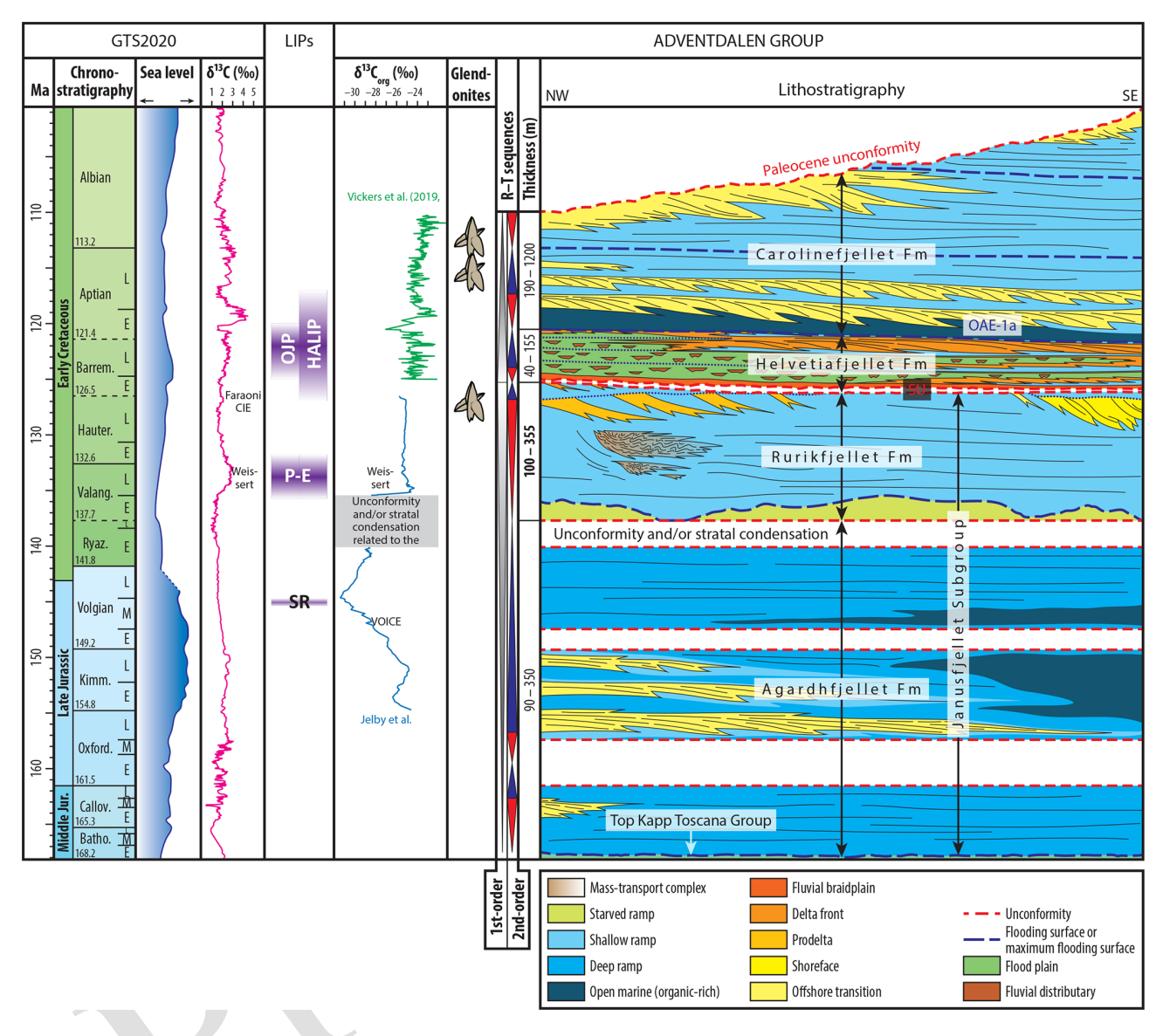


Figure 11. Overview of the Upper Jurassic and Lower Cretaceous stratigraphy of Svalbard plotted against time, from Jelby et al. (2025), based on Grundvåg et al. (2017, 2019). To the left of the stratigraphic summary chart, thicknesses of the formations, first- and second-order regressive-transgressive sequences, occurrence of glendonites (Vickers et al., 2019a), LIP volcanic episodes (see references in Vickers et al., 2023), and organic stable carbon isotopes (see Jelby et al., 2025, and references therein) are shown. These are plotted against global  $\delta^{13}$ C trends, sea level, and ages from the Geological Time Scale 2020 (Gale et al., 2020 [1820]; Hesselbo et al., 2020 [1821]).

In Svalbard, the  $\delta^{13}C_{org}$  record reveals an abrupt and pronounced positive excursion of up to 5.5% in the lower Valanginian, coincident with the base of the Rurikfjellet Formation (Fig. 11; Jelby et al., 2020b, 2025). The excursion is clearly observed in both core (DH-5 and DH-6 in Adventdalen) and outcrop (Myklegardfjellet) sections, where  $\delta^{13}C_{org}$  reaches the most positive values recorded since the Callovian–Oxfordian (Koevoets et al., 2016). Glendonites are found in numerous horizons in the Festningen locality, although a patchy  $\delta^{13}C_{org}$  curve and poor stratigraphic dating of this section due to local small-scale tectonism have led to uncertainty as to the relative age of the glendonites with re-

spect to the Weissert Event (Vickers et al., 2019a, 2023; Jelby et al., 2020b, 2025). Glendonites in the Canadian successions occur in Valanginian of the Deer Bay Formation (Grasby et al., 2017b; Galloway et al., 2020).

Examination of the Hg record across this interval at both Festningen and correlative sites in the Sverdrup Basin similarly yielded uncertain results, due to the poor age constraints preventing convincing identification of the Weissert Event CIE (Vickers et al., 2023). Nonetheless, Arctic Hg/TOC ratios are observed to increase across the proposed Weissert Event intervals in both Svalbard and the Sverdrup Basin. This supports recent work indicating that Paraná-Etendeka

volcanism was synchronous with the onset of the Weissert Event CIE (Gomes and Vasconcelos, 2021). In other localities on Svalbard (DH-5 borehole in Adventdalen and Myklegardfjellet in eastern Spitsbergen, Fig. 10), the Weissert 5 Event is well dated with age-diagnostic ammonites and palynomorphs (Jelby et al., 2020b, 2025) and with the observed  $\delta^{13}C_{org}$  trend being consistent with the globally recognized Weissert Event (Fig. 11; Lini et al., 1992; Weissert et al., 1998; Weissert and Erba, 2004). The onset of the 10 Weissert Event in Svalbard appears to have occurred earlier than in other Boreal sites, but this diachroneity may reflect a depositional hiatus and/or stratal condensation in the glauconitic plastic clay of the Myklegardfjellet Bed at the base of the Rurikfjellet Formation, corresponding to 15 the Tethyan T. pertransiens–N. neocomiensiformis ammonite zones (Jelby et al., 2020b, 2025).

In summary, the Weissert Event represents an important recoupling of the carbon cycle between Boreal (including Svalbard) and lower-latitude basins (including Tethyan, At-20 lantic, and Pacific), probably because of re-established ocean connections in response to a global eustatic sea-level rise and changing oceanic gateway connections (Haq, 2014; Galloway et al., 2020; Jelby et al., 2020b). However, Jelby et al. (2020b) recognized that the decay of the event in Sval-25 bard spanned the late Valanginian to early Barremian (Early Cretaceous; ca. 125.77–121.4 Ma) but is negligible compared to most other Boreal and lower-latitude records and that the signal remains relatively stable at near-peak values following the positive excursion. This indicates that the oceanographic 30 reconnection between higher and lower latitudes, and thus ocean ventilation, must have been sufficiently limited to keep some Boreal basins (including Svalbard) relatively deviated from prevailing global carbon cycle dynamics following the isotopic event due to water exchange only through narrow, 35 shallow straits (Price and Mutterlose, 2004).

#### The Cretaceous HALIP and OAE1a

The largest carbon cycle perturbation of the Early Cretaceous occurred in the early Aptian (a. 121-113 Ma). It is associated with Ocean Anoxic Event 1a (OAE1a, ~ 120 Ma), when 40 black shale deposition occurred across multiple marine sites, indicative of widespread ocean anoxia (e.g., Jenkyns, 1980). OAE1a is characterized by a globally recognized sharp negative CIE followed by a twin-peaked positive "recovery" CIE (Fig. 11; Jenkyns, 1995; Menegatti et al., 1998; Ando et al., 45 2002; Price, 2003; Weissert and Erba, 2004; Herrle et al., 2015; Dummann et al., 2021), which has also been recognized in multiple localities across Svalbard and in the Canadian Arctic (Herrle et al., 2015; Midtkandal et al., 2016; Vickers et al., 2016, 2019a, 2023; Grundvåg et al., 2019; 50 Dummann et al., 2021). Significant perturbations in global climate are believed to have occurred along with the CIE, with global warming followed by cooling being evident from multiple proxies in sites from across the globe (e.g., Bottini et al., 2015; Bodin et al., 2015; Harper et al., 2021; Galloway et al., 2022).

In Svalbard and other Arctic localities, the occurrence of numerous glendonite horizons immediately after the CIE (in-Aptian – Albian strata) supports the global extent of the post-OAE1a cooling (Fig. 11; Schröder-Adams et al., 2014; Herrle et al., 2015; Grasby et al., 2017b; Rogov et al., 2017; 60 Vickers et al., 2019a). The OAE1a is believed to be linked to LIP volcanism, as both the Greater Ontong Java Plateau (OJP) in the Pacific Ocean and the HALIP were being emplaced approximately synchronously with the onset of the event (Fig. 11; Midtkandal et al., 2016; Percival et al., 2021; 65 Galloway et al., 2022). However, uncertainties surrounding the exact relative timings of the volcanism and the OAE1a complicate the interpretation of the cause of the event (Tarduno et al., 1991; Mahoney et al., 1993; Parkinson et al., 2002; Tejada et al., 2002, 2009; Erba et al., 2004, 2015; 70 Chambers et al., 2004; Thordarson, 2004; Dockman et al., 2018; Kasbohm et al., 2021; Galloway et al., 2022).

Attempts to use Hg as a proxy for volcanism to resolve the question of relative timing of HALIP and OJP with regards to the OAE1a CIE and accompanying climatic/environmental 75 perturbations have yielded ambiguous results (Percival et al., 2021; Vickers et al., 2023), and recent work using palynology suggests HALIP-related landscape disturbances began to occur in the latest Barremian, coincident with the first pulse of the HALIP but prior to the early Aptian onset of OAE1a 80 (Galloway et al., 2022). The onset of the negative  $\delta^{13}$ C excursion across Svalbard occurs within a sapropel-rich interval which is highly impoverished in marine palynomorphs (dinocysts) but which yield a number of reworked taxa (e.g., in the Ullaberget outcrop section, the DH-2, and the DH-1 cores near Longyearbyen (Midtkandal et al., 2016; Grundvåg et al., 2019; Śliwińska et al., 2020), narrowing the age to the Barremian-Aptian transitional interval. The regional flooding event that is considered to correlate globally with the OAE1a yields well-preserved dinocysts and has been assigned an earliest Aptian age (Midtkandal et al., 2016; Grundvåg et al., 2017, 2019). Younger Cretaceous strata that elsewhere record other OAEs (e.g., OAE1b, OAE 2, OAE3) are absent from Svalbard (Fig. 4).

#### Cenozoic

The Paleogene succession in Svalbard includes Paleoceneage to possibly mid-Oligocene-age strata (61.8 to  $\sim$  30 Ma) and thus was deposited during the global climate transition from greenhouse to coolhouse conditions (Zachos et al., 2001; Westerhold et al., 2020). Since the Late Cretaceous, 100 Svalbard was already located north of the Arctic Circle (e.g., Harland, 1997) at paleolatitudes comparable to the present (Fig. 3). Therefore, the Cenozoic geological record in Spitsbergen provides a natural reference interval for future polar amplification to global warming in a warm Arctic.

105

The deposits of the CSB belong to the Van Mijenfjorden Group with thicknesses up to 2200 m. The basin fill begins with the Paleocene coal-bearing successions that demonstrates a transgressive trend from delta plain to prodelta/outer 5 shelf facies, followed by marine mudstones and intensely bioturbated sandstones that mainly were sourced from north and northeast of Svalbard (Petersen et al., 2016; Lüthje et al., 2020 [523]; Jochmann et al., 2020). The first evidence of WSFTB-derived sediments occurs in the latest Paleocene 10 with a westerly derived clastic wedge known as the Hollendardalen Formation. The upper part of the CSB continued to fill into the Eocene and possibly the Oligocene and consists of > 800 m thick deposits of shelf and shelf-edge deltas, slope clinotherms, and basin floor fans sourced from 15 the WSFTB to the west (Steel et al., 1981; Johannessen and Steel, 2005; Helland-Hansen and Grundvåg, 2021). Maximum subsidence occurred during the deposition of the Frysjaodden Formation, which contains a significantly expanded (> 30 m) Paleocene–Eocene Thermal Maximum (PETM) se-20 quence (Cui, 2010; Charles et al., 2011; Dypvik et al., 2011). The shallowing-upward uppermost CSB fill is seen as a transition from deepwater marine via shallow-marine/delta front to coastal plain and continental strata. The Norwegian-Greenland Seaway became severely restricted at this time, 25 isolating the Arctic from the Atlantic Ocean during the PETM and early Eocene (Blakey, 2021; Hovikoski et al., 2021; Jones et al., 2023). Overall, the Paleogene coal-bearing successions developed in several stratigraphic levels of Svalbard are an excellent archive for reconstruction of the past 30 vegetation and climate. These intervals provide an insight into the fauna/vegetation of Svalbard at these times (see Sect 6.3).

# 4.4.1 Paleocene hothouse from an Arctic Circle perspective

35 The Paleocene was characterized by a hothouse climate (Zachos et al., 2001; Westerhold et al., 2020). In Svalbard, the CSB Paleocene succession consists of the terrestrial to nearshore Firkanten Formation (yielding fossil fauna) and the offshore marine Basilika, Grumantbyen, and lower-40 most Frysjaodden formations. The Firkanten Formation of early Paleocene age (Selandian) contains fossil plant-bearing units, also known as the Barentsburg flora (see Golovneva et al., 2023). These deposits have been extensively investigated due to economic interest and exploitation of coal re-45 sources over the last century, yet there are relatively few publications describing the succession in detail (cf. Steel et al., 1981; Nøttvedt, 1985; Nagy, 2005; Jochmann et al., 2020; Lüthje et al., 2020). Coal exploration over the past few decades has provided more than 500 drill cores through the 50 early Paleogene of Svalbard and focuses in particular on the coal-bearing Todalen Member of the Firkanten Formation. Fission-track ages from the Firkanten Formation dated the unit to  $63\pm2$  and  $64\pm2$  Ma (Blythe and Kleinspehn, 1998). A more precise age is derived from an ash layer that cross-cuts the lowermost coal seam in the Firkanten Formation. It has 55 been dated using U-Pb methods to  $61.596 \pm 0.028 \,\mathrm{Ma}_{1524}$ (Jones et al., 2017) at the Danian-Selandian boundary, constraining the main coal deposition to the early Selandian. The Paleocene coals have recently been shown to comprise much higher-resolution stratigraphic records than previously anticipated (Large and Marshall, 2015; Large et al., 2021), especially when coals are formed from peat growing in colder climates. The age model developed by Large and Marshall (2015) and an improved understanding of long-term storage of peatland carbon (Large et al., 2021) can be implemented to assess accumulation rates. For example, the 1.5 m thick Longyear coal seam has a modeled accumulation rate of 59 and 99 kyr for temperate and boreal climates, respectively, which suggests a high-resolution record that can be used to infer variation in atmospheric dust input and the effects of forest fires (Marshall, 2013). Material has been collected from the now closed coal mines in ongoing research projects to expand on these existing datasets. The Selandian coal seams provide details of the vegetation on Svalbard at that time. The paleoflora from Svalbard reveal a temperate 75 (mean annual temperature  $10.1 \pm 2^{\circ}$ ), maritime, humid climate, with warm summers and cool mild winters (e.g., Uhl et al., 2007; Golovneva et al., 2023). Temperate Arctic paleotemperatures are corroborated by Pantodont tracks discovered at the upper boundary of the coal layer of the Firkanten 80 Formation (Lüthje et al., 2010). The climatic conditions were similar in the larger Arctic region (e.g., O'Regan et al., 2011).

## 4.4.2 The Paleocene–Eocene Thermal Maximum (PETM)

The PETM was a transient period ( $\sim 150-200 \, \mathrm{kyr}$ ) of rapid 85 global warming that began around 56 Ma, superimposed on already greenhouse conditions of the early Paleogene (Zachos et al., 2001). The event is recognized as a global negative CIE in sections worldwide, attributed to a massive release of <sup>13</sup>C-depleted carbon to the ocean–atmosphere system (McInerney and Wing, 2011). Potential sources include surface reservoirs such as dissociation of methane hydrates from marine sediments (e.g., Dickens et al., 1995) and/or volcanic and thermogenic degassing from the emplacement of the NAIP (e.g., Svensen et al., 2004; Gutjahr et al., 2017; Berndt et al., 2023; Jones et al., 2023). Existing High Arctic records for the PETM and following hyperthermal events suggest subtropical temperatures in both marine and terrestrial realms (e.g., Suc et al., 2020; Sluijs et al., 2000). In Svalbard, the PETM and its various environmental effects 100 have been thoroughly documented in several chemostratigraphic to biostratigraphic multi-proxy studies (Charles et al., 2011; Dypvik et al., 2011; Harding et al., 2011; Nagy et al., 2013; Wieczorek et al., 2013; Jones et al., 2019; Cui et al., 2021; Pogge von Strandmann et al., 2021). The bulk 105 of these studies are focused on a SNSK drill core (BH09/05)

from a coal exploration well located on the eastern flank of the CSB (Fig. 2).

The timing and duration of the PETM are well constrained from Svalbard strata with a high-precision U-Pb ra-5 diometric age of an ash layer within the CIE outcropping near Longyearbyen, coupled with evidence of orbital cycles within the strata of the BH09/05 core (Charles et al., 2011). Other studies explore the myriad consequences of extreme warming in Svalbard strata. The abundance of kaolinite in 10 the PETM interval (Dypvik et al., 2011) and a large negative lithium isotope excursion coincident with the CIE (Pogge von Strandmann et al., 2021) suggests increased weathering rates in response to warmer and wetter conditions. Increased runoff rates resulted in a stratified water column with 15 a freshwater surface layer and oxygen depleted bottom waters, which severely reduced the diversity of various fauna elements in the basin (Harding et al., 2011; Dypvik et al., 2011; Nagy et al., 2013). Osmium isotopes (Wieczorek et al., 2013) and mercury anomalies (Jones et al., 2019) show key 20 variations in the activity of the NAIP at this time, supporting the hypothesis that NAIP volcanism and magmatism was at least partially responsible for the extreme carbon emissions at the PETM onset. While studies on the BH09/05 core are now plentiful, there are numerous other cores and outcrops 25 that contain the PETM strata that have received little to no attention.

#### 4.4.3 The decline of the Eocene greenhouse climate

The hothouse conditions of the early Eocene were followed by a gradual global cooling that culminated in the transition 30 into the icehouse climate at around 34 Ma (e.g., Westerhold et al., 2020; Hutchinson et al., 2021). Paleobotanical records from the Arctic suggest that during the middle Eocene, the mean annual precipitation was  $> 120 \,\mathrm{cm} \,\mathrm{yr}^{-1}$  (Greenwood et al., 2010). In Svalbard, the continental, flora-35 bearing units are found within the Aspelintoppen Formation (Steel et al., 1978, 1985), probably spanning the middle Eocene and not younger than late Eocene or early Oligocene (Matthiessen, 1986; Cepek and Krutzsch, 2001), and the upper Eocene (Golovneva and Zolina, 2023) or early 40 Oligocene (Head, 1984) Renardodden Formation. Abundant paleoflora from the Aspelintoppen Formation and the Renardodden Formation (Manum, 1962; Kvaček and Manum, 1993; Kvaček et al., 1994; Cepek and Krutzsch, 2001; Uhl et al., 2007) indicates mean annual precipitation rates of  $_{45}$  1423 and 1716 mm yr<sup>-1</sup>, respectively (Golovneva, 2000). Angiosperm morphotypes indicate a strong seasonal precipitation pattern (from 356 to 656 mm in the three wettest months and 112-247 mm for the three driest months; Clifton, 2012). The high rates of precipitation and increased weath-50 ering rates, in combination with active tectonism, promoted the transfer of sand into deeper settings via flood-generated hyperpycnal flows at this time (Grundvåg et al., 2023). In the late Eocene, Svalbard was only a few degrees south of the present 78° N (Fig. 3), but fossil plant material indicates that the temperature at that time was much warmer than today, and the estimated mean annual air temperature was around +9 °C (Golovneva, 2000; Golovneva et al., 2023; Uhl et al., 2007). Several studies have evaluated the abundance and diversity of fossil plants and the occurrence of coal seams and fossil insects in the terrestrial parts of the Eocene Aspelintoppen Formation (e.g., Dallmann et al., 1999; Uhl et al., 2007; Marshall et al., 2015). In other areas of the High Arctic, such as Ellesmere Island, fossil remnants of a varanid lizard, the tortoise *Geochelone*, and the alligator *Allognathosuchus* confirm warm temperatures that remained above freezing (e.g., 65 Estes and Hutchinson, 1980; Eberle and Greenwood, 2012).

The sporadic occurrence of glendonites and outsized clasts, the latter possibly indicating rafting by temporal sea ice, in the marine parts of the succession suggests strong seasonal or temporal temperature variations in Svalbard (Kellogg, 1975; Dalland, 1976; Spielhagen and Tripati, 2009). This is in accordance with some of the paleofloristic/insect studies that infer freezing temperatures during winter months and an overall cooling trend for the entire interval (Golovneva, 2000; Uhl et al., 2007; Wappler and Denk, 75 2011). Some of the signals preserved in the sedimentary rock record may be caused by other allogenic forcing factors than climate fluctuations, such as tectonics and relative sea-level changes, but similar results from a range of proxies including plant morphotypes support the validity of paleoclimate 80 reconstructions. As such, deconvolving climatic and tectonic signals in tectonically active basins is of major importance. In the restricted Arctic Ocean during the early middle Eocene (ca. 49 Ma), increased runoff caused stratification of the water column (with a fresh-water lid) and led to the well-known Azolla freshwater algal blooms that eventually contributed to the withdrawing of the atmospheric CO<sub>2</sub> and cooling of the global climate from the middle Eocene onwards (Brinkhuis et al., 2006; Speelman et al., 2009).

### 4.4.4 The Eocene–Oligocene Transition and connection 90 with the Arctic Ocean

A major step in the long-term Cenozoic climate evolution took place at the Eocene Oligocene Transition (EOT;  $\sim$  34 Ma), when decreasing atmospheric CO<sub>2</sub> and changes to ocean gateways led to a development of the first permanent ice cap in Antarctica and initiated the icehouse type of climate which still exists today (Straume et al., 2020; Westerhold et al., 2020; Hutchinson et al., 2021). However, the global scale of the transition is not fully understood, since in contrast to the well-studied deep sea sites from southern and equatorial regions, the signature of the EOT for the northern high latitudes remains poorly constrained. Climate models suggest that closing and opening the gateways to the Arctic Ocean (such as the Fram Strait) had equally large impact on the temperature development in the high northern latitudes as the CO<sub>2</sub> decrease (e.g., Hutchinson et al., 2019,

2021; Straume et al., 2022; Śliwińska et al., 2023). However, the number of proxy records from the northern polar regions to evaluate the history of the Fram Strait and validate the climate models is limited. The ACEX core (IODP Ex-5 pedition 302) from the Arctic Ocean contains a hiatus that misses an estimated interval from 44.4 to 18.2 Ma (Backman et al., 2008). The ODP site 913 from the Greenlandic Sea suffers from a hiatus at the EOT (Eldrett et al., 2004; Sangiorgi et al. 2008). Furthermore, the existing sea surface 10 temperature proxy data are of extremely low resolution (Liu et al., 2009) in comparison with time-equivalent records from the Labrador Sea and the North Sea (Śliwińska et al., 2019, 2023). Molecular fossil (alkenone) records suggest at least 5 °C cooling in the northern high latitudes, associated with 15 the transition towards the coolhouse climate (Liu et al., 2009; Śliwińska et al., 2023). The existing pollen record revealed a significant cooling of ca. 5 °C in cold months mean temperatures on East Greenland across the EOT (Eldrett et al., 2009).

During the EOT, Svalbard was already located at  $\sim 80 \,^{\circ} \text{N}$ 20 and therefore provides insights into the climate evolution across the EOT in the northern high latitudes. In the CSB the youngest Paleogene unit is the Aspelintoppen Formation, which is assigned to the late Eocene (plant fragments) or Oligocene (mollusks) (Manum and Throndsen, 1986). Un-25 fortunately, the age model for this formation remains poorly constrained. With an improved age model, the Eocene-Oligocene succession could provide a valuable contribution to the atmospheric temperature evolution across the EOT in the northern high latitudes and be further resolved with 30 pollen records, comparable with the Norwegian-Greenland Sea (Eldrett et al., 2009). Marine to terrestrial deposits of possible late Eocene to Oligocene age have also been reported mainly from the exposed parts of the Forlandsundet and Bellsund grabens on the West Spitsbergen mar-35 gin (Gabrielsen et al., 1992; Weber, 2019; Śliwińska and Head, 2020; Schaaf et al., 2021). However, these studies are very limited. The foraminifera assemblages collected from the Sarstangen conglomerate at the Balanuspynten profile on the eastern side of the Forlandsundet Graben re-40 veal the presence of marine Oligocene strata assigned to the Buchananisen Group (Feyling-Hanssen and Ulleberg, 1984). This age has later been substantiated by palynostratigraphic analyses, which suggests an early to middle Oligocene age, at least for the sediments exposed along the eastern basin 45 margin (Schaaf et al., 2021). The two foraminiferal zones (TA and TB) that were originally assigned to the middle to upper Oligocene can more accurately be assigned to the lower Oligocene (lower Rupelian; the TA zone) and the upper Oligocene (lower Chattian; the TB zone). The early 50 Oligocene age of the marine strata is confirmed by the presence of dinocyst Svalbardella cooksoniae (Manum, 1960). The appearance interval of S. cooksoniae in the earliest Oligocene seems to be associated with a cooling interval (Śliwińska and Heilmann-Clausen, 2011). A single sample 55 from the Calypsostranda Group at the Renardodden section on the southern shore of Bellsund, a structural outlier interpreted to be an exposed part of the Bellsund Graben, has yielded dinocysts of late Eocene or early Oligocene age (Head, 1984; Śliwińska and Head, 2020). Based on the association of pollen in the Skilvika Formation, an upper Paleocene to Eocene age can be suggested for the lower part of the section (Weber, 2019).

#### 4.4.5 Neogene hiatus

Svalbard experienced two uplift phases in recent times. The first and major uplift phase started in the Eocene (> 36 Ma) 65 and persisted to ca. 10 Ma. This was followed by less prominent uplift from ca. 10 Ma onwards that generated the modern topography of the archipelago (Dörr et al., 2013). These uplift events are matched by contemporaneous uplift phases in Greenland, the Barents Shelf, and Baltica (Dörr et al., 70 2013) and are attributed to crustal thinning and the onset of ocean spreading in the Arctic and North Atlantic driven by mantle processes related to anomalously hot mantle underlying this part of the Arctic (Green and Duddy, 2010). The presence of thick pre-glacial (Miocene and Pliocene? 23 to 75 2.58 Ma) and glacial (late Pliocene and Pleistocene) offshore clastic wedges along the western and northern margins of Spitsbergen (Hjelstuen et al., 1996; Lasabuda et al., 2018; Alexandropoulou et al., 2021) suggests a net denudation of ca. 3 km (Riis and Fjeldskaar, 1992; Lasabuda et al., 2021). 80 The overall amplitude of Neogene uplift decreases eastwards with the uplift along parts of WSFTB exceeding 2.5 km and over 1.5 km in the CSB (Dörr et al., 2013). Estimates based on organic geochemical proxies suggest total uplift of 2.5 to 3.5 km (Throndsen, 1982; Marshall et al., 2015; Olaussen et al., 2019). As a result, Miocene and Pliocene sedimentary strata are not preserved anywhere on Svalbard, while only intermittent remains of Pleistocene glacial deposits are found (Ingólfsson and Landvik, 2013). Uplift of 9 mm yr<sup>-1</sup> continues in central-western Spitsbergen today, with only 90  $1 \,\mathrm{mm}\,\mathrm{yr}^{-1}$  of that attributed to isostatic rebound due to the recent Weichselian glaciation (Kierulf et al., 2022).

#### 5 Absolute radiochronology of Svalbard stratigraphy

Despite the extensive stratigraphic successions spanning much of the Phanerozoic in Svalbard, robust absolute radiometric stratigraphic age constraints are scarce. Except for data on Devonian and older magmatic and metamorphic rocks from the pre-Caledonian "basement" (e.g., Myhre et al., 2008; Pettersson et al., 2009; Majka and Kośmińska, 100 2017; McClelland et al., 2019), no robust ages are published from the stratigraphy pre-dating the Permian–Triassic boundary. The first radiometric age comes from an ash layer from the Festningen section (Fig. 6; Grasby et al., 2015 1832) and from the Deltadalen section at the Permian–Triassic boundary (Fig. 9; Zuchuat et al., 2020). In Deltadalen, a zir-

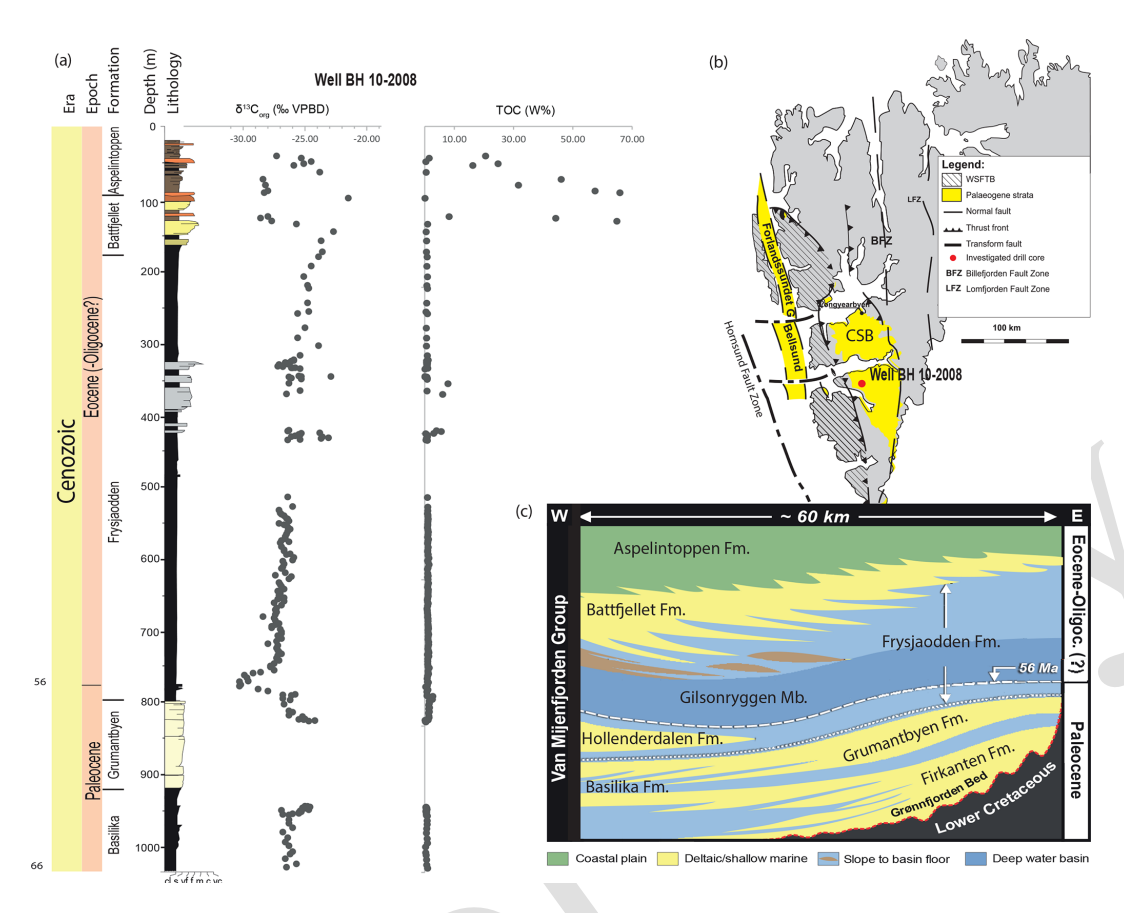


**Figure 12.** (a) Geochemical data from well BH 10-2008 are from Doerner et al. (2020), and borehole stratigraphy is after Grundvåg et al. (2014). (b) Geological map showing the outline of Paleocene deposits and position of BH 10-2008 from Helland-Hansen and Grundvåg (2021). (c) Lithostratigraphic summary of the Paleogene deposits of the Central Spitsbergen Basin. Modified from Helland-Hansen and Grundvåg (2021). The age of the Paleocene–Eocene boundary is from Charles et al. (2011) and Harding et al. (2011).

con U–Pb chemical abrasion isotope dilution thermal ionization mass spectrometry (CA-ID-TIMS) age of  $252.13 \pm 0.62$  Ma from a bentonite bed (volcanic ash) ca. 15 cm above the first appearance datum (FAD) of the age diagnostic H.  $_5$  parvus (onset Triassic) in the Vikinghøgda Fm. ties the biostratigraphic record to an absolute age. This age records the onset of the Triassic in Svalbard and the Panthalassic Ocean within error (Zuchuat et al., 2020). Given the sedimentation rate constraints for this section (Zuchuat et al., 2020), and the uncertainty in the age of the bentonite, there is overlap in age between the FAD of H. parvus in Svalbard and the FAD of H. parvus of  $251.902 \pm 0.024$  Ma at the Induan GSSP (Burgess et al., 2014). This indicates synchronicity of the End-Permian Mass Extinction in the Panthalassic and Tethyan domains at 15 a 0.2 % ( $2\sigma$ ) level of uncertainty.

The next absolute stratigraphic tie point occurs in the Barremian to lower Aptian Helvetiafjellet Formation, where a bentonite layer from two cores taken in Longyearbyen (DH-3 and DH-7; Fig. 4) was dated to 123.1 ± 0.3 Ma (zircon U–Pb CA-ID-TIMS; Corfu et al., 2013; Midtkandal et al., 2016). Bio- and chemo-stratigraphical evidence suggests that this bentonite layer is of mid-Barremian age (Midtkandal et

al., 2016) and that it occurs  $\sim 40\,\mathrm{m}$  below the Barremian– Aptian boundary and the onset of the Early Aptian Oceanic Anoxic event 1a (OAE1a). Subsequent magnetostratigraphy 25 tied this bentonite age to the magnetic polarity record, and hence Zhang et al. (2021a) were able to calculate an age of  $121.2 \pm 0.4 \,\mathrm{Ma}$  for the Barremian-Aptian boundary, accepting the M0r magnetochron as a boundary marker. Based on available ages for the HALIP in Svalbard (124.7  $\pm$  0.3 to  $_{30}$  $123.9 \pm 0.3$  Ma; Corfu et al., 2013) and Franz Josef Land ( $\sim$  122–123 Ma; Corfu et al., 2013), there is no overlap in age with a HALIP magmatic pulse of this event with the OAE1a. However, mafic lavas and intrusives from the Sverdrup basin in northern Canada do show overlapping ages (Evenchick et al., 2015; Dockman et al., 2018) with the updated Barremian-Aptian boundary age not precluding a relationship between a pulse of the HALIP with the AOE1a.

To our knowledge, there are no further absolute age constraints published for the Mesozoic stratigraphy of Svalbard. However, the onset of Paleogene sedimentation in the CSB (Fig. 4) and the Paleocene to early Eocene stratigraphy is well constrained through high precision zircon CA-ID-TIMS U–Pb ages (Charles et al., 2011; Jones et al., 2017;

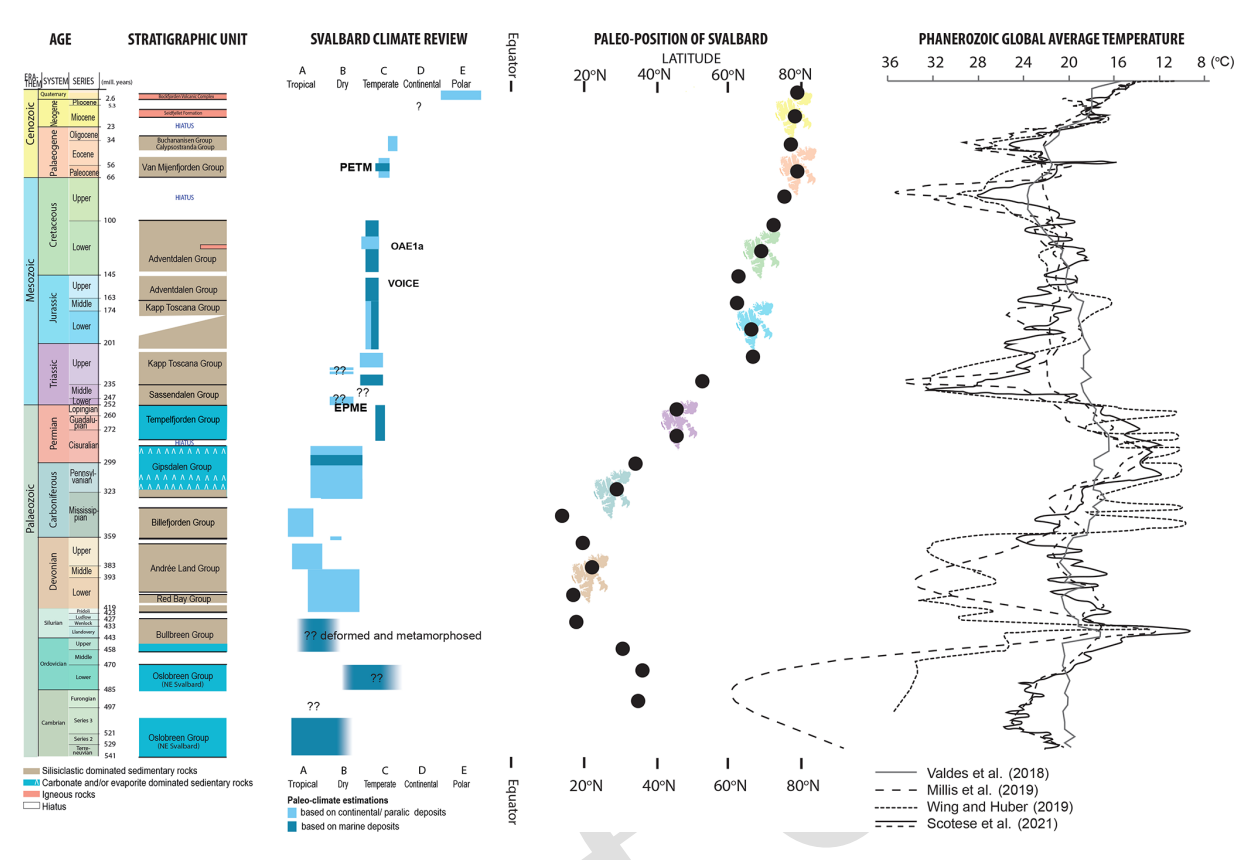


**Figure 13.** Correlation of the Phanerozoic climate plot based mainly on climate-sensitive facies (see Supplement), supplemented by biological and geochemical proxies with the paleogeographic position of Svalbard (Scotese and Wright, 2018) and compilation of the published global average temperature curves.

Jochmann et al., 2020). A bentonite bed towards the base of the Firkanten Formation (see diagram in Fig. 12), dated from three different parts of the basin, yielded an age of  $61.596 \pm$ 0.028 Ma overlapping with the Danian–Selandian boundary, 5 and a bentonite layer from the lower part of the overlying Basilika Formation has an age of  $59.32 \pm 0.19$  Ma overlapping with the Selandian-Thanetian boundary (Jones et al., 2017). Based on these marker horizons, deposition within the CSB was estimated to start around  $61.76 \pm 0.09$  Ma. A ben-10 tonite horizon within the Frysjaodden Formation was dated to  $55.785 \pm 0.034$  Ma by Charles et al. (2011). This ash layer is a key marker bed for constraining the Paleocene–Eocene boundary as it is found within the PETM CIE in Svalbard strata. Charles et al. (2011) used this age and possible pre-15 cession cycles within borehole BH09/05 to estimate an age of  $55.866 \pm 0.098$  Ma for the Paleocene–Eocene boundary (i.e., the PETM onset).

To date, there are no further robust and precise radiometric ages from Svalbard's Paleozoic strata. However, well-studied outcrop successions and abundant drill core material from much of the Paleozoic offer an excellent possibility to search for target volcanic rocks in the stratigraphy that may be dated by high-precision zircon U–Pb methods, thus improving the

chronostratigraphy not only of Svalbard but potentially also globally (e.g., Zhang et al., 2021a).

#### 6 Evolution of the Phanerozoic climate in Svalbard

The parameters controlling the Phanerozoic climate in Svalbard can be simplified to the two core elements: global distribution of paleoclimatic zones (Köppen belts; e.g., Boucot et al., 2013) and the paleolatitude of Svalbard (e.g., Steel 30 and Worsley, 1984; Torsvik and Cocks, 2017, Olaussen et al., 2025). The deep-time models of Phanerozoic climate for either low-latitude regions between 40°N and 40°S (Fig. 13; based on oxygen isotope record (Song et al., 2019; Vérard and Veizer, 2019; Veizer and Prokoph, 2015; Grossman, 2012; Royer et al., 2004) or global average temperature (GAT; Wing and Huber, 2019; Valdes et al., 2018; Mills et al., 2019) are characterized by a "Double Hump" pattern (Fig. 13; Fischer, 1981, 1982, 1984; Frakes et al., 1992; Scotese et al., 1999; Summerhayes, 2015). The GAT 40 trends show high temperatures during the early Paleozoic and cooler temperatures during the late Paleozoic, followed by warmer and monsoonal Mesozoic and early Cenozoic temperatures, finally returning to cooler temperatures in the late Cenozoic (Fig. 13). This pattern is formed in response 45

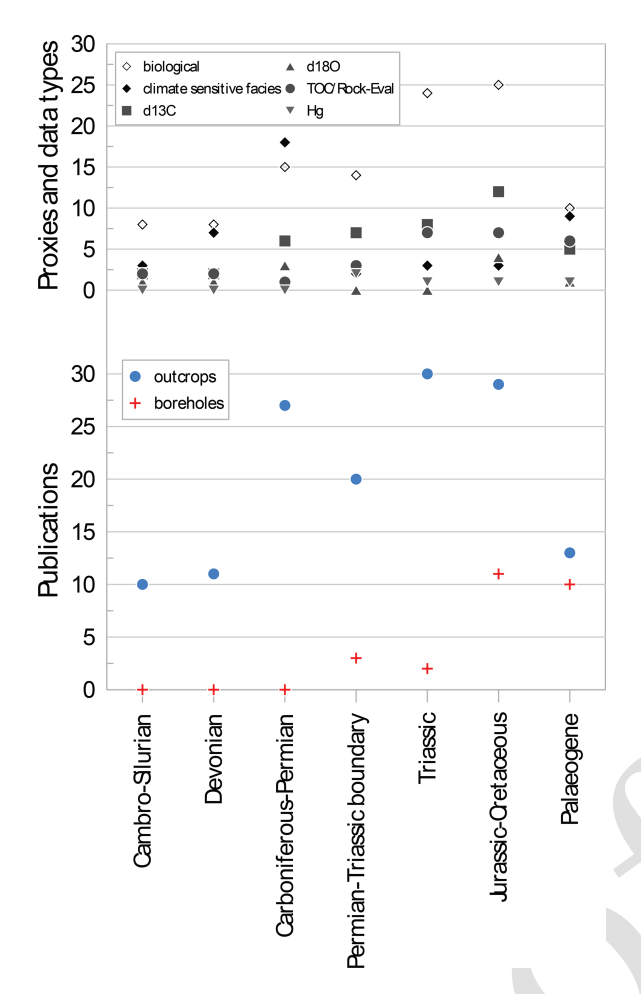


**Figure 14.** Compilation plot of main proxies as a function of geological time, based on Table 2.

to breakup and accretion of supercontinents (van der Meer et al., 2014, 2017). The geochemical proxies, such as oxygen isotopes, have limited application in Svalbard due to burial, diagenetic, and hydrothermal alterations (e.g., Bug-5 gies, 2013; Matysik et al., 2018). Therefore, the overall Phanerozoic climate trends illustrated in Fig. 14 are based on climate-sensitive lithofacies supplemented by biological and geochemical proxies where possible. The datasets used for all deep-time paleoclimatic and paleoenvironmental studies in Svalbard mainly come from the outcrop's investigations (See Fig. 14). Only about 18 % of the studies mainly of the Mesozoic and Cenozoic strata address borehole data (Fig. 14).

#### 6.1 Paleozoic

<sup>15</sup> The warm and tropical to subtropical climate recorded in the early Paleozoic sedimentary succession in Svalbard reflects its near equatorial position (Fig. 3). The Paleozoic climate slightly oscillates between the tropical and subtropical, dry climate. While the Late Ordovician cooling (ca. 460–

440 Ma) is not recorded in Svalbard, likely due to a strati- 20 graphic gap, the highest temperatures were reached in the Mississippian (Fig. 13). The northward drift of the continental plate on which Svalbard is located accelerated in the Mississippian to the late Triassic (Fig. 13; Torsvik and Cocks, 2019), while its impact on the climate can be recognized 25 in the Carboniferous-Permian succession. The Mississippian to Pennsylvanian shift in climate seen as a transition of climate-sensitive facies from the Mississippian coal-bearing deposits indicating tropical humid climate, through the Pennsylvanian semi-arid subtropical evaporites and siliciclastic 30 red beds, and warm-water carbonate facies (Sect. 4) is potentially accommodated by the changes in paleolatitude (Steel and Worsley, 1984; Torsvik and Cocks, 2019); however, the impact of global cooling related to the LPIA (e.g., Isbell et al., 2008) should also be considered. The following cooling trend expressed by the shift from cool-water to cold-water carbonate platform deposits (Sect. 4) takes place despite the overall increased trend of global temperature in the Permian (Fig. 13).

40

#### 6.2 Mesozoic

Despite the general northward migration through different climate zones, Svalbard's sedimentary Mesozoic strata recorded a more complex story, reflecting both global and regional climatic and environmental trends, and the control from the paleolatitude position of Svalbard, which is evident 45 in the Paleozoic, is not clearly seen. Indeed, the Mesozoic is characterized at the global scale by overall warm conditions, with overall mega-monsoonal climate, especially in the Triassic (Parrish, 1993; Mutti and Weissert, 1995; Preto et al., 2010), punctuated by several established hyperthermal 50 events and potential ones, such as the EPME, the late Dienerian biotic crisis, the Smithian-Spathian transition, and the Carnian Pluvial Episode. Most of these hyperthermals are associated with the emplacement of LIPs or smaller-scale volcanic activities (see Sect. 4 for details). The emplacement of one LIP, however, might have triggered a global cooling rather than a global warming episode (the Weissert Event; Martinez et al., 2023). In addition to these individual events, longer-lived climate perturbations and oscillations are recorded in the Mesozoic strata of Svalbard, including periodic cooling-warming episodes during the Middle Jurassic to Early Cretaceous, as testified by the presence of cool-climate-indicators such as glendonite crystals in certain stratigraphic intervals. These climatic cycles generated (glacio-?)eustatic sea-level variations, leading to changes in 65 global oceanic circulation as shallow seaways were periodically exposed during sea-level lowstands. These climatic and (glacio-?)eustatic sea-level variations impacted the amount and the redistribution of precipitation, runoff, temperature, salinity, water-mass stratification, nutrients, and productiv- 70 ity between basins, as well as notably impacting the global

carbon- and phosphorus cycles. One of these periodic perturbations recorded in Svalbard was the VOICE event.

#### 6.3 Cenozoic

The Late Cretaceous climate maximum along with the Neo-5 gene cooling (Fig. 13) is not recorded in Svalbard due to stratigraphic gaps. During the Cenozoic, Svalbard was positioned at the high northern latitudes (the Arctic Circle). Under the greenhouse conditions of the Paleocene and Eocene, paleoflora of Svalbard suggest a humid and temperate cli-10 mate at that time, punctuated by hyperthermal conditions during the PETM (Sect. 4). Therefore, palynoflora from Svalbard provides a unique insight into the high-latitude end member for estimating the latitudinal gradient under the greenhouse conditions of the early Cenozoic. Notably, the 15 paleoflora suggests slightly warmer temperatures and higher mean annual precipitation during the Paleocene than in the Eocene-earliest Oligocene. This may be an effect of the decline of the greenhouse climate. During the early Oligocene, Svalbard (located at approximately 80° N) experienced sig-20 nificant cooling: the presence of specific dinocysts suggests a notable cooling interval during this period. The cooling trend is a direct response to the global cooling and the transition to the modern icehouse climate state with a bipolar glaciation (Fig. 13).

#### 25 7 Conclusions

40

In this contribution we synthesized the review of the Pre-Quaternary Phanerozoic (ca. 541 to 2.588 Ma) deep-time paleoclimatic research conducted on Svalbard's sedimentary succession and conclude the following:

- Svalbard represents an excellent location for studying multiple globally relevant paleoclimatic events within a spatially constrained area.
  - Svalbard's geological record is influenced by both its northward drift and the recurring influence of large igneous provinces that affected its climate. These include, at least, the End-Permian Siberian Traps LIP, the Early Cretaceous High Arctic LIP, and the Paleogene North Atlantic Igneous Province.
  - Specific events that record environmental perturbations at the global scale imprinted on Svalbard's geological record include the LPIA, the End-Permian Mass Extinction, Early Cretaceous anoxic events and cold snaps, and the Paleocene–Eocene Thermal Maximum.
- These are recorded as changes in biological, lithological, and chemical proxies of past climates preserved in both outcrops and drill cores.

- Absolute radiometric ages constrain the continuous stratigraphic successions but are unevenly distributed throughout the stratigraphy.
- Of the 148 key publications, the most used proxies to quantify past environments and climate are sedimentological studies of biological indicators (104), climatesensitive facies (45), carbon isotopes  $\delta^{13}$ C (42), oxygen isotopes  $\delta^{18}$ O (10), and mercury (5).

This contribution serves as a foundation for future deep-time paleoclimate studies utilizing outcrops, opportunistic drill cores, or dedicated deep-time paleoclimate scientific drilling planned in the near future.

**Data availability.** All datasets come from published scientific contributions or are part of the paper, including Sects. S2 and S3 in the 60 Supplement.

Supplement. Section S1 consists of Table S1 illustrating an overview of selected sedimentary and biological climate indicators used to construct the Svalbard paleoclimate review plot in Fig. 4. Section S2 consists of (a) a table with data plot- 65 ted in Fig. 4, along with (b) an interactive plot displaying the individual datasets (Smyrak-Sikora and Betlem, 2025). Section S2 can be accessed at https://doi.org/10.5281/zenodo.15405159 (Smyrak-Sikora et al., 2024). Section S3 (Table S3) presents a comprehensive table summarizing 148 scientific articles. The 70 table outlines the diverse proxies utilized in deep-time climate studies conducted in Svalbard, highlighting their respective methodologies, findings, stratigraphic succession, and implications for paleoenvironmental reconstructions. It can be accessed at https://doi.org/10.5281/zenodo.16928063. The supplement related to this article is available online at [the link will be implemented upon publication].

Author contributions. AASS – data curation, conceptualization, writing (original draft and editing), visualization, project administration. PB – writing (review and editing), visualization. VSE – 80 writing (original draft), writing (review and editing). WJF – writing (original draft), writing (review and editing). SAG - writing (original draft), writing (review and editing). MEJ – writing (original draft), writing (review and editing), visualization. MTJ - writing (original draft), writing (review and editing). GES - writing (original draft), writing (review and editing), visualization. KKS - writing (original draft), writing (review and editing). MLV - writing (original draft), writing (review and editing), visualization. VZ – writing (original draft), writing (review and editing), visualization. LEA – writing (original draft). JIF – conceptualization. JMG – writing (original draft). WHH - editing. MAJ - writing (review and editing). EJ - writing (review and editing). MK - Visualization and editing. DK - writing (review and editing). GL - writing (original draft). TM - data curation. AM - writing (original draft). SO - writing (original draft). SP - conceptualization. GDP - writing (origi- 95 nal draft). LS - writing (original draft). KiS - conceptualization,

writing (original draft), writing (review and editing), visualization, supervision, funding acquisition.

**Competing interests.** The contact author has declared that none of the authors has any competing interests.

5 Disclaimer. Publisher's note: Copernicus Publications remains neutral with regard to jurisdictional claims made in the text, published maps, institutional affiliations, or any other geographical representation in this paper. While Copernicus Publications makes every effort to include appropriate place names, the final responsibility lies with the authors.

Acknowledgements. Lilith Kuckero and Moritz Boehme kindly contributed with reference formatting. Atle Mørk is acknowledged for comments on the manuscript. Copilot was used to help organize the references. We would like to acknowledge Gerilyn Soreghan, <sup>15</sup> Helmut Weissert, and an anonymous reviewer for constructive feedback on the manuscript. Steve Grasby is acknowledged for his additional and unique suggestions for the manuscript.

Financial support. This research has been supported by the Norges Forskningsråd (grant nos. 283488, 295781, 352811, 20 326238, 336293, 257579, 223272, and 332523), Horizon 2020 (grant nos. 101024218 and 754513), the Danmarks Frie Forskningsfond (grant no. 11-107497), the Commission Géologique du Canada, the Carlsbergfondet (grant no. CF22-0122 and CF24-1960), industry funding (Locra, ARCEx), international funding 25 agencies (MagellanPlus), and University of Arctic (UArctic) collaboration projects.

**Review statement.** This paper was edited by Shiling Yang and reviewed by Gerilyn (Lynn) Soreghan, Helmut Weissert, and one anonymous referee.

#### 30 References

- Abay, T. B., Karlsen, D. A., Olaussen, S., Pedersen, J. H., and Hanken, N.-M.: Organic geochemistry of Cambro-Ordovician succession of Ny Friesland, Svalbard, High Arctic Norway: Petroleum generation potential and bulk geochemical properties, J. Petrol. Sci. Eng., 218, 111033, https://doi.org/10.1016/j.petrol.2022.111033, 2022.
- Abdelmalak, M. M., Gac, S., Faleide, J. I., Shephard, G., Tsikalas, F., Polteau, S., Zastrozhnov, D., and Torsvik, T. H.: Quantification and restoration of the pre-drift extension across the NE Atlantic conjugate margins during the mid-Permian-early Cenozoic multi-rifting phases, Tectonics, 42, e2022TC007386,
- Aguirre-Urreta, M. B., Price, G. D., Ruffell, A. H., Lazo, D. G., Kalin, R. M., Ogle, N., and Rawson, P. F.: Southern hemisphere Early Cretaceous (Valanginian-Early Barremian) carbon

https://doi.org/10.1029/2022TC007386, 2023.

- and oxygen isotope curves from the Neuquén basin, Argentina, Cretaceous Res., 29, 87–99, 2008.
- Ahlborn, M. and Stemmerik, L.: Depositional evolution of the Upper Carboniferous–Lower Permian Wordiekammen carbonate platform, Nordfjorden High, central Spitsbergen, Arctic Norway, 50 Norw. J. Geol., 95, 91–126, https://doi.org/10.17850/njg95-1-03, 2015.
- Alexandropoulou, N., Winsborrow, M., Andreassen, K., Plaza-Faverola, A., Dessandier, P. A., Mattingsdal, R., Baeten, N., and Knies, J.: A continuous seismostratigraphic framework for the Western Svalbard-Barents Sea Margin over the last 2.7 Ma: Implications for the late Cenozoic Glacial history of the Svalbard-Barents Sea Ice Sheet, Front. Earth Sci., 9, 656732, https://doi.org/10.3389/feart.2021.656732, 2021.
- Allen, K. C.: Lower and Middle Devonian spores of North and Central Vestspitsbergen, Palaeontology 8, 687–748, 1965.
- Allen, K. C.: Spore assemblages and their stratigraphical application in the Lower and Middle Devonian of North and Central Vestspitsbergen, Palaeontology, 10, 280–97, 1967.
- Alley, N. F., Hore, S. B., and Frakes, L. A.: Glaciations at high-latitude Southern Australia during the Early Cretaceous, Aust. J. Earth Sci., 67, 1045-1095, 2020.
- Anderson, T. F. and Arthur, M. A.: Stable isotopes in sedimentary geology and their application to sedimentologic and paleoenvironmental problems, in: Society of Economic Paleontologists and Mineralogists Short Course Notes, edited by: Arthur, M. A. et al. 1823, SEPM 10, 1–151, 1983.
- Ando, A., Kakegawa, T., Takashima, R., and Saito, T.: New perspective on Aptian carbon isotope stratigraphy: data from  $\delta^{13}$ C records of terrestrial organic matter, Geology, 30, 227–230, 2002.
- Anell, I., Braathen, A., Olaussen, S., and Osmundsen, P.: Evidence of faulting contradicts a quiescent northern Barents Shelf during the Triassic, First Break, 31, 67–76, https://doi.org/10.3997/1365-2397.2013017, 2013.
- Backman, J., Jakobsson, M., Frank, M., Sangiorgi, F., Brinkhuis, H.,
  Stickley, C., O'Regan, M., Løvlie, R., Pälike, H., Spofforth, D.,
  Gattacecca, J., Moran, K., King, J., and Heil, C.: Age model and
  core-seismic integration for the Cenozoic Arctic Coring Expedition sediments from the Lomonosov Ridge, Paleoceanography,
  23, PS1S03, https://doi.org/10.1029/2007PA001476, 2008.
- Bajnai, D., Guo, W., Spötl, C., Coplen, T. B., Methner, K., Löffler, N., Krsnik, E., Gischler, E., Hansen, M., Henkel, D., and Price, G. D.: Dual clumped isotope thermometry resolves kinetic biases in carbonate formation temperatures, Nat. Commun., 11, 4005, https://doi.org/10.1038/s41467-020-17501-0, 2020.
- Baranyi, V., Miller, C. S., Ruffell, A., Hounslow, M. W., and Kürschner, W. M.: A continental record of the Carnian Pluvial Episode (CPE) from the Mercia Mudstone Group (UK): palynology and climatic implications, J. Geol. Society, 176, 149–166, 2019.
- Beauchamp, B. and Grasby, S. E.: Permian lysocline shoaling and ocean acidification along NW Pangea led to carbonate eradication and chert expansion, Palaeogeogr. Palaeoclimatol. Palaeoecol., 350, 73–90, 2012.
- Bédard, J. H., Saumur, B. M., Tegner, C., Troll, V. R., Deegan, F. 100 M., Evenchick, C. A., Grasby, S. E., and Dewing, K.: Geochemical systematics of High Arctic Large Igneous Province continental tholeites from Canada – evidence for progressive crustal

- contamination in the plumbing system, J. Petrol., 62, egab041, https://doi.org/10.1093/petrology/egab041, 2021.
- Benton, M. J., Bernardi, M., and Kinsella, C.: The Carnian Pluvial Episode and the origin of dinosaurs, J. Geol. Soc., 175, 1019– 1026, 2018.
- Beranek, L. P., Gee, D. G., and Fisher, C. M.: Detrital zircon U-Pb-Hf isotope signatures of Old Red Sandstone strata constrain the Silurian to Devonian paleogeography, tectonics, and crustal evolution of the Svalbard Caledonides, GSA Bull., 132, 1987–2003, https://doi.org/10.1130/b35318.1, 2020.
- Bergh, S., Maher Jr., H., and Braathen, A.: Late Devonian transpressional tectonics in Spitsbergen, Svalbard, and implications for basement uplift of the Sørkapp–Hornsund High, J. Geol. Soc., 168, 441–456, 2011.
- 15 Bergh, S. G., Braathen, A., and Andresen, A.: Interaction of Basement-Involved and Thin-Skinned Tectonism in the Tertiary Fold-Thrust Belt of Central Spitsbergen, Svalbard, AAPG Bull., 81, 637–661, https://doi.org/10.1306/522b43f7-1727-11d7-8645000102c1865d, 1997.
- 20 Bergström, S. M.: Conodonts as paleotemperature tools in Ordovician rocks of the Caledonides and adjacent areas in Scandinavia and the British Isles, Geol. Fören. Stock. För., 102, 377–392, 1980.
- Bernardi, M., Petti, F. M., and Benton, M. J.: Tetrapod distribution and temperature rise during the Permian—Triassic mass extinction, P. Roy. Soc. B, 285, 20172331, https://doi.org/10.1098/rspb.2017.2331, 2018.
- Berndt, C., Planke, S., Alvarez Zarikian, C. A., Frieling, J., Jones, M. T., Millett, J. M., Brinkhuis, H., Bünz, S., Svensen, H. H.,
- Longman, J., Scherer, R. P., Karstens, J., Manton, B., Nelissen, M., Reed, B., Faleide, J. I., Huismans, R. S., Agarwal, A., Andrews, G. D. M., Betlem, P., Bhattacharya, J., Chatterjee, S., Christopoulou, M., Clementi, V. J., Ferré, E. C., Filina, I. Y., Guo, P., Harper, D. T., Lambart, S., Mohn, G., Nakaoka, R., Tegner, C.,
- Varela, N., Wang, M., Xu, W., and Yager, S. L.: Shallow-water hydrothermal venting linked to the Palaeocene–Eocene Thermal Maximum, Nat. Geosci., 16, 803–809, 2023.
- Berner, R. A.: Paleozoic atmospheric CO<sub>2</sub>: importance of solar radiation and plant evolution, Science, 261, 68–70, https://doi.org/10.1126/science.261.5117.68, 1993.
- Berner, R. A.: The rise of trees and how they changed Paleozoic atmospheric CO<sub>2</sub>, climate, and geology, in: A History of Atmospheric CO<sub>2</sub> and Its Effects on Plants, Animals, and Ecosystems, 1–7 pp., New York, NY: Springer New York, https://doi.org/10.1007/0-387-27048-5\_1, 2005.
- Berry, C. M.: 'Hyenia'vogtii Høeg from the Middle Devonian of Spitsbergen Its morphology and systematic position, Rev. Palaeobot. Palynol., 135, 109–116, 2005.
- Berry, C. M. and Marshall, J. E. A.: Lycopsid forests in the early Late Devonian paleoequatorial zone of Svalbard, Geology, 43, 1043–1046, https://doi.org/10.1130/g37000.1, 2015.
- Betlem, P., Rodés, N., Birchall, T., Dahlin, A., Smyrak-Sikora, A., and Senger, K.: Svalbox Digital Model Database: A geoscientific window into the High Arctic, Geosphere, 19, 1640–1666, 2023.
- 55 Betlem, P., Birchall, T., Lord, G., Oldfield, S., Nakken, L., Ogata, K., and Senger, K.: High-resolution digital outcrop model of the faults, fractures, and stratigraphy of the Agardhfjellet Formation cap rock shales at Konusdalen West, central Spitsbergen, Earth

- Syst. Sci. Data, 16, 985—1006, https://doi.org/10.5194/essd-16-985-2024, 2024.
- Biakov, A. S., Zakharov, Y. D., Horacek, M., Richoz, S., Kutygin, R.
  V., Ivanov, Y. Y., Kolesov, E. V., Konstantinov, A. G., Tuchkova,
  M. I., and Mikhalitsyna, T. I.: New data on the structure and age of the terminal Permian strata in the South Verkhoyansk region (northeastern Asia), Russ. Geol. Geophys.+, 57, 282–293, 2016.
- Bjerager, M., Alsen, P., Bojesen-Koefoed, J. A., Fyhn, M. B. W., Hovikoski, J., Keulen, N., Lindström, S., Therkelsen, J., and Thomsen, T. B.: Triassic in the northernmost Atlantic Linking North Greenland and the southwestern Barents Sea, Terra Nova, 35, 250–259, https://doi.org/10.1111/ter.12649, 2023.
- Black, B. A., Lamarque, J.-F., Shields, C. A., Elkins-Tanton, L. T., and Kiehl, J. T.: Acid rain and ozone depletion from pulsed Siberian Traps magmatism, Geology, 42, 67–70, https://doi.org/10.1130/g34875.1, 2014.
- Blakey, R.: Paleotectonic and paleogeographic history of the Arctic region, Atl. Geol., 57, 007–039, 2021.
- Blattmann, F. R., Schneebeli-Hermann, E., Adatte, T., Bucher, H. F., Vérard, C., Hammer, Ø., Luz, Z. A. S., and Vennemann, T. W.: Palaeoenvironmental variability and carbon cycle perturbations during the Smithian-Spathian (Early Triassic) in Central Spitsbergen, Lethaia, 57, 1–14, 2024.
- Blinova, M., Thorsen, R., Mjelde, R., and Faleide, J. I.: Structure and evolution of the Bellsund Graben between Forlandsundet and Bellsund (Spitsbergen) based on marine seismic data, Norw. J. Geol., 89, 215–228, 2009.
- Blinova, M., Faleide, J. I., Gabrielsen, R. H., and Mjelde, R.: Analysis of structural trends of sub-sea-floor strata in the Isfjorden area of the West Spitsbergen Fold-and-Thrust Belt based on multichannel seismic data, J. Geol. Soc., 170, 657–668, https://doi.org/10.1144/jgs2012-109, 2013.
- Blomeier, D., Wisshak, M., Dallmann, W., Volohonsky, E., and Freiwald, A.: Facies analysis of the old Red Sandstone of Spitsbergen (Wood Bay Formation): Reconstruction of the depositional environments and implications of basin development, Facies, 49, 151–174, https://doi.org/10.1007/s10347-003-0030-1, 95 2003a.
- Blomeier, D., Wisshak, M., Joachimski, M., Freiwald, A., and Volohonsky, E.: Calcareous, alluvial and lacustrine deposits in the Old Red Sandstone of central north Spitsbergen (Wood Bay Formation, Early Devonian), Norw. J. Geol./Norsk Geologisk Forening, 100 83, 281–298, 2003b.
- Blomeier, D., Scheibner, C., and Forke, H.: Facies arrangement and cyclostratigraphic architecture of a shallow-marine, warm-water carbonate platform: the Late Carboniferous Ny Friesland Platform in eastern Spitsbergen (Pyefjellet Beds, 105 Wordiekammen Formation, Gipsdalen Group), Facies, 55, 291–324, https://doi.org/10.1007/s10347-008-0163-3, 2009.
- Blomeier, D., Dustira, A., Forke, H., and Scheibner, C.: Environmental change in the Early Permian of NE Svalbard: from a warm-water carbonate platform (Gipshuken Formation) to a temperate, mixed siliciclastic-carbonate ramp (Kapp Starostin Formation), Facies, 57, 493–523, https://doi.org/10.1007/s10347-010-0243-z, 2011.
- Blomeier, D., Dustira, A. M., Forke, H., and Scheibner, C.: Facies analysis and depositional environments of a storm-dominated, 115 temperate to cold, mixed siliceous-carbonate ramp: the Permian

- Kapp Starostin Formation in NE Svalbard, Norw. J. Geol., 93, 75–93, 2013.
- Blumenberg, M., Weniger, P., Kus, J., Scheeder, G., Piepjohn, K., Zindler, M., and Reinhardt, L.: Geochemistry of a middle Devonian cannel coal (Munindalen) in comparison with Carbonifer-
- ous coals from Svalbard, Arktos, 4, 1–8, 2018.
- Blythe, A. E. and Kleinspehn, K. L.: Tectonically versus climatically driven Cenozoic exhumation of the Eurasian plate margin, Svalbard: Fission track analyses, Tectonics, 17, 621–639, 1998.
- 10 Bodin, S., Meissner, P., Janssen, N. M., Steuber, T., and Mutter-lose, J.: Large igneous provinces and organic carbon burial: Controls on global temperature and continental weathering during the Early Cretaceous, Global Planet. Change, 133, 238–253, 2015.
- Bond, D. P., Wignall, P. B., and Grasby, S. E.: The Capitanian (Guadalupian, Middle Permian) mass extinction in NW Pangea (Borup Fiord, Arctic Canada): A global crisis driven by volcanism and anoxia, GSA Bull., 132, 931–942, https://doi.org/10.1130/B35281.1, 2020.
- Bond, D. P. G., Wignall, P. B., Joachimski, M. M., Sun, Y., Savov, I., Grasby, S. E., Beauchamp, B., and Blomeier, D. P. G.: An abrupt extinction in the Middle Permian (Capitanian) of the Boreal Realm (Spitsbergen) and its link to anoxia and acidification, GSA Bull., 127, 1411–1421, https://doi.org/10.1130/b31216.1, 2015.
- 25 Bottini, C., Erba, E., Tiraboschi, D., Jenkyns, H. C., Schouten, S., and Sinninghe Damsté, J. S.: Climate variability and ocean fertility during the Aptian Stage, Clim. Past, 11, 383–402, https://doi.org/10.5194/cp-11-383-2015, 2015.
- Boucot, A. J., Xu, C., and Scotese, C. R.: Phanerozoic Paleoclimate:

  An Atlas of Lithologic Indicators of Climate, SEPM Concepts in Sedimentology and Paleontology, (Print-on-Demand Version),

  No. 11, 478 pp., ISBN 978-1-56576-289-3, 2013.
  - Braathen, A. and Bergh, S. G.: Kinematics of Tertiary deformation in the basement-involved fold-thrust complex, western Norden-
- skiøld Land, Svalbard: tectonic implications based on fault-slip data analysis, Tectonophysics, 249, 1–29, 1995.
- Braathen, A., Bergh, S., and Maher Jr, H.: Structural outline of a Tertiary Basement-cored uplift/inversion structure in western Spitsbergen, Svalbard: Kinematics and controlling factors, Tectonics, 14, 95–119, 1995.
- Braathen, A., Bergh, S. G., and Maher Jr., H. D.: Application of a critical wedge taper model to the Tertiary transpressional fold-thrust belt on Spitsbergen, Svalbard, GSA Bull., 11, 1468–1485, https://doi.org/10.1130/0016-7606(1999)111<1468:Aoacwt>2.3.Co;2 1999.
- Braathen, A., Bælum, K., Maher Jr, H., and Buckley, S. J.: Growth of extensional faults and folds during deposition of an evaporite-dominated half-graben basin; the Carboniferous Billefjorden Trough, Svalbard, Norw. J. Geol., 91, 137–160, 2012.
- 50 Braathen, A., Osmundsen, P. T., Maher, H., and Ganerød, M.: The Keisarhjelmen detachment records Silurian–Devonian extensional collapse in northern Svalbard, Terra Nova, 30, 34–39, 2018.
- Bratvold, J.: Chondrichthyans from the Grippia bonebed (Early Triassic) of Marmierfjellet, Spitsbergen (Master's thesis, University od Oslo), https://doi.org/10.17850/njg98-2-03, 2016.
  - Breda, A., Preto, N., Roghi, G., Furin, S., Meneguolo, R., Ragazzi, E., Fedele, P., and Gianolla, P.: The Carnian Pluvial Event in the

- Tofane area (Cortina d'Ampezzo, Dolomites, Italy), Geo. Alp, 6, 80–115, 2009.
- Brinkhuis, H., Schouten, S., Collinson, M. E., Sluijs, A., Damsté, J. S. S., Dickens, G. R., Huber, M., Cronin, T. M., Onodera, J., and Takahashi, K.: Episodic fresh surface waters in the Eocene Arctic Ocean, Nature, 441, 606–609, 2006.
- Bruhn, R. and Steel, R.: High-resolution sequence stratigraphy of a clastic foredeep succession (Paleocene, Spitsbergen): An example of peripheral-bulge-controlled depositional architecture, J. Sedim. Res., 73, 745–755, 2003.
- Brune, S., Williams, S. E., and Müller, R. D. Potential links between continental rifting, CO<sub>2</sub> degassing and 70 climate change through time, Nat. Geosci., 10, 941–946, https://doi.org/10.1038/s41561-017-0003-6, 2017.
- Bryan, S. E. and Ernst, R. E.: Revised definition of large igneous provinces (LIPs), Earth-Sci. Rev., 86, 175–202, 2008.
- Buchan, K. L. and Ernst, R. E.: A giant circumferential dyke 75 swarm associated with the High Arctic Large Igneous Province (HALIP), Gondwana Res., 58, 39–57, 2018.
- Buchan, S., Challinor, A., Harland, W., and Parker, J.: The Triassic stratigraphy of Svalbard, Norsk Polarinst. Skrifter, 135, 1829, 1965.
- Buggisch, W., Blomeier, D., and Joachimski, M. M.: Facies, diagenesis and carbon isotopes of the Early Permian Gipshuken Formation (Svalbard). Zeitschrift der Deutschen Gesellschaft für Geowissenschaften, 163, 309–321, https://doi.org/10.1127/1860-1804/2012/0163-0309, 2012.
- Burger, B. J., Vargas Estrada, M., and Gustin, M. S.: What caused Earth's largest mass extinction event? New evidence from the Permian-Triassic boundary in northeastern Utah, Global Planet. Change, 177, 81–100, https://doi.org/10.1016/j.gloplacha.2019.03.013, 2019.
- Burgess, S. D. and Bowring, S. A.: High-precision geochronology confirms voluminous magmatism before, during, and after Earth's most severe extinction, Sci. Adv., 1, e1500470, https://doi.org/10.1126/sciadv.1500470, 2015.
- Burgess, S. D., Bowring, S., and Shen, S. Z.: High-precision timeline for Earth's most severe extinction, P. Natl. Acad. Sci. USA, 111, 3316–3321, 2014.
- Burgess, S. D., Muirhead, J. D., and Bowring, S. A.: Initial pulse of Siberian Traps sills as the trigger of the end-Permian mass extinction, Nat. Commun., 8, 164, https://doi.org/10.1038/s41467-100 017-00083-9, 2017.
- Canadell, J. G., Monteiro, P. M., Costa, M. H., Cotrim da Cunha, L., Cox, P. M., Eliseev, A. V., ... and Zickfeld, K.: 1830 Intergovernmental Panel on Climate Change (IPCC). Global carbon and other biogeochemical cycles and feedbacks, in: Climate change 105 2021: The physical science basis. Contribution of working group I to the sixth assessment report of the intergovernmental panel on climate change 673–816 pp., Cambridge University Press, 2023.
- Capelli, I. A., Scasso, R. A., Spangenberg, J. E., Kietzmann, 110 D. A., Cravero, F., Duperron, M., and Adatte, T.: Mineralogy and geochemistry of deeply-buried marine sediments of the Vaca Muerta-Quintuco system in the Neuquén Basin (Chacay Melehue section), Argentina: Paleoclimatic and paleoenvironmental implications for the global Tithonian-Valanginian 115 reconstructions, J. South Am. Earth Sci., 107, 103103, https://doi.org/10.1016/j.jsames.2020.103103, 2021.

- Cavalheiro, L., Wagner, T., Steinig, S., Bottini, C., Dummann, W., Esegbue, O., Gambacorta, G., Giraldo-Gómez, V., Farnsworth, A., and Flögel, S.: Impact of global cooling on Early Cretaceous high pCO<sub>2</sub> world during the Weissert Event, Nat. Commun., 12, 5411, https://doi.org/10.1038/s41467-021-25706-0, 2021.
- Celestino, R., Wohlwend, S., Reháková, D., and Weissert, H.: Carbon isotope stratigraphy, biostratigraphy and sedimentology of the Upper Jurassic–Lower Cretaceous Rayda Formation, Central Oman Mountains, Newsl. Stratigr., 50, 91–109, 2017.
- Cepek, P. and Krutzsch, W.: Conflicting interpretations of the Tertiary Biostratigraphy of Spitsbergen and New Palynological Results, in: Intra-continental fold belts, CASE 1: West Spitsbergen, edited by: Tessensohn F., Geologisches Jahrbuch Reihe B, Polar Issue 7. Federal Institute for Geosciences and Natural Resources,
   Hannover, 551–602 pp., ISBN 3-510-95834-9, 2001.
  - Charles, A. J., Condon, D. J., Harding, I. C., Pälike, H., Marshall, J. E., Cui, Y., Kump, L., and Croudace, I. W.: Constraints on the numerical age of the Paleocene-Eocene boundary, Geochem. Geophys. Geosyst., 12, https://doi.org/10.1029/2010GC003426, 2011.
  - Chambers, L. M., Pringle, M. S., and Fitton, J. G.: Phreatomagmatic eruptions on the Ontong Java Plateau: an Aptian <sup>40</sup>Ar/<sup>39</sup>Ar age for volcaniclastic rocks at ODP Site 1184, Geol. Soc. London, Special Publications, 229, 325–331 pp., https://etheses.whiterose.ac.uk/id/eprint/21133/1/589040.pdf 1832, 2004.
- Chen, J., Shen, S., Li, X., Xu, Y., Joachimski, M. M., Bowring, S. A., Erwin, D. H., Yuan, D., Chen, B., Zhang, H., Wang, Y., Cao, C., Zheng, Q., and Mu, L.: High-resolution SIMS oxygen isotope analysis on condodont apatite from South China and implications for the end-Permian mass extinction, Palaeogeogr. Palaeoclimatol. Palaeoecol., 448, 26–38, 2016.
- Chen, Z. Q., Tong, J., and Fraiser, M. L.: Trace fossil evidence for restoration of marine ecosystems following the end-Permian mass extinction in the Lower Yangtze region, South China, Palaeogeogr. Palaeoclimatol. Palaeoecol., 299, 449–474, 2011.
- Clemmensen, A. and Thomsen, E.: Palaeoenvironmental changes across the Danian–Selandian boundary in the North Sea Basin, Palaeogeogr. Palaeoclimatol. Palaeoecol., 219, 351–394, https://doi.org/10.1016/j.palaeo.2005.01.005, 2005.
- 40 Clifton, A.: The Eocene flora of Svalbard and its climatic significance, unpublished PhD Thesis, The University of Leeds, Leeds, 401 pp., https://etheses.whiterose.ac.uk/id/eprint/21133/1/589040.pdf 1833, 2012.
- Corfu, F., Polteau, S., Planke, S., Faleide, J. I., Svensen, H., Zayoncheck, A., and Stolbov, N.: U–Pb geochronology of Cretaceous magmatism on Svalbard and Franz Josef Land, Barents Sea large igneous province, Geol. Mag., 150, 1127–1135, https://doi.org/10.1017/S0016756813000162, 2013.
- Cui, Y.: Carbon addition during the Paleocene-Eocene Thermal
  Maximum: model inversion of a new, high-resolution carbon isotope record from Svalbard, (Master Thesis, The Pennsylvania
  State University), 1834, 2010.
- Cui, Y., Kump, L. R., Ridgwell, A. J., Charles, A. J., Junium, C. K.,
  Diefendorf, A. F., Freeman, K. H., Urban, N. M., and Harding, I.
  C.: Slow release of fossil carbon during the Palaeocene–Eocene
  Thermal Maximum, Nat. Geosci., 4, 481–485, 2011.
- Cui, Y., Kump, L. R., and Ridgwell, A.: Spatial and temporal patterns of ocean acidification during the end-Permian mass extinction-An Earth system model evaluation, in: Volcanism

- and global environmental change, 291–307 pp., Cambridge University Press, https://doi.org/10.1017/CBO9781107415683.023, 2015.
- Cui, Y., Diefendorf, A. F., Kump, L. R., Jiang, S., and Freeman, K. H.: Synchronous marine and terrestrial carbon cycle perturbation in the high arctic during the PETM, Paleoceanogr. Paleoclimatol., 36, e2020PA003942, https://doi.org/10.1029/2020PA003942, 2021.
- Cutbill, J. and Challinor, A.: Revision of the stratigraphical scheme for the Carboniferous and Permian rocks of Spitsbergen and Bjørnøya, Geol. Mag., 102, 418–439, 1965.
- Daëron, M., Drysdale, R. N., Peral, M., Huyghe, D., Blamart, D., Coplen, T. B., Lartaud, F., and Zanchetta, G.: Most Earth-surface calcites precipitate out of isotopic equilibrium, Nat. Commun., 10, 429, https://doi.org/10.1038/s41467-019-08336-5, 2019.
- Dal Corso, J., Ruffell, A., and Preto, N.: The Carnian Pluvial 75 Episode (Late Triassic): New insights into this important time of global environmental and biological change, J. Geol. Soc., 175, 986–988, 2018.
- Dal Corso, J., Mills, B. J., Chu, D., Newton, R. J., and Song, H.: Background Earth system state amplified Carnian (Late Triassic) environmental changes, Earth Planet. Sci. Lett., 578, 117321, https://doi.org/10.1016/j.epsl.2021.117321, 2022.
- Dalland, A.: Erratic clasts in the Lower Tertiary deposits of Svalbard–evidence of transport by winter ice, Norsk Polarinstitutt Arbok, 151–165, 1976.
- Dalland, A.: Mesozoic sedimentary succession at Andoy, northern Norway, and relation to structural development of the North Atlantic area, Geology of the North Atlantic Borderlands Memoir 7, CSPG Special Publications 563–584, ISSS, 1981. ISSS
- Dallmann, W. (Ed.): Lithostratigraphic lexicon of Svalbard. Norwegian Polar Institute, 1837, 1999.
- Dallmann, W. K., Andresen, A., Bergh, S. G., Maher Jr., H. D., and
   Ohta, Y.: Tertiary fold-and-thrust belt of Spitsbergen, Svalbard,
   Norsk Polarinstitutt, *Meddelelser* Nr 128, Oslo, 1838, 1993.
- Dallmann, W. K., Gjelberg, J. G., Harland, W. B., Johannessen, E. 95 P., Keilen, H. B., Lønøy, A., Nilson, I., and Worsley, D.: Upper palaeozoic lithostratigraphy, in: Lithostratigraphic Lexicon of Svalbard, edited by: Dallmann, W. K., Norsk Polarinstitutt, Tromsø, 25–126 pp., 1839, 1999.
- Dallmann, W. K. E. (Ed.): Geoscience Atlas of Svalbard, Norsk Polarinst. Rapportserie, 148, http://hdl.handle.net/11250/2580810 (last access: 1540), 2015.
- Dalseg, T. S., Nakrem, H. A., and Smelror, M.: Dinoflagellate cyst biostratigraphy, palynofacies, depositional environment and sequence stratigraphy of the Agardhfjellet Formation (Upper 105 Jurassic-Lower Cretaceous) in central Spitsbergen (Arctic Norway), Norw. J. Geol., 96, 1–14, 2016.
- Davies, N. S., Berry, C. M., Marshall, J. E., Wellman, C. H., and Lindemann, F.-J.: The Devonian landscape factory: plant–sediment interactions in the Old Red Sandstone of Svalbard and the rise of vegetation as a biogeomorphic agent, J. Geol. Soc., 178, 1–27, https://doi.org/10.1144/jgs2020-225, 2021.
- Davis, W. J., Schroeder-Adams, C. J., Galloway, J. M., Herrle, J. O., and Pugh, A. T.: U-Pb geochronology of bentonites from the Upper cretaceous Kanguk Formation, Sverdrup 115 Basin, Arctic Canada: constraints on sedimentation rates, biostratigraphic correlations and the late magmatic history of the

- High Arctic large Igneous Province, Geol. Mag., 154, 757–776, https://doi.org/10.1017/S0016756816000376, 2017.
- Delsett, L. L., Novis, L. K., Roberts, A. J., Koevoets, M. J., Hammer, Ø., Druckenmiller, P. S., and Hurum, J. H.: The Slottsmøya
- marine reptile Lagerstätte: depositional environments, taphonomy and diagenesis, Geological Society, London, Special Publications, 434, 165–188, 2016.
- Delsett, L. L., Roberts, A. J., Druckenmiller, P. S., and Hurum, J. H.: A new ophthalmosaurid (Ichthyosauria) from Svalbard, Norway, and evolution of the ichthyopterygian pelvic girdle, PloS One, 12, e0169971, https://doi.org/10.1371/journal.pone.0169971, 2017.
- Dickens, G. R., O'Neil, J. R., Rea, D. K., and Owen, R. M.: Dissociation of oceanic methane hydrate as a cause of the carbon isotope excursion at the end of the Paleocene, Paleoceanography, 10, 965–971, 1995.
- Dimakis, P., Braathen, B. I., Faleide, J. I., Elverhøi, A., and Gudlaugsson, S. T.: Cenozoic erosion and the preglacial uplift of the Svalbard–Barents Sea region, Tectonophysics, 300, 311–327, https://doi.org/10.1016/S0040-1951(98)00245-5, 1998a.
- Dimakis, P., Braathen, B. I., Faleide, J. I., Elverhøi, A., and Gudlaugsson, S. T.: Cenozoic erosion and the preglacial uplift of the Svalbard–Barents Sea region, Tectonophysics, 300, 311–327, 1998b.
- <sup>25</sup> Ditchfield, P. W.: High northern palaeolatitude Jurassic-Cretaceous palaeotemperature variation: new data from Kong Karls Land, Svalbard, Palaeogeogr. Palaeoclimatol. Palaeoecol., 130, 163– 175, 1997.
- Dockman, D., Pearson, D., Heaman, L., Gibson, S., and Sarkar, C.: Timing and origin of magmatism in the Sverdrup Basin, Northern Canada Implications for lithospheric evolution in the High Arctic Large Igneous Province (HALIP), Tectonophysics, 742, 50–65, 2018.
- Dodd, S. C., Mac Niocaill, C., and Muxworthy, A. R.: Long duration (> 4 Ma) and steadystate volcanic activity in the early cretaceous Paraná-Etendeka Large Igneous Province: new palaeomagnetic data from Namibia, Earth Planet. Sci. Lett., 414, 16–29, 2015.
- Doerner, M., Berner, U., Erdmann, M., and Barth, T.: Geochemical characterization of the depositional environment of Paleocene and Eocene sediments of the Tertiary Central Basin of Svalbard, Chem. Geol., 542, 119587, https://doi.org/10.1016/j.chemgeo.2020.119587, 2020.
- Drachev, S.: Fold belts and sedimentary basins of the Eurasian Arctic, Arktos, 2, 21, 1–30, https://doi.org/10.1007/s41063-015-0014-8, 2016.
  - Duchamp-Alphonse, S., Gardin, S., Fiet, N., Bartolini, A., Blamart, D., and Pagel, M.: Fertilization of the northwestern Tethys (Vocontian basin, SE France) during the Valanginian carbon isotope perturbation: evidence from calcareous nannofossils and trace el-
- ement data, Palaeogeogr. Palaeoclimatol. Palaeoecol., 243, 132–151, 2007.
- Dummann, W., Schröder-Adams, C., Hofmann, P., Rethemeyer, J., and Herrle, J. O.: Carbon isotope and sequence stratigraphy of
- the upper Isachsen Formation on Axel Heiberg Island (Nunavut, Canada): High Arctic expression of oceanic anoxic event 1a in a deltaic environment, Geosphere, 17, 501–519, 2021.
- Dummann, W., Wennrich, V., Schröder-Adams, C. J., Leicher, N., and Herrle, J. O.: Ash deposits link Oceanic Anoxic

- Event 2 to High Arctic volcanism, Geology, 52, 927–932, 60 https://doi.org/10.1130/G52368.1, 2024.
- Dustira, A. M., Wignall, P. B., Joachimski, M., Blomeier, D., Hartkopf-Fröder, C., and Bond, D. P. G.: Gradual onset of anoxia across the Permian–Triassic Boundary in Svalbard, Norway, Palaeogeogr. Palaeoclimatol. Palaeoecol., 374, 303–313, https://doi.org/10.1016/j.palaeo.2013.02.004, 2013.
- Dypvik, H., Riber, L., Burca, F., Rüther, D., Jargvoll, D., Nagy, J., and Jochmann, M.: The Paleocene–Eocene thermal maximum (PETM) in Svalbard clay mineral and geochemical signals, Palaeogeogr. Palaeoclimatol. Palaeoecol., 302, 156–169, 2011.
- Dörr, N., Clift, P., Lisker, F., and Spiegel, C.: Why is Svalbard an island? Evidence for two-stage uplift, magmatic underplating, and mantle thermal anomalies, Tectonics, 32, 473–486, 2013.
- Dzyuba, O. S., Izokh, O. P., and Shurygin, B. N.: Carbon isotope excursions in Boreal Jurassic-Cretaceous 75 boundary sections and their correlation potential, Palaeogeogr. Palaeoclimatol. Palaeoecol., 381–382, 33–46, https://doi.org/10.1016/j.palaeo.2013.04.013, 2013.
- Eberle, J. and Greenwood, D.: Life at the top of the greenhouse Eocene world–A review of the Eocene flora and vertebrate fauna so from Canada's High Arctic, Geol. Soc. Am. Bull., 124, 3–23, https://doi.org/10.1130/B30571.1, 2012.
- Edwards, C. T. and Saltzman, M. R.: Paired carbon isotopic analysis of Ordovician bulk carbonate ( $\delta^{13}$ Ccarb) and organic matter ( $\delta^{13}$ Corg) spanning the Great Ordovician Biodiversification Event, Palaeogeogr. Palaeoclimatol. Palaeoecol., 458, 102–117, 2016.
- Ekeheien, C., Delsett, L. L., Roberts, A. J., and Hurum, J. H.: Preliminary report on ichthyopterygian elements from the Early Triassic (Spathian) of Spitsbergen, Norw. J. Geol., 98, 219–238, 90 2018.
- Eldrett, J., Greenwood, D., Harding, I., and Huber, M.: Increased seasonality in the latest Eocene to earliest Oligocene in northern high latitudes, Nature, 459, 969–973, 2009.
- Eldrett, J. S., Harding, I. C., Firth, J. V., and Roberts, A. P.: Magnetostratigraphic calibration of Eocene–Oligocene dinoflagellate cyst biostratigraphy from the Norwegian–Greenland Sea, Mar. Geol., 204, 91–127, 2004.
- Engelschiøn, V. S., Delsett, L. L., Roberts, A. J., and Hurum, J. H.:

  Large-sized ichthyosaurs from the Lower Saurian niveau of the 100

  Vikinghøgda formation (Early Triassic), Marmierfjellet, Spitsbergen, Norw. J. Geol., 98, 239–266, 2018.
- Engelschiøn, V. S., Bernhardsen, S., Wesenlund, F., Hammer, Ø., Hurum, J. H., and Mørk, A.: Bivalve beds reveal rapid changes in ocean oxygenation in the Boreal Middle Triassic—a 105 case study from Svalbard, Norway, Norw. J. Geol.,, 103, 1–25, https://doi.org/10.17850/njg103-2-1, 2023.
- Erba, E., Bartolini, A., and Larson, R. L.: Valanginian Weissert oceanic anoxic event, Geology, 32, 149–152, 2004.
- Ernst, R. E. and Youbi, N.: How Large Igneous Provinces affect 110 global climate, sometimes cause mass extinctions, and represent natural markers in the geological record, Palaeogeogr. Palaeoclimatol. Palaeoecol., 478, 30–52, 2017.
- Estes, R. and Hutchinson, J. H.: Eocene Lower Vertebrates from Ellesmere Island, Canadian Arctic Archipelago, Palaeogeogr. 115 Palaeocl., 30, 325–347, 1980.
- Estrada, S. and Henjes-Kunst, F.: <sup>40</sup>Ar-<sup>39</sup>Ar and U-Pb dating of Cretaceous continental rift-related magmatism on the northeast

- Canadian Arctic margin, Z. Dtsch. Ges. Geowiss., 164, 107–130, 2013.
- Evans, D., Sagoo, N., Renema, W., Cotton, L. J., Müller, W., Todd, J. A., Saraswati, P. K., Stassen, P., Ziegler, M., and Pearson, P.
- N.: Eocene greenhouse climate revealed by coupled clumped isotope-Mg/Ca thermometry, P. Natl. Acad. Sci. USA, 115, 1174–1179, https://doi.org/10.1073/pnas.1714744115, 2018.
- Ezaki, Y., Kawamura, T., and Nakamura, K.: Kapp Starostin Formation in Spitsbergen: a sedimentary and faunal record of Late Permian palaeoenvironments in an Arctic region, in: Pangea: Global Environments and Resources Memoir 17, 647–655 pp., 1994.
- Fairchild, I. J.: The Orustdalen Formation of Brøggerhalvøya, Svalbard: A fan delta complex of Dinantian/Namurian age, Polar Res., 1982, 17–34, https://doi.org/10.1111/j.1751-8369.1982.tb00470.x, 1982.
- Faleide, J. I., Tsikalas, F., Breivik, A. J., Mjelde, R., Ritzmann, O., Engen, Ø., Wilson, J., and Eldholm, O.,: Structure and evolution of the continental margin off Norway and the Barents Sea, Episodes J. Int. Geosci., 31, 82–91, 2008.
- <sup>20</sup> Faleide, J. I., Pease, V., Curtis, M., Klitzke, P., Minakov, A., Scheck-Wenderoth, M., Kostyuchenko, S., and Zayonchek, A.: Tectonic implications of the lithospheric structure across the Barents and Kara shelves, Geological Society, London, Special Publications, 460, 285–314, https://doi.org/10.1144/SP460.18, 2018.
- 25 Fallatah, M. I., Alnazghah, M., Kerans, C., and Al-Hussaini, A.: Sedimentology and carbon isotope stratigraphy from the Late Jurassic Early Cretaceous of the Arabian plate: The Weissert event and the VOICE in the Tethys Realm?, Mar. Petrol. Geol., 161, 106670, https://doi.org/10.1016/j.marpetgeo.2023.106670, 2024
  - Feyling-Hanssen, R. W. and Ulleberg, K.: A Tertiary-Quaternary section at Sarsbukta, Spitsbergen, Svalbard, and its foraminifera, Polar Res.h, 2, 77–106, https://doi.org/10.3402/polar.v2i1.6963, 1984.
- 35 Fischer, A. G.: Climatic oscillations in the biosphere. Biotic crises in ecological and evolutionary time, Academic Press,, 331, 103– 131, https://doi.org/10.24382/4485, 1981.
  - Fischer, A. G.: Long-term climate oscillations recorded in stratigraphy, Climate in Earth history, Academy Press, Washington, D.C, 97–104, https://doi.org/10.17226/11798, 1982.
  - Fischer, A. G.: The two Phanerozoic supercycles, in: Catastrophes and Earth history, edited by: Berggren, W. A. and Van Couvering, J. A., Princetown University Press, 129–150, https://doi.org/10.1515/9781400853281.129, 1984.
- 45 Fortey, R. and Bruton, D.: Cambrian-Ordovician rocks adjacent to Hinlopenstretet, North Ny Friesland, Spitsbergen, Geol. Soc. Am. Bull., 84, 2227–2242, 1973.
  - Foster, W. J.: Palaeoecology of the late Permian mass extinction and subsequent recovery, Unpublished PhD thesis, Plymouth University, 1841, 2015.
  - Foster, W. J., Danise, S., Price, G. D., and Twitchett, R. J.: Subsequent biotic crises delayed marine recovery following the late Permian mass extinction event in northern Italy, PLoS One, 12, e0172321, https://doi.org/10.1371/journal.pone.0172321, 2017a.
- Foster, W. J., Danise, S., and Twitchett, R. J.: A silicified Early Triassic marine assemblage from Svalbard, J. Syst. Palaeontol., 15, 851–877, https://doi.org/10.1080/14772019.2016.1245680, 2017b.

- Foster, W. J., Lehrmann, D. J., Yu, M., Ji, L., and Martindale, R. C.: Persistent environmental stress delayed the recovery of marine communities in the aftermath of the latest Permian mass extinction, Paleoceanogr. Paleoclimatol., 33, 338–353, 2018.
- Foster, W. J., Hirtz, J. A., Farrell, C., Reistroffer, M., Twitchett, R. J., and Martindale, R. C.: Bioindicators of severe ocean acidification are absent from the end-Permian mass extinction, Sci. Rep., 12, 1202, https://doi.org/10.1038/s41598-022-04991-9, 2022.
- Foster, W. J., Asatryan, G., Rauzi, S., Botting, J., Buchwald, S., Lazarus, D., Isson, T., Renaudie, J., and Kiessling, W.: Response of Siliceous Marine Organisms to the Permian-Triassic Climate Crisis Based on New Findings From Central Spitsbergen, 70 Svalbard, Paleoceanogr. Paleoclimatol., 38, e2023PA004766, https://doi.org/10.22541/essoar.169447472.26881234/v1, 2023.
- Frakes, L. A. and Francis, J. E.; A guide to Phanerozoic cold polar climates from high-latitude ice-rafting in the Cretaceous, Nature, 333, 547–549, 1988.
- Frakes, L. A., Francis, J. E., and Syktus, J. I.: Climate modes of the Phanerozoic, Cambridge University Press, Cambridge, 274 pp., https://doi.org/10.1017/CBO9780511628948, 1992.
- Franks, P. J., Berry, J. A., Lombardozzi, D. L., and Bonan, G. B.: Stomatal Function across Temporal and Spatial Scales: Deep-Time Trends, Land-Atmosphere Coupling and Global Models, Plant Physiol., 174, 583–602, https://doi.org/10.1104/pp.17.00287, 2017.
- Friend, P.: Fluviatile sedimentary structures in the Wood Bay series (Devonian) of Spitsbergen, Sedimentology, 5, 39–68, 1965.
- Friend, P., Harland, W., Rogers, D., Snape, I., and Thornley, R.: Late Silurian and Early Devonian stratigraphy and probable strike-slip tectonics in northwestern Spitsbergen, Geol. Mag., 134, 459– 479, 1997.
- Friend, P. F.: The Devonian stratigraphy of north and central Spitsbergen, P. Yorks. Geol. Soc., 33, 77–118, https://doi.org/10.1144/pygs.33.1.77, 1961.
- Fyhn, M. B. W. and Hopper, J. R.: NE Greenland Composite Tectono-Sedimentary Element, northern Greenland Sea and Fram Strait, Geol. Soc. London, Memoirs, 57, 1843, https://doi.org/10.1144/M57-2017-12, 2025.
- Gabrielsen, R. H., Kløvjan, O. S., Haugsbø, H., Midbøe, P. S., Nøttvedt, A., Rasmussen, E., and Skott, P. H.: A structural outline of Forlandsundet Graben, Prins Karls Forland, Svalbard, Norsk Geol. Tidsskrift, 72, 105–120, 1992.
- Gale, A. S., Mutterlose, J., Batenburg, S., Gradstein, F. M., Agterberg, F. P., Ogg, J. G., and Petrizzo, M. R. 2020: The Cretaceous Period, in: Geological Time Scale 2020, edited by: Gradstein, F. M., Ogg, J. G., Schmitz, M. D., and Ogg, G. M., Elsevier, Boston, MA, 1023–1086 pp., 2020.
- Galfetti, T., Hochuli, P. A., Brayard, A., Bucher, H., Weissert, H., and Vigran, J. O.: Smithian-Spathian boundary event: Evidence for global climatic change in the wake of the end-Permian biotic crisis, Geology, 35, 291–294, https://doi.org/10.1130/g23117a.1, 2007.
- Galloway, J. M. and Lindström, S.: Impacts of Large-scale Magmatism on Land Plant Ecosystems, Elements, 19, 289–295, 2023a.

Galloway, J. M., Vickers, M. L., Price, G. D., Poulton, T., Grasby, S. E., Hadlari, T., Beauchamp, B., and Sulphur, K.: Finding the VOICE: organic carbon isotope chemostratigraphy of Late Juras-sic – Early Cretaceous Arctic Canada, Geol. Mag., 157, 1643–1657, https://doi.org/10.1017/s0016756819001316, 2020.

- Galloway, J. M., Fensome, R. A., Swindles, G. T., Hadlari, T., Fath, J., Schröder-Adams, C., Herrle, J. O., and Pugh, A.: Exploring the role of High Arctic Large Igneous Province volcanism on Early Cretaceous Arctic forests, Cretaceous Res., 129, 105022, https://doi.org/10.1016/j.cretres.2021.105022, 2022.
- Galloway, J. M., Grasby, S. E., Wang, F., Hadlari, T., Dewing, K., Bodin, S., and Sanei, H.: A mercury and trace element geochemical record across Oceanic Anoxic Event 1b in Arctic Canada, Palaeogeogr. Palaeoclimatol. Palaeoecol., 617, 111490, https://doi.org/10.1016/j.palaeo.2023.111490, 2023.
- Galloway, J. M., Hadlari, T., Dewing, K., Poulton, T., Grasby, S. E., Reinhardt, L., Rogov, M., Longman, J., and Vickers, M.: The silent VOICE Searching for geochemical markers to track the impact of Late Jurassic rift tectonics, Geochem. Geophys. Geosyst., 25, e2024GC011490, https://doi.org/10.1029/2024GC011490, 2024.
- Gastaldo, R. A., DiMichele, W. A., and Pfefferkorn, H. W.: Out of the icehouse into the greenhouse: a late Paleozoic analogue for modern global vegetational change, GSA Today, 6, 1–7, 1996.
- 20 Gee, D. G. and Teben'kov, A.: Svalbard: a fragment of the Laurentian margin, Geol. Soc. London, Memoirs, 30, 191–206, 2004.
  - Gee, D. G., Bogolepova, O. K., and Lorenz, H.: The Timanide, Caledonide and Uralide orogens in the Eurasian high Arctic, and relationships to the palaeo-continents Laurentia, Baltica and Siberia, Geol. Soc. London, Memoirs, 32, 507–520,
  - https://doi.org/10.1144/GSL.MEM.2006.032.01.31, 2006. Gensel, P. G.: The earliest land plants, Annu. Rev. Ecol. Evol. S., 39, 459–477, 2008.
- Gilmullina, A., Klausen, T. G., Doré, A. G., Rossi, V. M., Suslova, A., and Eide, C. H.: Linking sediment supply variations and tectonic evolution in deep time, source-to-sink systems The Triassic Greater Barents Sea Basin, GSA Bulletin, 134, 1760–1780, 2022.
- Gion, A. M., Williams, S. E., and Müller, R. D.: A reconstruction of the Eurekan Orogeny incorporating deformation constraints, Tectonics, 36, 304–320, 2017.
- Gjelberg, J. and Steel, R.: An outline of Lower-Middle Carboniferous sedimentation on Svalbard: Effects of tectonic, climatic and sea level changes in rift basin sequences, Geology of the North Atlantic Borderlands – Memoir, 7, 543–561, 1981.
- Gjelberg, J. and Steel, R. J.: Helvetiafjellet Formation (Barremian-Aptian), Spitsbergen: characteristics of a transgressive succession, Norwegian Petroleum Society Special Publications, Elsevier, 571–593 https://doi.org/10.1016/S0928-8937(06)80087-1, 1005
- Glørstad-Clark, E., Faleide, J. I., Lundschien, B. A., and Nystuen, J. P.: Triassic seismic sequence stratigraphy and paleogeography of the western Barents Sea area, Mar. Petrol. Geol., 27, 1448–1475, https://doi.org/10.1016/j.marpetgeo.2010.02.008, 2010
- 50 Gobbett, D. J. and Wilson, C.: The Oslobreen Series, Upper Hecla Hoek of Ny Friesland, Spitsbergen, Geol. Mag., 97, 441–457, 1960.
  - Golovneva, L. and Zolina, A.: The Renardodden flora of Spitsbergen, Biol. Commun., 68, 307–319, https://doi.org/10.21638/spbu03.2023.410, 2023.
  - Golovneva, L. B.: Palaeogene climates of Spitsbergen, GFF (Geological Society of Sweden), 122, 62–63, https://doi.org/10.1080/11035890001221062, 2000.

- Golovneva, L. B., Zolina, À. À., and Spicer, R. A.: The early Paleocene (Danian) climate of Svalbard based on palaeobotanical data, Papers in Palaeontology, 9, e1533, https://doi.org/10.1002/spp2.1533, 2023.
- Gomes, A. S. and Vasconcelos, P. M.: Geochronology of the Parana-Etendeka large igneous province, Earth Sci. Rev., 220, 103716, https://doi.org/10.1016/j.earscirev.2021.103716, 2021.
- Grasby, S., Sanei, H., and Beauchamp, B.: Catastrophic dispersion of coal fly ash into oceans during the latest Permian extinctionm Nat. Geosci., 4, 104–107. https://doi.org/10.1038/ngeo1069, 2011.
- Grasby, S. E. and Beauchamp, B.: Latest Permian to early Triassic basin-to-shelf anoxia in the Sverdrup Basin, Arctic Canada, Chem. Geol., 264, 232–246, 2009.
- Grasby, S. E. and Bond, D. P.: How large igneous provinces have killed most life on Earth – Numerous times, Elements, 19, 276– 281, 2023.
- Grasby, S. E., Beauchamp, B., Embry, A., and Sanei, H.: Recurrent Early Triassic Ocean anoxia, Geology, 41, 175–178, https://doi.org/10.1130/g33599.1, 2013.
- Grasby, S. E., Beauchamp, B., Bond, D. P. G., Wignall, P., Talavera, C., Galloway, J. M., Piepjohn, K., Reinhardt, L., and Blomeier, D.: Progressive environmental deterioration in northwestern Pangea leading to the latest Permian extinction, GSA Bull., 127, 1331–1347, https://doi.org/10.1130/b31197.1, 2015.
- Grasby, S. E., Beauchamp, B., Bond, D. P., Wignall, P. B., and Sanei, H.: Mercury anomalies associated with three extinction events (Capitanian crisis, latest Permian extinction and the Smithian/Spathian extinction) in NW Pangea, Geol. Mag., 153, 285–297, 2016a.
- Grasby, S. E., Beauchamp, B., and Knies, J.: Early Triassic productivity crises delayed recovery from world's worst mass extinction, Geology, 44, 779–782, 2016b.
- Grasby, S. E., McCune, G. E., Beauchamp, B., and Galloway, J. M.: Lower Cretaceous cold snaps led to widespread glendonite occurrences in the Sverdrup Basin, Canadian High Arctic, Bulletin, 129, 771–787, 2017.
- Grasby, S. E., Liu, X., Yin, R., Ernst, R. E., and Chen, Z.: Toxic mercury pulses into late Permian terrestrial and marine environments, Geology, 48, 830–833, https://doi.org/10.1130/g47295.1, 2020.
- Green, T., Renne, P. R., and Brenhin Kneller, C.: Continental flood basalts drive Phanerozoic extinctions, P. Natl. Acad. Sci. USA, 119, e2120441119, https://doi.org/10.1073/pnas.212044111, 2022.
- Green, P. F. and Duddy, I. R.: Synchronous exhumation events around the Arctic including examples from Barents Sea and 105 Alaska North Slope, in: Geological Society, London, Petroleum Geology Conference Series, Vol. 7, No. 1, 633–644 pp., London: The Geological Society of London, 2010.
- Greenwood, D. R., Basinger, J. F., and Smith, R. Y.: How wet was the Arctic Eocene rain forest? Estimates of precipita- 110 tion from Paleogene Arctic macrofloras, Geology, 38, 15–18, https://doi.org/10.1130/g30218.1, 2010.
- Grossman, E. L.: Applying Oxygen Isotope Paleothermometry in Deep Time, The Paleontological Society Papers, 18, 39–68, https://doi.org/10.1017/S1089332600002540, 2012.

Grossman, E. L., Yancey, T. E., Jones, T. E., Bruckschen, P., Chuvashov, B., Mazzullo, S. J., and Mii, H. S.: Glaciation, aridifica-

- tion, and carbon sequestration in the Permo-Carboniferous: the isotopic record from low latitudes, Palaeogeogr. Palaeoclimatol. Palaeoecol., 268, 222–233, 2008.
- Grundvåg, S.-A. and Olaussen, S.: Sedimentology of the Lower
   Cretaceous at Kikutodden and Keilhaufjellet, southern Spitsbergen: implications for an onshore-offshore link, Polar Res., 36, 1302124, https://doi.org/10.1080/17518369.2017.1302124, 2017.
- Grundvåg, S. A., Johannessen, E. P., Helland-Hansen, W., and Plink-Björklund, P.: Depositional architecture and evolution of progradationally stacked lobe complexes in the E ocene Central Basin of Spitsbergen, Sedimentology, 61, 535–569, https://doi.org/10.1111/sed.12067, 2014.
- Grundvåg, S. A., Marin, D., Kairanov, B., Śliwińska, K. K., Nøhr-Hansen, H., Jelby, M. E., Escalona, A., and Olaussen, S.: The Lower Cretaceous succession of the northwestern Barents Shelf: Onshore and offshore correlations, Mar. Petrol. Geol., 86, 834– 857, https://doi.org/10.1016/j.marpetgeo.2017.06.036, 2017.
- Grundvåg, S.-A., Jelby, M. E., Śliwińska, K. K., Nøhr-Hansen, H., Aadland, T., Sandvik, S. E., Tennvassås, I., Engen, T. M., and Olaussen, S.: Sedimentology and palynology of the Lower Cretaceous succession of central Spitsbergen: integration of subsurface and outcrop data, Norw. J. Geol., 99, 253–284, ISSN 0029-196X, https://doi.org/10.17850/njg99-2-02, 2019.
- 25 Grundvåg, S. A., Helland-Hansen, W., Johannessen, E. P., Eggenhuisen, J., Pohl, F., and Spychala, Y.: Deep-water sand transfer by hyperpycnal flows, the Eocene of Spitsbergen, Arctic Norway, Sedimentology, 70, 2057–2107, 2023.
- Gruszczyński, M., Hałas, S., Hoffman, A., and Małkowski, K.: A brachiopod calcite record of the oceanic carbon and oxygen isotope shifts at the Permian/Triassic transition, Nature, 337, 64–68, 1989.
- Gröcke, D. R., Price, G. D., Robinson, S. A., Baraboshkin, E. Y., Mutterlose, J., and Ruffell, A. H.: The Upper Valanginian (Early
- Cretaceous) positive carbon–isotope event recorded in terrestrial plants, Earth Planet. Sci. Lett., 240, 495–509, 2005.
- Guarnieri, P.: Pre-break-up palaeostress state along the East Greenland margin, J. Geol. Soc., 172, 727–739, https://doi.org/10.1144/jgs2015-053, 2015.
- 40 Gutjahr, M., Ridgwell, A., Sexton, P. F., Anagnostou, E., Pearson, P. N., Pälike, H., Norris, R. D., Thomas, E., and Foster, G. L.: Very large release of mostly volcanic carbon during the Palaeocene–Eocene Thermal Maximum, Nature, 548, 573–577, https://doi.org/10.1038/nature23646, 2017.
- <sup>45</sup> Haaland, L. C., Slagstad, T., Osmundsen, P. T., and Redfield, T.: U-Pb calcite ages date oblique rifting of the Arctic-North Atlantic gateway, Geology, 52, 615–619, 2024.
  - Hammer, Ø., Nakrem, H. A., Little, C. T., Hryniewicz, K., Sandy, M. R., Hurum, J. H., Druckenmiller, P., Knutsen, E. M., and
- Høyberget, M.: Hydrocarbon seeps from close to the Jurassic– Cretaceous boundary, Svalbard, Palaeogeogr. Palaeoclimatol. Palaeoecol., 306, 15–26, 2011.
- Hammer, Ø., Collignon, M., and Nakrem, H. A.: Organic carbon isotope chemostratigraphy and cyclostratigraphy in the Volgian of Svalbard, Norw. J. Geol., 92, 103–112, ISSN 029-196X, 2012.
- Hammer, Ø., Jones, M. T., Schneebeli-Hermann, E., Hansen, B. B., and Bucher, H.: Are Early Triassic extinction events associated with mercury anomalies? A reassessment of the Smithi-

- an/Spathian boundary extinction, Earth-Sci. Rev., 195, 179–190, https://doi.org/10.1016/j.earscirev.2019.04.016, 2019.
- Hansen, J. and Holmer, L. E.: Diversity fluctuations and biogeography of Ordovician brachiopod faunas in northeastern Spitsbergen, Bull. Geosci., 85, 497–504, 2010.
- Hansen, B. B., Bucher, H. F., Schneebeli-Hermann, E., and Hammer, Ø.: Smithian and Spathian palaeontological records of the Vikinghøgda Formation in Central Spitsbergen, Lethaia, 57, 1–15, 2024.
- Haq, B. U.: Cretaceous eustasy revisited, Global Planet. Change, I, 113, 44–58, https://doi.org/10.1016/j.gloplacha.2013.12.007, 2014.
- Harding, I. C., Charles, A. J., Marshall, J. E. A., Pälike, H., Roberts, A. P., Wilson, P. A., Jarvis, E., Thorne, R., Morris, E., Moremon, R., Pearce, R. B., and Akbari, S.: Sea-level and salinity fluctuations during the Paleocene–Eocene thermal maximum in Arctic Spitsbergen, Earth Planet. Sci. Lett., 303, 97–107, https://doi.org/10.1016/j.epsl.2010.12.043, 2011.
- Harland, W. B.: Geology of Svalbard, Svalbard, edited by: Harland, W. B., Geological Society, London, Memoirs, ISBN 1-897799-93-4, https://doi.org/10.1144/gsl.mem.1997.017.01.26, 1997.
- Harland, W. B. and Wilson, C.: The Hecla Hoek succession in Ny Friesland, Spitsbergen, Geol. Mag., 93, 265–286, 1956.
- Harland, W. B., Cutbill, J., Friend, P. F., Gobbett, D. J., Holliday, D., Maton, P., Parker, J., and Wallis, R. H.: The Billefjorden Fault Zone, Spitsbergen: the long history of a major tectonic lineament, Nor. Polarinst. Skr., 161, 1841, 1974.
- Harper, D. T., Suarez, M. B., Uglesich, J., You, H., Li, D., and Dodson, P.: Aptian–Albian clumped isotopes from northwest China: cool temperatures, variable atmospheric *p*CO<sub>2</sub> and regional shifts in the hydrologic cycle, Clim. Past, 17, 1607—1625, https://doi.org/10.5194/cp-17-1607-2021, 2021.
- Hatleberg, E. and Clark, D. L.: Lower Triassic conodonts and biofacies interpretations: Nepal and Svalbard, Geol. Palaeontol., 18, 101–125, 1984.
- Hayes, J. M., Strauss, H., and Kaufman, A. J.: The abundance of 13C in marine organic matter and isotopic fractionation in the 95 global biogeochemical cycle of carbon during the past 800 Ma, Chem. Geol., 161, 103–125, 1999.
- Head, M.: A palynological investigation of Tertiary strata at Renardodden, West Spitsbergen, 6th International Palynological Conference, Abstract, 61 pp., 1984.
- Helland-Hansen, W.: Sedimentation in Paleogene Foreland Basin, Spitsbergen, AAPG Bulletin, 74, 260–272, https://doi.org/10.1306/0c9b22bd-1710-11d7-8645000102c1865d, 1990.
- Helland-Hansen, W. and Grundvåg, S. A.: The Svalbard 105 Eocene-Oligocene (?) Central Basin succession: Sedimentation patterns and controls, Basin Res., 33, 729–753, https://doi.org/10.1111/bre.12492, 2021.
- Henderson, C. M. and Baud, A.: Correlation of the Permian-Triassic boundary in Arctic Canada and comparison with Meishan, 110 China, Proceedings, 30th International Geological Congress, 11, 143–152, 1997.
- Henriksen, E., Bjørnseth, H., Hals, T., Heide, T., Kiryukhina, T., Kløvjan, O., Larssen, G. B., Ryseth, A., Rønning, K., and Sollid, K.: Chapter 17 Uplift and erosion of the greater Barents Sea: impact on prospectivity and petroleum systems, Geol. Soc. Lond., 35, 271–281, 2011a.

- Henriksen, E., Ryseth, A. E., Larssen, G. B., Heide, T., Rønning, K., Sollid, K., and Stoupakova, A. V.: Chapter 10 Tectonostratigraphy of the greater Barents Sea: implications for petroleum systems, Geol. Soc. Lond., 35, 163–195, https://doi.org/10.1144/M35.10, 2011b.
- Herrle, J. O., Schröder-Adams, C. J., Davis, W., Pugh, A. T., Galloway, J. M., and Fath, J.: Mid-Cretaceous High Arctic stratigraphy, climate, and oceanic anoxic events, Geology, 43, 403–406, 2015.
- Hesselbo, S. P., Ogg, J. G., Ruhl, M., Hinnov, L. A., and Huang, C. J.: The Jurassic Period, in: Geological Time Scale 2020, edited by: Gradstein, F. M., Ogg, J. G., Schmitz, M. D., and Ogg, G. M., Elsevier, Boston, MA, 955–1021 pp., 2020.
- Heyn, B. H., Shephard, G. E., and Conrad, C. P.: Prolonged multi-phase magmatism due to plume-lithosphere interaction as applied to the High Arctic Large Igneous Province, Geochem. Geophys. Geosyst., 25, e2023GC011380, https://doi.org/10.1029/2023GC011380, 2024.
- Hjelstuen, B. O., Elverhøi, A., and Faleide, J. I.: Cenozoic erosion and sediment yield in the drainage area of the Storfjorden Fan, Global Planet. Change, 12, 95–117, 1996.
  - Hochuli, P. A., Hermann, E., Vigran, J. O., Bucher, H., and Weissert, H.: Rapid demise and recovery of plant ecosystems across the end-Permian extinction event, Global Planet. Change, 74, 144– 155, https://doi.org/10.1016/j.gloplacha.2010.10.004, 2010.
- Hoel, A. and Orvin, A. K.: Das Festungsprofil auf Spitzbergen. I, Karbon-Kreide: Vermessungsresultate, 1845, 1937.
- Hofmann, R., Goudemand, N., Wasmer, M., Bucher, H., and Hautmann, M.: New trace fossil evidence for an early recovery signal in the aftermath of the end-Permian mass extinction, Palaeogeogr. Palaeoclimatol. Palaeoecol., 310, 216–226, 2011.
- Hofmann, R., Hautmann, M., Brayard, A., Nützel, A., Bylund, K. G., Jenks, J. F., Vennin, E., Oliver, N., and Bucher, H., Recovery of benthic marine communities from the end-P ermian mass extinction at the low latitudes of eastern Panthalassa, Palaeontology, 57, 547–589, 2014.
- Hofmann, R., Hautmann, M., and Bucher, H., Recovery dynamics of benthic marine communities from the Lower Triassic Werfen Formation, northern Italy, Lethaia, 48, 474–496, 2015.
- 40 Holliday, D. and Cutbill, J.: The Ebbadalen Formation (Carboniferous), Spitsbergen, P. Yorks. Geol. Soc., 39, 1–32, 1972.
  - Holmden, C., Creaser, R. A., Muehlenbachs, K., Leslie, S. A., and Bergström, S. M.: Isotopic evidence for geochemical decoupling between ancient epeiric seas and bordering oceans: Implications for secular curves, Geology, 26, 567–570,
- https://doi.org/10.1130/0091-7613(1998)0262.3.Co;2, 1998.

  Hönisch B Ridgwell A Schmidt D Thomas F Gibbs S
- Hönisch, B., Ridgwell, A., Schmidt, D., Thomas, E., Gibbs, S., Sluijs, A., Zeebe, R., Kump, L., Martindale, R. C., Greene, S. E., Kiessling, W., Ries, J., Zachos, J. C., Royer, D., Barker, S.,
- Marchitto Jr., T. M., Moyer, R., Pelejero, C., Ziveri, P., Foster, G., and Williams, B.: The Geological Record of Ocean Acidification, Science, 335, 1058–1063, 2012.
- Horota, R. K., Rossa, P., Marques, A., Gonzaga, L., Senger, K., Cazarin, C. L., Spigolon, A., and Veronez, M. R.: An Immersive Virtual Field Experience Structuring Method for Geoscience Ed-
- Hochuli, P. A., Schneebeli-Hermann, E., Mangerud, G., and Bucher,H.: Evidence for atmospheric pollution across the Permian-Triassic transition, Geology, 45, 1123–1126, 2017.

ucation, IEEE T. Learn. Technol., 16, 121-132, 2022.

- Hovikoski, J., Fyhn, M. B. W., Nøhr-Hansen, H., Hopper, J. R., Andrews, S., Barham, M., Nielsen, L. H., Bjerager, M., Bojesen-Koefoed, J., Lode, S., Sheldon, E., Uchman, A., Skorstengaard, P. R., and Alsen, P.: Paleocene-Eocene volcanic segmentation of the Norwegian-Greenland seaway reorganized highlatitude ocean circulation, Commun. Earth Environ., 2, 1–10, 65 https://doi.org/10.1038/s43247-021-00249-w, 2021.
- Hryniewicz, K., Nakrem, H. A., Hammer, Ø., Little, C. T., Kaim, A., Sandy, M. R., and Hurum, J. H.: The palaeoecology of the latest Jurassic–earliest Cretaceous hydrocarbon seep carbonates from Spitsbergen, Svalbard, Lethaia, 48, 353–374, 2015.
- Hu, Y., Li, X., Boos, W. R., Guo, J., Lan, J., Lin, Q., Han, J., Zhang, J., Bao, X., Yuan, S., Wei, Q., Liu, Y., Yang, J., Nie, J., and Guo, Z.: Emergence of the modern global monsoon from the Pangaea megamonsoon set by palaeogeography, Nat. Geosci., 16, 1041–1046, 2023.
- Hurum, J. H., Nakrem, H. A., Hammer, Ø., Knutsen, E. M., Druckenmiller, P. S., Hryniewicz, K., and Novis, L. K.: An Arctic Lagerstätte–the Slottsmøya Member of the Agardhfjellet Formation (Upper Jurassic–Lower Cretaceous) of Spitsbergen, Norw. J. Geol., 92, 55–64 pp., 2012.
- Hurum, J. H., Roberts, A. J., Nakrem, H. A., Stenløkk, J. A., and Mørk, A.: The first recovered ichthyosaur from the Middle Triassic of Edgeøya, Svalbard, Norw. Petrol. Directorate Bull., 11, 97–110, 2014.
- Hurum, J. H., Druckenmiller, P. S., Hammer, Ø., Nakrem, H. 85 A., and Olaussen, S.: The theropod that wasn't: an ornithopod tracksite from the Helvetiafjellet Formation (Lower Cretaceous) of Boltodden, Svalbard, Geol. Soc. Lond., 434, 189–206, https://doi.org/10.1144/SP434.10, 2016a.
- Hurum, J. H., Roberts, A. J., Dyke, G. J., Grundvåg, S.-A., Nakrem,
  H. A., Midtkandal, I., Sliwinska, K., and Olaussen, S.: Bird or maniraptoran dinosaur? A femur from the Albian strata of Spitsbergen, Palaeontol. Polonica, 67, 137–47, 2016b.
- Hurum, J. H., Engelschiøn, V. S., Økland, I. H., Bratvold, J., Ekeheien, C., Roberts, A. J., Delsett, L. L., Hansen, B. B., Mørk,
  A., and Nakrem, H. A.: The history of exploration and stratigraphy of the Early to Middle Triassic vertebrate-bearing strata of Svalbard (Sassendalen Group, Spitsbergen), Norw. J. Geol., 98, 165–174, 2018.
- Hutchinson, D. K., Coxall, H. K., O'Regan, M., Nilsson, J., Caballero, R., and de Boer, A. M.: Arctic closure as a trigger for Atlantic overturning at the Eocene-Oligocene Transition, Nat. Commun., 10, 3797, https://doi.org/10.1038/s41467-019-11828-2-2019
- Hutchinson, D. K., Coxall, H. K., Lunt, D. J., Steinthorsdottir, M., de Boer, A. M., Baatsen, M., von der Heydt, A., Huber, M., Kennedy-Asser, A. T., Kunzmann, L., Ladant, J.-B., Lear, C. H., Moraweck, K., Pearson, P. N., Piga, E., Pound, M. J., Salzmann, U., Scher, H. D., Sijp, W. P., Śliwińska, K. K., Wilson, P. A., and Zhang, Z.: The Eocene–Oligocene transition: a review of marine and terrestrial proxy data, models and model–data comparisons, Clim. Past, 17, 269–315, https://doi.org/10.5194/cp-17-269-2021, 2021.
- Hüneke, H., Joachimski, M., Buggisch, W., and Lützner, H.: Marine carbonate facies in response to climate and nutrient level: The upper carboniferous and permian of central spitsbergen (Svalbard), Facies, 45, 93–135, https://doi.org/10.1007/BF02668107, 2001.

- Høy, T. and Lundschien, B.: Triassic deltaic sequences in the northern Barents Sea, Geol. Soc. Lond., 35, 249–260, https://doi.org/10.1144/M35.15, 2011.
- Ingólfsson, Ó. and Landvik, J. Y.: The Svalbard–Barents Sea icesheet–Historical, current and future perspectives, Quaternary Sci. Rev., 64, 33–60, 2013.
- Isbell, J. L., Fraiser, M. L., and Henry, L. C.: Examining the Complexity of Environmental Change during the Late Paleozoic and Early Mesozoic, PALAIOS, 23, 267–269, https://doi.org/10.2110/palo.2008.S03, 2008.
- Ivanov, A. V., He, H., Yan, L., Ryabov, V. V., Shevko, A. Y., Palesskii, S. V., and Nikolaeva, I. V.: Siberian Traps large igneous province: Evidence for two flood basalt pulses around the Permo-Triassic boundary and in the Middle Triassic, and contemporaneous granitic magmatism, Earth-Sci. Rev., 122, 58–76, https://doi.org/10.1016/j.earscirev.2013.04.001, 2013.
- Jakobsson, M., Backman, J., Rudels, B., Nycander, J., Frank, M., Mayer, L., Jokat, W., Sangiorgi, F., O'Regan, M., and Brinkhuis, H.: The early Miocene onset of a ventilated circulation regime in the Arctic Ocean, Nature, 447, 986–990, 2007.
- Janocha, J., Wesenlund, F., Thießen, O., Grundvåg, S.-A., Koehl, J.-B., and Johannessen, E. P.: Petroleum geochemistry of Upper Paleozoic strata on Bjørnøya, western Barents Shelf, Mar. Petrol. Geol., 163, 106768, https://doi.org/10.1016/j.marpetgeo.2024.106768, 2024.
- Jansen, E., Overpeck, J., Briffa, K. R., Duplessy, J.-C., Joos, F.,
  Masson-Delmotte, V., Olago, D., Otto-Bliesner, B., Peltier, W.
  R., Rahmstorf, S., Ramesh, R., Raynaud, D., Rind, D., Solomina, O., Villalba, R., and Zhang, D.: Palaeoclimate, in: Climate Change 2007: The Physical Science Basis. Contribution
- of Working Group I to the Fourth Assessment Report of the Intergovernmental Panel on Climate Change, edited by: Solomon, S., Qin, D., Manning, M., Chen, Z., Marquis, M., Averyt, K. B., Tignor, M., and Miller, H. L., Cambridge University Press, Cambridge, United Kingdom and New York, NY, USA, 1846, 2007.
- Jelby, M. E., Grundvåg, S. A., Helland-Hansen, W., Olaussen, S., and Stemmerik, L.: Tempestite facies variability and storm-depositional processes across a wide ramp: Towards a polygenetic model for hummocky cross-stratification, Sedimentology, 67, 742–781, https://doi.org/10.1111/sed.12671, 2020a.
- Jelby, M. E., Śliwińska, K. K., Koevoets, M. J., Alsen, P., Vickers, M. L., Olaussen, S., and Stemmerik, L.: Arctic reappraisal of global carbon-cycle dynamics across the Jurassic–Cretaceous boundary and Valanginian Weissert
- Event, Palaeogeogr. Palaeoclimatol. Palaeoecol., 555, 109847, https://doi.org/10.1016/j.palaeo.2020.109847, 2020b.
- Jelby, M. E., Grundvåg, S. A., Śliwińska, K. K., Alsen, P., Vickers, M. L., Olaussen, S., and Stemmerik, L.: Lower Cretaceous holostratigraphy in Svalbard: the Arctic key piece of the Boreal basin puzzle. Geol. Soc. Lond. Spec. Publ. 545, SP545–2023.
- basin puzzle, Geol. Soc. Lond. Spec. Publ., 545, SP545–2023, 2025.
- Jenkyns, H.: Cretaceous anoxic events: from continents to oceans, J. Geol. Soc. Lond., 137, 171–188, 1980.
- Jenkyns, H. C.: Carbon-isotope stratigraphy and paleoceanographic
   significance of the Lower Cretaceous shallow-water carbonates
   of Resolution Guyot, Mid-Pacific Mountains, Proc. Ocean Drill.
   Program Sci. Results, 143, 99–104, 1995.

- Jenkyns, H. C.: Geochemistry of oceanic anoxic events, Geochem. Geophys. Geosyst., 11, 1–30, https://doi.org/10.1029/2009GC002788, 2010.
- Jenkyns, H. C., Schouten-Huibers, L., Schouten, S., and Sinninghe Damsté, J. S.: Warm Middle Jurassic–Early Cretaceous high-latitude sea-surface temperatures from the Southern Ocean, Clim. Past, 8, 215—226, https://doi.org/10.5194/cp-8-215-2012, 2012.
- Jin, X., Tomimatsu, Y., Yin, R., Onoue, T., Franceschi, M., Grasby, S. E., and Rigo, M.: Climax in Wrangellia LIP activity coincident with major Middle Carnian (Late Triassic) climate and biotic changes: Mercury isotope evidence from the Panthalassa pelagic domain, Earth Planet. Sci. Lett., 607, 118075, https://doi.org/10.1016/j.epsl.2023.118075, 2023.
- Jin, Y., Wang, Y., Wang, W., Shang, Q., Cao, C., and Erwin, D. H.: Pattern of marine mass extinction near the Permian-Triassic boundary in South China, Science, 289, 432–436, 2000.
- Joachimski, M. M., Lai, X., Shen, S., Jiang, H., Luo, G., Chen, B., 75 Chen, J., and Sun, Y.: Climate warming in the latest Permian and the Permian–Triassic mass extinction, Geology, 40, 195–198, https://doi.org/10.1130/g32707.1, 2012.
- Joachimski, M. M., Alekseev, A. S., Grigoryan, A., and Gatovsky, Y. A.: Siberian Trap volcanism, global warming and the Permian-Triassic mass extinction: New insights from Armenian Permian-Triassic sections, GSA Bull., 132, 427–443, 2020.
- Jochmann, M. M., Augland, L. E., Lenz, O., Bieg, G., Haugen, T., Grundvåg, S. A., Jelby, M. E., Midtkandal, I., Dolezych, M., and Hjálmarsdóttir, H. R.: Sylfjellet: a new outcrop of the Paleogene Van Mijenfjorden Group in Svalbard, Arktos, 6, 17–38, https://doi.org/10.1007/s41063-019-00072-w, 2020.
- Johannessen, E. P. and Steel, R. J.: Shelf-margin clinoforms and prediction of deepwater sands, Basin Res., 17, 521–550, 2005.
- Johannessen, E. P. and Steel, R. J.: Mid-Carboniferous extension and rift-infill sequences in the Billefjorden Trough, Svalbard, Nor. Geol. Tidsskr., 72, 35–48, 1992.
- Johannessen, E. P., Henningsen, T., Bakke, N. E., Johansen, T. A., Ruud, B. E., Riste, P., Elvebakk, H., Jochmann, M., Elvebakk, G., and Woldengen, M. S.: Palaeogene clinoform succession on Svalbard expressed in outcrops, seismic data, logs and cores, First Break, 29, 35–44, https://doi.org/10.3997/1365-2397.2011004, 2011.
- Johansson, Å., Larionov, A. N., Gee, D. G., Ohta, Y., Tebenkov, A. M., and Sandelin, S.: Grenvillian and 100 Caledonian tectono-magmatic activity in northeasternmost Svalbard, Geol. Soc. Lond. Mem., 30, 207–232, https://doi.org/10.1144/GSL.MEM.2004.030.01.17, 2004.
- Johansson, Å., Gee, D. G., Larionov, A. N., Ohta, Y., and Tebenkov, A. M.: Grenvillian and Caledonian evolution of eastern Svalbard–a tale of two orogenies, Terra Nova, 17, 317–325, 2005.
- Jokat, W. and Herter, U.: Jurassic failed rift system below the Filchner-Ronne-Shelf, Antarctica: New evidence from geophysical data, Tectonophysics, 688, 65–83, 2016.
- Jones, M. T., Jerram, D. A., Svensen, H. H., and Grove, C.: The effects of large igneous provinces on the global carbon and sulphur cycles, Palaeogeogr. Palaeoclimatol. Palaeoecol., 441, 4– 21, https://doi.org/10.1016/j.palaeo.2015.06.042, 2016.
- Jones, M. T., Augland, L. E., Shephard, G. E., Burgess, S. 115 D., Eliassen, G. T., Jochmann, M. M., Friis, B., Jerram,

- D. A., Planke, S., and Svensen, H. H.: Constraining shifts in North Atlantic plate motions during the Palaeocene by U-Pb dating of Svalbard tephra layers, Sci. Rep., 7, 6822, https://doi.org/10.1038/s41598-017-06170-7, 2017.
- 5 Jones, M. T., Percival, L. M. E., Stokke, E. W., Frieling, J., Mather, T. A., Riber, L., Schubert, B. A., Schultz, B., Tegner, C., Planke, S., and Svensen, H. H.: Mercury anomalies across the Palaeocene–Eocene Thermal Maximum, Clim. Past, 15, 217– 236, https://doi.org/10.5194/cp-15-217-2019, 2019.
- Jones, M. T., Stokke, E. W., Rooney, A. D., Frieling, J., Pogge von Strandmann, P. A. E., Wilson, D. J., Svensen, H. H., Planke, S., Adatte, T., Thibault, N., Vickers, M. L., Mather, T. A., Tegner, C., Zuchuat, V., and Schultz, B. P.: Tracing North Atlantic volcanism and seaway connectivity across the Paleocene–
   Eocene Thermal Maximum (PETM), Clim. Past, 19, 1623–1652, https://doi.org/10.5194/cp-19-1623-2023, 2023.
  - Kasbohm, J., Schoene, B., and Burgess, S.: Radiometric constraints on the timing, tempo, and effects of large igneous province emplacement, in: Large Igneous Provinces: A Driver of Global Environmental and Biotic Changes, edited by: Ernst, R. E., Dick-

son, A. J., and Bekker, A., Am. Geophys. Union, John Wiley Sons, Inc., 27–82, https://doi.org/10.1002/9781119507444.ch2, 2021.

- Kear, B. P., Engelschiøn, V. S., Hammer, Ø., Roberts, A. J., and Hurum, J. H.: Earliest Triassic ichthyosaur fossils push back oceanic reptile origins, Curr. Biol., 33, R178–R179, 2023.
- Kele, S., Breitenbach, S. F., Capezzuoli, E., Meckler, A. N., Ziegler, M., Millan, I. M., Kluge, T., Deák, J., Hanselmann, K., John, C. M., and Yan, H.: Temperature dependence of oxygen-
- and clumped isotope fractionation in carbonates: a study of travertines and tufas in the 6–95 °C temperature range, Geochim. Cosmochim. Acta, 168, 172–192, 2015.
- Kellogg, H. E.: Tertiary stratigraphy and tectonism in Svalbard and continental drift, AAPG Bull., 59, 465–485, 1975.
- 35 Kemp, D., Eichenseer, K., and Kiessling, W.: Maximum rates of climate change are systematically underestimated in the geological record, Nat. Commun., 6, 8890, https://doi.org/10.1038/ncomms/9890, 2015
- Kenrick, P., Wellman, C. H., Schneider, H., and Edgecombe, G. D.:
  A timeline for terrestrialization: consequences for the carbon cycle in the Palaeozoic, Philos. Trans. R. Soc. B-Biol. Sci., 367, 519–536, 2012.
- Kidder, D. L. and Worsley, T. R.: Causes and consequences of extreme Permo-Triassic warming to globally equable cli-
- mate and relation to the Permo-Triassic extinction and recovery, Palaeogeogr. Palaeoclimatol. Palaeoecol., 203, 207–237, https://doi.org/10.1016/S0031-0182(03)00667-9, 2004.
- Kierulf, H. P., Kohler, J., Boy, J. P., Geyman, E. C., Mémin, A.,
  Omang, O. C., and Steffen, R.: Time-varying uplift in Svalbard
   an effect of glacial changes, Geophys. J. Int., 231, 1518–1534, 2022.
- Kim, S.-T. and O'Neil, J. R.: Equilibrium and nonequilibrium oxygen isotope effects in synthetic carbonates, Geochim. Cosmochim. Acta, 61, 3461–3475, 1997.
- 55 Klausen, T. G., Müller, R., Slama, J., and Helland-Hansen, W.: Evidence for Late Triassic provenance areas and Early Jurassic sediment supply turnover in the Barents Sea Basin of northern Pangea, Lithosphere, 9, 14–28, 2017.

- Klausen, T. G., Nyberg, B., and Helland-Hansen, W.: The largest delta plain in Earth's history, Geology, 47, 470–474, 60 https://doi.org/10.1130/G45507.1, 2019.
- Kleinspehn, K. L. and Teyssier, C.: Oblique rifting and the Late Eocene–Oligocene demise of Laurasia with inception of Molloy Ridge: Deformation of Forlandsundet Basin, Svalbard, Tectonophysics, 693, 363–377, 2016.
- Knies, J., Schönenberger, J., Zwingmann, H., van der Lelij, R., Smelror, M., Vullum, P. E., Brönner, M., Vogt, C., Fredin, O., Müller, A., Grasby, S. E., Beauchamp, B., and Viola, G.: Continental weathering and recovery from ocean nutrient stress during the Early Triassic Biotic Crisis, Commun. Earth Environ., 3, 161, 70 1–12, https://doi.org/10.1038/s43247-022-00480-z, 2022.
- Koevoets, M. J., Abay, T. B., Hammer, Ø., and Olaussen, S.: High-resolution organic carbon–isotope stratigraphy of the Middle Jurassic–Lower Cretaceous Agardhfjellet Formation of central Spitsbergen, Svalbard, Palaeogeogr. Palaeoclimatol. Palaeoecol., 75 449, 266–274, https://doi.org/10.1016/j.palaeo.2016.02.029, 2016.
- Koevoets, M. J., Hammer, Ø., Olaussen, S., Senger, K., and Smelror, M.: Integrating subsurface and outcrop data of the Middle Jurassic to Lower Cretaceous Agardhfjellet Formation in central Spitsbergen, Nor. Geol. Tidsskr., 98, 1–34, https://doi.org/10.17850/njg98-4-01, 2018.
- Koevoets, M., Hammer, Ø., and Little, C. T.: Palaeoecology and palaeoenvironments of the Middle Jurassic to lowermost Cretaceous Agardhfjellet Formation (Bathonian-Ryazanian), Spitsbergen, Svalbard, Nor. J. Geol., 99, 1–24, https://doi.org/10.17850/njg99-1-02, 2019.
- Korte, C. and Kozur, H. W.: Carbon-isotope stratigraphy across the Permian–Triassic boundary: A review, J. Asian Earth Sci., 39, 215–235, https://doi.org/10.1016/j.jseaes.2010.01.005, 2010.
- Korte, C., Jasper, T., Kozur, H. W., and Veizer, J.:  $\delta^{18}$ O and  $\delta^{13}$ C of Permian brachiopods: a record of seawater evolution and continental glaciation, Palaeogeogr. Palaeoclimatol. Palaeoecol., 224, 333–351, 2005.
- Krajewski, K. P.: The Botneheia Formation (Middle Triassic) in Edgeøya and Barentsøya, Svalbard: lithostratigraphy, facies, phosphogenesis, paleoenvironment, Pol. Polar Res., 29, 319–364, 2008.
- Krajewski, K. P.: Organic matter–apatite–pyrite relationships in the Botneheia Formation (Middle Triassic) of eastern Svalbard: Relevance to the formation of petroleum source rocks in the NW Barents Sea shelf, Mar. Petrol. Geol., 45, 69–105, 2013.
- Kristoffersen, Y.: On the tectonic evolution and paleoceanographic significance of the Fram Strait gateway, in: Geological history of the polar oceans: Arctic versus Antarctic, 105 edited by: Bleil, U. and Thiede, J., Springer, Dordrecht, 63–76, https://doi.org/10.1007/978-94-009-2029-3\_4, 1990.
- Kristoffersen, Y. and Husebye, E. S.: Multi-channel seismic reflection measurements in the Eurasian Basin, Arctic Ocean, from US ice station FRAM-IV, Tectonophysics, 114, 103–115, 1985.

110

- Kristoffersen, Y., Ohta, Y., and Hall, J. K.: On the origin of the Yermak Plateau north Svalbard, Arctic Ocean, Nor. J. Geol., 100, 1–33, 2020.
- Kröger, B., Finnegan, S., Franeck, F., and Hopkins, M. J.: The Ordovician Succession Adjacent to Hinlopenstretet, Ny Friesland, 115 Spitsbergen, Am. Mus. Novit., 3882, 1–28, 2017.

- Kvaček, Z. and Manum, S. B.: Ferns of the Spitsbergen Palaeogene, Palaeontogr. Abt. B, 230, 169–181, 1993.
- Kvaček, Z., Manum, S. B., and Boulter, M. C.: Angiosperms from the Palaeogene of Spitsbergen, including an unfinished work by A. G. Nathorst, Palaeontogr. Abt. B, 232, 103–128, 1994.
- Large, D. J. and Marshall, C.: Use of carbon accumulation rates to estimate the duration of coal seams and the influence of atmospheric dust deposition on coal composition, Geol. Soc. Lond. Spec. Publ., 404, 303–315, 2015.
- Large, D. J., Marshall, C., Jochmann, M., Jensen, M., Spiro, B. F., and Olaussen, S.: Time, Hydrologic Landscape, and the Long-Term Storage of Peatland Carbon in Sedimentary Basins, J. Geophys. Res.-Earth Surf., 126, e2020JF005762, https://doi.org/10.1029/2020JF005762, 2021.
- 15 Larson, R. L. and Erba, E.: Onset of the Mid-Cretaceous greenhouse in the Barremian-Aptian: Igneous events and the biological, sedimentary, and geochemical responses, Paleoceanogr., 14, 663–678, 1999.
- Lasabuda, A., Laberg, J. S., Knutsen, S. M., and Safronova, P.: Cenozoic tectonostratigraphy and pre-glacial erosion: A mass-balance study of the northwestern Barents Sea margin, Norwegian Arctic, J. Geodyn., 119, 149–166, 2018.
- Lasabuda, A. P. E., Johansen, N. S., Laberg, J. S., Faleide, J. I., Senger, K., Rydningen, T. A., Patton, H., Knutsen, S.-M.,
- and Hanssen, A.: Cenozoic uplift and erosion of the Norwegian Barents Shelf A review, Earth-Sci. Rev., 217, 103609, https://doi.org/10.1016/j.earscirev.2021.103609, 2021.
- Lauritzen, O. and Worsley, D.: Observations of the Upper Palaeozoic stratigraphy of the Ny Friesland area, Norsk Polarinstitutt A51, 41 pp., 1975.
- Lawver, L., Müller, R., Srivastava, S., and Roest, W.: The opening of the Arctic Ocean, in: Geological history of the polar oceans: Arctic versus Antarctic, edited by: Bleil, U. and Thiede, J., Springer, Dordrecht, 29–62, https://doi.org/10.1007/978-94-009-2029-3\_3, 1990.
- Lawver, L., Scotese, C., Grantz, A., Johnson, L., and Sweeney, J.: A review of tectonic models for the evolution of the Canada Basin, in: The Geology of North America, edited by: Grantz, A., Johnson, G. L., and Sweeney, J. F., Geological Society of America, Boulder, CO, 593–618, 1990b.
- Lee, C., Love, G. D., Hopkins, M. J., Kröger, B., Franeck, F., and Finnegan, S.: Lipid biomarker and stable isotopic profiles through Early-Middle Ordovician carbonates from Spitsbergen, Norway, Org. Geochem., 131, 5–18, https://doi.org/10.1016/j.orggeochem.2019.02.008, 2019.
- Lee, S., Shi, G. R., Nakrem, H. A., Woo, J., and Tazawa, J.-I.: Mass extinction or extirpation: Permian biotic turnovers in the northwestern margin of Pangea, GSA Bull., 134, 2399–2414, https://doi.org/10.1130/b36227.1, 2022.
- 50 Leever, K. A., Gabrielsen, R. H., Faleide, J. I., and Braathen, A.: A transpressional origin for the West Spitsbergen fold-and-thrust belt: Insight from analog modelling, Tectonics, 30, TC2014, https://doi.org/10.1029/2010TC002753, 2011.
- Lehnert, O., Stouge, S., and Brandl, P. A.: Conodont biostratigraphy
  in the Early to Middle Ordovician strata of the Oslobreen Group
  in Ny Friesland, Svalbard, Z. Dtsch. Ges. Geowiss., 164, 149–172, 2013
  - Leu, M., Schneebeli-Hermann, E., Hammer, Ø., Lindemann, F. J., and Bucher, H.: Spatiotemporal dynamics of nektonic biodiver-

- sity and vegetation shifts during the Smithian–Spathian transition: conodont and palynomorph insights from Svalbard, Lethaia, 57, 1–19, 2024.
- Leung, J. Y., Zhang, S., and Connell, S. D.: Is ocean acidification really a threat to marine calcifiers? A systematic review and meta-analysis of 980+ studies spanning two decades, Small, 18, 2107407, https://doi.org/10.1002/smll.202107407, 2022.
- Lini, A., Weissert, H., and Erba, E.: The Valanginian carbon isotope event: a first episode of greenhouse climate conditions during the Cretaceous, Terra Nova, 4, 374–384, https://doi.org/10.1111/j.1365-3121.1992.tb00826.x, 1992.
- Lipinski, M., Warning, B., and Brumsack, H. J.: Trace metal signatures of Jurassic/Cretaceous black shales from the Norwegian Shelf and the Barents Sea, Palaeogeogr. Palaeoclimatol. Palaeoecol., 190, 459–475, https://doi.org/10.1016/S0031-0182(02)00619-3, 2003.
- Liu, Z., Pagani, M., Zinniker, D., DeConto, R., Huber, M., Brinkhuis, H., Shah, S. R., Leckie, R. M., and Pearson, A.: Global Cooling During the Eocene-Oligocene Climate Transition, Science, 323, 1187–1190, https://doi.org/10.1126/science.1166368, 2009.
- Lopes, G., Mangerud, G., and Clayton, G.: The palynostratigraphy of the Mississippian Birger Johnsonfjellet section, Spitsbergen, Svalbard, Palynology, 43, 631–649, 2019.
- Lord, G. S., Johansen, S. K., Støen, S. J., and Mørk, A.: Facies development of the Upper Triassic succession on Barentsøya, Wilhelmøya and NE Spitsbergen, Svalbard, Nor. J. Geol., 97, 1–62, https://doi.org/10.17850/njg97-1-03, 2017.
- Lord, G. S., Mørk, A., Haugen, T., Boxaspen, M. A., Husteli, B., Forsberg, C. S., and Olaussen, S.: Stratigraphy and palaeosol profiles of the Upper Triassic Isfjorden Member, Svalbard, Nor. J. Geol., https://doi.org//10.17850/njg102-4-02, 2022.
- Lüthje, C. J., Milàn, J., and Hurum, J. H.: Paleocene tracks of the mammal pantodont genus Titanoides in coal-bearing strata, Svalbard, Arctic Norway, J. Vertebr. Paleontol., 30, 521–527, 2010.
- Lüthje, C. J., Nichols, G., and Jerrett, R.: Sedimentary facies and reconstruction of a transgressive coastal plain with coal formation, Paleocene, Spitsbergen, Arctic Norway, Nor. J. Geol., 100, 1–49, 2020.
- Macdonald, F. A.:. Deep-Time paleoclimate proxies, AGU Advances, 1, e2020AV000244,  $_{\rm 100}$  https://doi.org/10.1029/2020av000244, 2020.
- Maher Jr., H. D., Braathen, A., Bergh, S., Dallmann, W., and Harland, W. B.: Tertiary or Cretaceous age for Spitsbergen's fold-thrust belt on the Barents Shelf, Tectonics, 14, 1321–1326, https://doi.org/10.1029/95TC01257, 1995.
- Maher, Jr. H. D., IS47: Manifestations of the Cretaceous High Arctic Large Igneous Province in Svalbard, The J. Geol., 109, 91–104, https://doi.org/10.1086/317960, 2001.
- Mahoney, J., Storey, M., Duncan, R., Spencer, K., and Pringle, M.: Geochemistry and age of the Ontong Java Plateau, in: The Mesozoic Pacific: Geology, tectonics, and volcanism, edited by: Pringle, M. S., Sager, W. W., Sliter, W. V., and Stein, S., Wiley, Washington, D. C: American Geophysical Union, 233–261, https://doi.org/10.1029/GM077p0233 1993.
- Majka, J. and Kośmińska, K.: Magmatic and metamorphic events recorded within the Southwestern Basement Province of Svalbard, Arktos, 3, 5, https://doi.org/10.1007/s41063-017-0034-7, 2017.

- Major, H., Nagy, J., Haremo, P., Dallmann, W. K., Andersen, A., and Salvigsen, O.: Adventdalen, in: Geological Map Svalbard 1:100 000, Sheet C9G. Norsk Polarinstitutt, 1992.
- Mangerud, G. and Konieczny, R.: Palynology of the Permian succession of Spitsbergen, Svalbard, Polar Res., 12, 65–93, https://doi.org/10.3402/polar.v12i1.6704, 1993.
- Manum, S.: Some dinoflagellates and hystrichosphaerids from the Lower Tertiary of Spitsbergen, Nytt Magasin for Botanik, 8, 17–25, 1960.
- Manum, S.: Studies in the Tertiary Flora of Spitsbergen: With Notes on Tertiary Floras of Ellesmere Island, Greenland, and Iceland, a Palynological Investigation, Norsk Polarinst. Skrifter, 125, 128+21 pp., plates, Norsk Polarinstitutt, Oslo University Press, 127 p., 1962.
- 15 Manum, S. B. and Throndsen, T.: Age of Tertiary formations on Spitsbergen, Polar Res., 4, 103–131, https://doi.org/10.3402/polar.v4i2.6927, 1986.
  - Marshall, C. J.: Palaeogeographic development and economic potential of the coal-bearing Palaeocene Todalen Member, Spitsbergen, PhD University of Nottingham, 360 pp., https://eprints.nottingham.ac.uk/13794/ (last access: 1848), 2013.
  - Marshall, C., Large, D. J., Meredith, W., Snape, C. E., Uguna, C., Spiro, B. F., Orheim, A., Jochmann, M., Mokogwu, I., Wang, Y., and Friis, B.: Geochemistry and petrology of Palaeocene coals from Spitsbergen Part 1: Oil potential

and depositional environment, Int. J. Coal Geol., 143, 22–33, https://doi.org/10.1016/j.coal.2015.03.006.2015

https://doi.org/10.1016/j.coal.2015.03.006, 2015.

- Martinez, M., Aguirre-Urreta, B., Dera, G., Lescano, M., Omarini,
   J., Tunik, M., O'Dogherty, L., Aguado, R., Company, M., and
   Bodin, S.: Synchrony of carbon cycle fluctuations, volcanism and orbital forcing during the Early Cretaceous, Earth-Sci. Rev., 239, 104356, https://doi.org/10.1016/j.earscirev.2023.104356, 2023.
- Matthiessen, J.: Biostratigraphie tertiärer Ablagerungen (Paläozän) Am Van Keulenfjord (Spitzbergen) nach Dinoflagellaten-Zysten,
- (Diploma thesis), Christian-Albrechts-Universität zu Kiel, Kiel, 94 pp., 1849, 1986.
- Matysik, M., Stemmerik, L., Olaussen, S., and Brunstad, H.: Diagenesis of spiculites and carbonates in a Permian temperate ramp succession–Tempelfjorden Group, Spitsbergen, Arctic Norway,
- Sedimentology, 65, 745–774, https://doi.org/10.1111/sed.12404, 2018.
- Maxwell, E. E. and Kear, B. P.:.Triassic ichthyopterygian assemblages of the Svalbard archipelago: a reassessment of taxonomy and distribution, J. Geol. Soc. Sweden, 135, 85–94, https://doi.org/10.1080/11035897.2012.759145, 2013.
- McArthur, J. M., Mutterlose, J., Price, G. D., Rawson, P. F., Ruffell, A., and Thirlwall, M. F.: Belemnites of Valanginian, Hauterivian and Barremian age: Sr-isotope stratigraphy, composition (<sup>87</sup>Sr/<sup>86</sup>Sr, δ<sup>13</sup>C, δ<sup>18</sup>O, Na, Sr, Mg), and palaeo-oceanography, Palaeogeogr. Palaeoclimatol. Palaeoecol.,
- o paraeo-oceanography, Paraeogeogr. Paraeocrimator. Paraeoecor., 202, 253–272, https://doi.org/10.1016/S0031-0182(03)00638-2, 2004.
- McArthur, J. M., Janssen, N. M. M., Reboulet, S., Leng, M. J., Thirlwall, M. F., and Van de Schootbrugge, B.: Palaeotemperatures, polar ice-volume, and isotope stratigraphy (Mg/Ca,  $\delta^{18}$ O,  $\delta^{13}$ C,  $\delta^{87}$ Sr/ $\delta^{86}$ Sr): the early cretaceous (Berriasian, Valanginian, Hauterivian), Palaeogeogr. Palaeoclimatol. Palaeoecol., 248, 391–430, https://doi.org/10.1016/j.palaeo.2006.12.0152007, 2007.

- McCann, A. J.: Deformation of the Old Red Sandstone of 60 NW Spitsbergen; links to the Ellesmerian and Caledonian orogenies, Geol. Soc. London, 180, 567–584, https://doi.org/10.1144/GSL.SP.2000.180.01.30, 2000.
- McClelland\*, W. C., von Gosen\*, W., and Piepjohn\*, K.: Tonian and Silurian magmatism in Nordaustlandet: Svalbard's place in the Caledonian orogen, in: Circum-Arctic Structural Events: Tectonic Evolution of the Arctic Margins and Trans-Arctic Links with Adjacent Orogens, edited by: Piepjohn, K., Strauss, J. V., Reinhardt, L., and McClelland, W. C.: Boulder, Colorado, Geological Society of America, Special Paper, 541, 63–80, 70 https://doi.org/10.1130/2018.2541(04), 2019.
- McInerney, F. A. and Wing, S. L.: The Paleocene-Eocene Thermal Maximum: a perturbation of carbon cycle, climate, and biosphere with implications for the future, Annu. Rev. Earth Planet. Sci., 39, 489–516, https://doi.org/10.1146/annurev-earth-040610-133431, 2011.
- Meissner, P., Mutterlose, J., and Bodin, S.: Latitudinal temperature trends in the northern hemisphere during the Early Cretaceous (Valanginian–Hauterivian), Palaeogeogr. Palaeoclimatol. Palaeoecol., 424, 17–39, https://doi.org/10.1016/j.palaeo.2015.02.003, 2015.
- Menegatti, A. P., Weissert, H., Brown, R. S., Tyson, R. V., Farrimond, P., Strasser, A., and Caron, M.:High-resolution  $\delta^{13}$ C stratigraphy through the early Aptian "Livello Selli" of the Alpine Tethys, Paleoceanography, 13, 530–545, 1998.
- Midtkandal, I. and Nystuen, J.: Depositional architecture of a low-gradient ramp shelf in an epicontinental sea: The lower Cretaceous of Svalbard, Basin Res., 21, 655–675, https://doi.org/10.1111/j.1365-2117.2009.00399.x., 2009.
- Midtkandal, I., Nystuen, J. P., Nagy, J., and Mørk, A.: Lower Cretaceous lithostratigraphy across a regional subaerial unconformity in Spitsbergen: the Rurikfjellet and Helvetiafjellet formations, Nor. J. Geol., 88, 287–304, 2008.
- Midtkandal, I., Svensen, H. H., Planke, S., Corfu, F., Polteau, S., Torsvik, T. H., Faleide, J. I., Grundvåg, S.-A., Selnes, 95 H., Kürschner, W., and Olaussen, S.: The Aptian (Early Cretaceous) oceanic anoxic event (OAE1a) in Svalbard, Barents Sea, and the absolute age of the Barremian-Aptian boundary, Palaeogeogr. Palaeoclimatol. Palaeoecol., 463, 126–135, https://doi.org/10.1016/j.palaeo.2016.09.023, 2016.
- Mii, H.-S., Grossman, E. L., and Yancey, T. E.: Stable carbon and oxygen isotope shifts in Permian seas of West Spitsbergen-Global change or diagenetic artifact?, Geology, 25, 227–230, https://doi.org/10.1130/0091-7613(1997)025<0227:SCAOIS>2.3.CO;2, 1997.
- Miller, K. G., Kominz, M. A., Browning, J. V., Wright, J. D., Mountain, G. S., Katz, M. E., Sugarman, P. J., Cramer, B. S., Christie-Blick, N., and Pekar, S. F.: The Phanerozoic record of global sea-level change, Science, 310, 1293–1298, https://doi.org/10.1126/science.1116412, 2005.
- Montañez, I. P. and Poulsen, C. J.: The Late Paleozoic ice age: an evolving paradigm, Annu. Rev. Earth Plane. Sci., 41, 629–656, 2013.
- Montañez, I. P., Tabor, N. J., Niemeier, D., DiMichele, W. A., Frank, T.D., Fielding, C. R., Isbell, J. L., Birgenheier, L. P., 115 and Rygel, M. C.: CO<sub>2</sub>-forced climate and vegetation instability during Late Paleozoic deglaciation, Science, 315, 87–91, https://doi.org/10.1126/science.1134207, 2007.

- Moody-Stuart, M.: High- and low-sinuosity stream deposits, with examples from the Devonian of Spitsbergen, J. Sediment. Res., 36, 1102–1117, https://doi.org/10.1306/74D71609-2B21-11D7-8648000102C1865D, 1966.
- Morgans-Bell, H. S., Coe, A. L., Hesselbo, S. P., Jenkyns, H. C., Weedon, G. P., Marshall, J. E. A., Tyson, R. V., and Williams, C. J.: Integrated stratigraphy of the Kimmeridge Clay Formation (Upper Jurassic) based on exposures and boreholes in south Dorset, UK, Geol. Mag., 138, 511–539, 2001
- Mørk, A. and Bjorøy, M.: Mesozoic source rocks on Svalbard,
   Petroleum Geology of the North European Margin: Proceedings of the North European Margin Symposium (NEMS'83), organized by the Norwegian Petroleum Society and held at the Norwegian Institute of Technology (NTH) in Trondheim 9–11
   May, 1983, Springer, 371–382 pp., https://doi.org/10.1007/978-
- 94-009-5626-1\_28, 1984.
- Mørk, A. and Grundvåg, S.:Festningen-A 300-million-year journey through shoreline exposures of the Carboniferous and Mesozoic in 7 kilometers, Geological Society of
- Norway— geological guides 2020-7, https://www.geologi. no/images/GeologiskeGuider/Festningen\_red.pdf (last access: 1850), 2020.
- Mørk, A. and Worsley, D.: Triassic of Svalbard and the Barents shelf, in: NGF Abstracts and proceedings, Vol. 3, 23–29 pp., 2006.
- Mørk, A., Knarud, R., and Worsley, D.: Depositional and diagenetic environments of the Triassic and Lower Jurassic succession of Svalbard, Arctic Geology and Geophysics: Proceedings of the Third International Symposium on Arctic Geology – Memoir, 8, 371–398, 1982.
- Mørk, A., Embry, A. F., and Weitschat, W.: Triassic transgressiveregressive cycles in the Sverdrup Basin, Svalbard and the Barents Shelf, Correlation in Hydrocarbon Exploration: Proceedings of the conference Correlation in Hydrocarbon Exploration
- organized by the Norwegian Petroleum Society and held in Bergen, Norway, 3–5 October 1988, Springer, 113–130 pp., https://doi.org/10.1007/978-94-009-1149-9\_11, 1989.
- Mørk, A., Vigran, J. O., Korchinskaya, M. V., Pchelina, T. M., Fefilova, L. A., Vavilov, M. N., and Weitschat, W.: a Triassic rocks
- in Svalbard, the Arctic Soviet islands and the Barents Shelf: bearing on their correlations, in: Norwegian Petroleum Society Special Publications, edited by: ISSI, T. O., Bergsager, E., Dahl-Stamnes, Ø. A., Holter, E., B., Lie, E., and Lund, T. B., Elsevier, 457–479, https://doi.org/10.1016/B978-0-444-88943-0.50033-2, 1003
- Mørk, A., Dallmann, W., Dypvik, H., Johannessen, E., Larssen, G., Nagy, J., Nøttvedt, A., Olaussen, S., Pchelina, T., and Worsley, D.: Mesozoic lithostratigraphy, Lithostratigraphic lexicon of Svalbard, Upper Palaeozoic to Quaternary bedrock. Review and recommendations for nomenclature use: 127–214, ISS2, 1999a.
- Mørk, A., Elvebakk, G., Forsberg, A. W., Hounslow, M. W., Nakrem, H. A., Vigran, J. O., and Weitschat, W.: The type section of the Vikinghogda Formation: a new Lower Triassic unit in central and eastern Svalbard, Polar Res., 18, 51–82, 1999b.
- Müller, R., Klausen, T. G., Faleide, J. I., Olaussen, S., Eide, C. H., and Suslova, A.: Linking regional unconformities in the Barents Sea to compression-induced forebulge uplift at the Triassic-Jurassic transition, Tectonophysics, 765, 35–51, 2019.

- Müller, R. D. and Spielhagen, R. F.: Evolution of the Central Tertiary Basin of Spitsbergen: towards a synthesis of sediment and plate tectonic history, Palaeogeogr. Palaeoclimatol. Palaeoecol., 80, 153–172, 1990.
- Müller, R. D., Cannon, J., Qin, X., Watson, R. J., Gurnis, M., Williams, S., Pfaffelmoser, T., Seton, M., Russell, S. H. J., and Zahirovic S.: GPlates: Building a virtual Earth through deep time, Geochem. Geophys. Geosyst., 19, 2243–2261, https://doi.org/10.1029/2018GC007584, 2018.
- Mueller, S., Veld, H., Nagy, J., and Kürschner, W. M.: Depositional history of the Upper Triassic Kapp Toscana Group on Svalbard, Norway, inferred from palynofacies analysis and organic geochemistrym Sediment, Geol., 310, 16–29, 2014.
- Mueller, S., Hounslow, M. W., and Kürschner, W. M.: Integrated stratigraphy and palaeoclimate history of the Carnian Pluvial Event in the Boreal realm; new data from the Upper Triassic Kapp Toscana Group in central Spitsbergen (Norway), J. Geol. 75 Soc., 173, 186–202, 2016.
- Mutti, M. and Weissert, H.: Triassic monsoonal climate and its signature in Ladinian-Carnian carbonate platforms (Southern Alps, Italy), J. Sediment. Res., 65, 357–367, 1995.
- Mulrooney, M. J., Larsen, L., Van Stappen, J., Rismyhr, B., Senger, K., Braathen, A., Olaussen, S., Mørk, M. B. E., Ogata, K., and Cnudde, V.: Fluid flow properties of the Wilhelmøya Subgroup, a potential unconventional CO<sub>2</sub> storage unit in central Spitsbergen, Norw. J. Geol., 99, 85–116, 2018.
- Myhre, P. I., Corfu, F., and Andresen, A.: Caledonian anatexis of Grenvillian crust: a U/Pb study of Albert I Land, NW Svalbard., Norw. J. Geol., 89, e191, 173–191, ISSN 029-196X, 2008.
- Nabbefeld, B., Grice, K., Twitchett, R. J., Summons, R. E., Hays, L., Böttcher, M. E., and Asif, M.: An integrated biomarker, isotopic and palaeoenvironmental study through the Late Permian event at Lusitaniadalen, Spitsbergen, Earth Planet. Sci. Lett., 291, 84–96, 2010
- Naber, T. V., Grasby, S. E., Cuthbertson, J. P., Rayner, N., and Tegner, C.: New constraints on the age, geochemistry, and environmental impact of High Arctic Large Igneous Province magmatism: Tracing the extension of the Alpha Ridge onto Ellesmere Island, Canada, GSA Bull., 133, 1695–1711, 2021.
- Nagy, J.: Delta-influenced foraminiferal facies and sequence stratigraphy of Paleocene deposits in Spitsbergen, Palaeogeogr. Palaeoclimatol. Palaeoecol., 222, 161–179, 100 https://doi.org/10.1016/j.palaeo.2005.03.014, 2005.
- Nagy, J. and Berge, S. H.: Micropalaeontological evidence of brackish water conditions during deposition of the Knorringfjellet Formation, Late Triassic–Early Jurassic, Spitsbergen, Polar Res., 27, 413–427, https://doi.org/10.1111/j.1751-8369.2007.00038.x, 105 2008.
- Nagy, J., Jargvoll, D., Dypvik, H., Jochmann, M., and Riber, L.: Environmental changes during the Paleocene–Eocene Thermal Maximum in Spitsbergen as reflected by benthic foraminifera, Polar Res., 32, 19737, 110 https://doi.org/10.3402/polar.v32i0.19737, 2013.
- Nakrem, H. A. and Mørk, A.: New Early Triassic Bryozoa (Trepostomata) from Spitsbergen, with some remarks on the stratigraphy of the investigated horizons, Geol. Mag., 128, 129–140, 1991.
- Nakrem, H. A., Orchard, M. J., Weitschat, W., Hounslow, M. W., 115 Beatty, T. W., and Mørk, A.: Triassic conodonts from Sval-

- bard and their Boreal correlations, Polar Res., 27, 523–539, https://doi.org/10.1111/j.1751-8369.2007.00038.x, 2008.
- Nielsen, J. K., Błażejowski, B., Gieszcz, P., and Nielsen, J. K.: Carbon and oxygen isotope records of Permian brachiopods from relatively low and high palaeolatitudes: climatic seasonality and evaporation, Geol. Soc. Lond. Spec. Publ., 376, 387–406, 2013.
- Nøttvedt, A.: Askeladden delta sequence (Paleocene) on Spitsbergen sedimentation and controls on delta formation, Polar Res., 3, 21–48, 1985.
- Nøttvedt, A., Cecchi, M., Gjelberg, J., Kristensen, S., Lønøy, A., Rasmussen, A., Rasmussen, E., Skott, P., and Van Veen, P.: Svalbard-Barents Sea correlation: a short review, Nor. Pet. Soc. Spec. Publ., 2, 363–375, 1993.
- Oakey, G. N. and Chalmers, J. A.: A new model for the Paleogene motion of Greenland relative to North America: Plate reconstructions of the Davis Strait and Nares Strait regions between Canada and Greenland, J. Geophys. Res.-Sol. Ea., 117, B10401, https://doi.org/10.1029/2011jb008942, 2012.
- Ogata, K., Senger, K., Braathen, A., Tveranger, J., and Olaussen, S.:

  The importance of natural fractures in a tight reservoir for potential CO<sub>2</sub> storage: a case study of the upper Triassic-middle Jurassic Kapp Toscana Group (Spitsbergen, Arctic Norway), Geol. Soc. Lond. Spec. Publ., 374, 395–415, 2014a.
- Ogata, K., Senger, K., Braathen, A., Tveranger, J., and Olaussen, S.:
  Fracture systems and mesoscale structural patterns in the siliciclastic Mesozoic reservoir-caprock succession of the Longyear-byen CO<sub>2</sub> Lab project: Implications for geological CO<sub>2</sub> sequestration in Central Spitsbergen, Svalbard, Nor. J. Geol., 94, 121–154, 2014b.
- 30 Ogata, K., Weert, A., Betlem, P., Birchall, T., and Senger, K.: Shallow and deep subsurface sediment remobilization and intrusion in the Middle Jurassic to Lower Cretaceous Agardhfjellet Formation (Svalbard), Geosphere, 19, 801–822, 2023.
- Ogden, D. E. and Sleep, N. H.: Explosive eruption of coal and basalt and the end-Permian mass extinction, P. Natl. Acad. Sci. USA, 109, 59–62, https://doi.org/10.1073/pnas.1118675109, 2012.
- Økland, I. H., Delsett, L. L., Roberts, A. J., and Hurum, J. H.: A Phalarodon fraasi (Ichthyosauria: Mixosauridae) from the Middle Triassic of Svalbard, Norw. J. Geol., 98, 267–288. https://doi.org/10.17850/njg98-2-06, 2018.
- Olaussen, S., Larssen, G. B., Helland-Hansen, W., Johannessen, E. P., Nøttvedt, A., Riis, F., Rismyhr, B., Smelror, M., and Worsley, D.: Mesozoic strata of Kong Karls Land, Svalbard, Norway; a link to the northern Barents Sea basins and platforms, Nor. J.
- Geol., 98, 5, https://doi.org/10.17850/njg98-4-06, 2018.
- Olaussen, S., Senger, K., Braathen, A., Grundvåg, S.-A., and Mørk, A.: You learn as long as you drill; research synthesis from the Longyearbyen CO2 Laboratory, Svalbard, Norway, Nor. J. Geol., 99, 157–187, 2019.
- Olaussen, S., Grundvåg, S.-A., Senger, K., Anell, I., Betlem, P., Braathen, A., Dallmann, W., Jochmann, M., Johannessen, E. P., Lord, G., Mørk, A., Osmundsen, P. T., Smyrak-Sikora, A., and Stemmerik, L.: Svalbard Composite Tectono-Stratigraphic Element, Barents Sea, Geol. Soc. Lond. Mem., 57, https://doi.org/10.1144/M57-2021-36, 2025.
  - Olempska, E. and Błaszyk, J.: Ostracods from Permian of Spitsbergen, Pol. Polar Res., 17, 3–20, 1996.
  - Oordt, A. J., Soreghan, G. S., Stemmerik, L., and Hinnov, L. A.: A record of dust deposition in northern, mid-latitude Pangaea dur-

- ing peak icehouse conditions of the late Paleozoic ice age, J. Sediment. Res., 90, 337–363, https://doi.org/10.2110/jsr.2020.15, 2020.
- O'Regan, M., Williams, C. J., Frey, K. E., and Jakobsson, M.: A synthesis of the long-term paleoclimatic evolution of the Arctic, Oceanography, 24, 66–80, 2011.
- Park, J., Stein, H. J., Hannah, J. L., Georgiev, S. V., Hammer, Ø., and Olaussen, S.: Paleoenvironment in the circum-Arctic region from the Middle Jurassic to Lower Cretaceous: Trace element and stable isotope geochemistry of the Agardhfjellet Formation, Svalbard, Palaeogeogr. Palaeoclimatol. Palaeoecol., 112333, 649, 70 https://doi.org/10.1016/j.palaeo.2024.112333, 2024.
- Parkinson, I. J., Schaefer, B. F., and Arculus, R. J.: A lower mantle origin for the world's biggest LIP? A high precision Os isotope isochron from Ontong Java Plateau basalts drilled on ODP Leg 192, Geochim. Cosmochim. Acta, 66, A580, [1855], 2002.
- Patterson, W. P. and Walter, L. M.: Depletion of 13C in seawater ΣC02 on modern carbonate platforms: Significance for the carbon isotopic record of carbonates, Geology, 22, 885–888, https://doi.org/10.1130/0091-7613(1994)022<0885:Docise>2.3.Co;2, 1994.
- Paterson, N. W., Mangerud, G., Cetean, C. G., Mørk, A., Lord, G. S., Klausen, T. G., and Mørkved, P. T.: A multidisciplinary biofacies characterisation of the Late Triassic (late Carnian–Rhaetian) Kapp Toscana Group on Hopen, Arctic Norway, Palaeogeogr. Palaeoclimatol. Palaeoecol., 464, 16–42, 2016.
- Payne, J. L., Lehrmann, D. J., Wei, J., Orchard, M. J., Schrag, D. P., and Knoll, A. H.: Large perturbations of the carbon cycle during recovery from the end-Permian extinction, Science, 305, 506– 509, 2004.
- Percival, L., Tedeschi, L. R., Creaser, R., Bottini, C., Erba, E., Giraud, F., Svensen, H., Savian, J., Trindade, R., and Coccioni, R.: Determining the style and provenance of magmatic activity during the Early Aptian Oceanic Anoxic Event (OAE 1a), Global Planet. Change, 200, 103461, https://doi.org/10.1016/j.gloplacha.2021.103461, 2021.
- Petersen, T. G., Thomsen, T. B., Olaussen, S., and Stemmerik, L.: Provenance shifts in an evolving Eurekan foreland basin: the Tertiary Central Basin, Spitsbergen, J. Geol. Soc. Lond., 173, 634–648, 2016
- Pettersson, C. H., Pease, V., and Frei, D.: U–Pb zircon provenance of metasedimentary basement of the Northwestern Terrane, Svalbard: Implications for the Grenvillian–Sveconorwegian orogeny and development of Rodinia, Precambrian Res., 175, 206–220, 2009.
- Piepjohn, K.: The Svalbardian-Ellesmerian deformation of the Old 105 Red Sandstone and the pre-Devonian basement in NW Spitsbergen (Svalbard), Geol. Soc. Lond. Spec. Publ., 180, 585–601, https://doi.org/10.1144/GSL.SP.2000.180.01.31, 2000.
- Piepjohn, K. and Dallmann, W. K.: Stratigraphy of the uppermost Old Red Sandstone of Svalbard (Mimerdalen Subgroup), Polar 110 Res., 33, 19998, https://doi.org/10.3402/polar.v33.19998, 2014.
- Piepjohn, K. and von Gosen, W.: Structural transect through Ellesmere Island (Canadian Arctic): superimposed Palaeozoic Ellesmerian and Cenozoic Eurekan deformation, Geol. Soc. Lond. Spec. Publ., 460, 33–56, 2018.

Piepjohn, K., Brinkmann, L., Grewing, A., and Kerp, H.: New data on the age of the uppermost ORS and the lowermost post-ORS strata in Dickson Land (Spitsbergen) and implications for the age

- of the Svalbardian deformation, Geol. Soc. Lond. Spec. Publ., 180, 603–609, https://doi.org/10.1144/GSL.SP.2000.180.01.32, 2000.
- Piepjohn, K., von Gosen, W., Tessensohn, F., Reinhardt, L., McClelland, W. C., Dallmann, W., Gaedicke, C., and Harrison, J. C.: Tectonic map of the Ellesmerian and Eurekan deformation belts on Svalbard, North Greenland, and the Queen Elizabeth Islands (Canadian Arctic), Arktos, 1, 12, https://doi.org/10.1007/s41063-015-0015-7, 2015.
- Piepjohn, K., von Gosen, W., and Tessensohn, F.: The Eurekan deformation in the Arctic: an outline, J. Geol. Soc. Lond., 173, 1007–1024, 2016.
  - Pietsch, C. and Bottjer, D. J.: The importance of oxygen for the disparate recovery patterns of the benthic macrofauna in the Early Triassic, Earth-Sci. Rev., 137, 65–84, 2014.
  - Podlaha, O. G., Mutterlose, J., and Veizer, J.: Preservation of delta 18O and delta 13C in belemnite rostra from the Jurassic/Early Cretaceous successions, Am. J. Sci., 298, 324–347, 1998.
- Pogge von Strandmann, P. A. E., Jones, M. T., West, A. J., Murphy, M. J., Stokke, E. W., Tarbuck, G., Wilson, D. J., Pearce, C. R., and Schmidt, D. N.: Lithium isotope evidence for enhanced weathering and erosion during the Paleocene-Eocene Thermal Maximum, Sci. Adv., 7, eabh4224, https://doi.org/10.1126/sciadv.abh4224, 2021.
- 25 Polteau, S., Hendriks, B. W., Planke, S., Ganerød, M., Corfu, F., Faleide, J. I., Midtkandal, I., Svensen, H. S., and Myklebust, R.: The Early Cretaceous Barents Sea Sill Complex: distribution, 40Ar/39Ar geochronology, and implications for carbon gas formation, Palaeogeogr. Palaeoclimatol. Palaeoecol., 441, 83–95, 2016
  - Preto, N., Kustatscher, E., and Wignall, P. B.: Triassic climates state of the art and perspectives, Palaeogeogr. Palaeoclimatol. Palaeoecol., 290, 1–10, https://doi.org/10.1016/j.palaeo.2010.03.015, 2010.
- 35 Price, G. D.: The evidence and implications of polar ice during the Mesozoic, Earth-Sci. Rev., 48, 183–210, 1999.
  - Price, G. D.: New constraints upon isotope variation during the early Cretaceous (Barremian–Cenomanian) from the Pacific Ocean, Geol. Mag., 140, 513–522, 2003.
- <sup>40</sup> Price, G. D. and Mutterlose, J.: Isotopic signals from late Jurassic–early Cretaceous (Volgian–Valanginian) sub-Arctic belemnites, Yatria River, Western Siberia, J. Geol. Soc. Lond., 161, 959–968, https://doi.org/10.1144/0016-764903-169, 2004.
- Price, G. D. and Nunn, E. V.: Valanginian isotope variation in glendonites and belemnites from Arctic Svalbard: Transient glacial temperatures during the Cretaceous greenhouse, Geology, 38, 251–254, https://doi.org/10.1130/g30593.1, 2010.
- Price, G. D. and Passey, B. H.: Dynamic polar climates in a greenhouse world: Evidence from clumped isotope thermometry of Early Cretaceous belemnites, Geology, 41, 923–926, 2013.
- Price, G. D. and Rogov, M. A.: An isotopic appraisal of the Late Jurassic greenhouse phase in the Russian Platform, Palaeogeogr. Palaeoclimatol. Palaeoecol., 273, 41–49, https://doi.org/10.1016/j.palaeo.2008.11.011, 2009.
- 55 Price, G. D., Bajnai, D., and Fiebig, J.: Carbonate clumped isotope evidence for latitudinal seawater temperature gradients and the oxygen isotope composition of Early Cretaceous seas, Palaeogeogr. Palaeoclimatol. Palaeoecol., 552, 109777, https://doi.org/10.1016/j.palaeo.2020.109777, 2020.

- Price, G. D., Főzy, I., and Pálfy, J.: Carbon cycle history through the Jurassic–Cretaceous boundary: A new global  $\delta^{13}$ C stack, Palaeogeogr. Palaeoclimatol. Palaeoecol., 451, 46–61, https://doi.org/10.1016/j.palaeo.2016.03.016, 2016.
- Pörtner, H.-O., Roberts, D. C., Adams, H., Adler, C., Aldunce, P., Ali, E., Begum, R. A., Betts, R., Kerr, R. B., Biesbroek, R., Birkmann, J., Bowen, K., Castellanos, E. C., Constable, A., Cramer, W., Dodman, D., Eriksen, S. H., Fischlin, A., Garschagen, M., Glavovic, B., Gilmore, E., Haasnoot, M., Harper, S., Hasegawa, T., Hayward, B., Hirabayashi, Y., Howden, M., Kalaba, K., Kiessling, W., Lasco, R., Lawrence, J., Lemos, M. F., 70 Lempert, R., Ley, D., Lissner, T., Lluch-Cota, S., Loeschke, S., Lucatello, S., Luo, Y., Mackey, B., Maharaj, S., Mendez, C., Mintenbeck, K., Moncassim Vale, M., Morecroft, M. D., Mukherji, A., Mycoo, M., Mustonen, T., Nalau, J., Okem, A., Ometto, J. P., Parmesan, C., Pelling, M., Pinho, P., Poloczanska, 75 E., Racault, M.-F., Reckien, D., Pereira, J., Revi, A., Rose, S., Sanchez-Rodriguez, R., Schipper, E. L. F., Schmidt, D., Schoeman, D., Shaw, R., Singh, C., Solecki, W., Stringer, L., Thomas, A., Totin, E., Trisos, C., Viner, D., van Aalst, M., Wairiu, M., Warren, R., Yanda, P., and Zaiton Ibrahim, Z.: Climate change 80 2022: Impacts, adaptation and vulnerability, IPCC Sixth Assessment Report, https://edepot.wur.nl/565644 (last access: TS54), 2022.
- Pucéat, E., Lécuyer, C., Sheppard, S. M., Dromart, G., Reboulet, S., and Grandjean, P.: Thermal evolution of Cretaceous Tethyan marine waters inferred from oxygen isotope composition of fish tooth enamels, Paleoceanography, 18, https://doi.org/10.1029/2002PA000823, 2003.
- Rantanen, M., Karpechko, A. Y., Lipponen, A., Nordling, K., Hyvärinen, O., Ruosteenoja, K., Vihma, T., and Laaksonen, A.: The Arctic has warmed nearly four times faster than the globe since 1979, Commun. Earth Environ., 3, 1–10, https://doi.org/10.1038/s43247-022-00498-3, 2022.
- Rauzi, S., Foster, W. J., Takahashi, S., Hori, R. S., Beaty, B. J., Tarhan, L. G., and Isson, T.: Lithium isotopic evidence of renhanced reverse weathering during the Early Triassic warm period, P. Natl. Acad. Sci. USA, 121, e2318860121, https://doi.org/10.1073/pnas.2318860121, 2024.
- Reichow, M. K., Pringle, M. S., Al'Mukhamedov, A. I., Allen, M., Andreichev, V. L., Buslov, M. M., Davies, C., Fedoseev, G. S., 100 Fitton, J. G., and Inger, S.: The timing and extent of the eruption of the Siberian Traps large igneous province: Implications for the end-Permian environmental crisis, Earth Planet. Sci. Lett., 277, 9–20, 2009.
- Rigo, M. and Joachimski, M. M.: Palaeoecology of Late Triassic 105 conodonts: Constraints from oxygen isotopes in biogenic apatite, Acta Palaeontol. Pol., 55, 471–478, 2010.
- Rigo, M., Preto, N., Roghi, G., Tateo, F., and Mietto, P.: A rise in the carbonate compensation depth of western Tethys in the Carnian (Late Triassic): deep-water evidence for the Carnian Pluvial Event, Palaeogeogr. Palaeoclimatol. Palaeoecol., 246, 188–205, 2007.
- Riis, F. and Fjeldskaar, W.: On the magnitude of the Late Tertiary and Quaternary erosion and its significance for the uplift of Scandinavia and the Barents Sea, in: Structural and tectonic modelling and its application to petroleum geology, edited by: Larsen, R. M., Brekke, H., Larsen, B. T., and Talleraas, E., Else-

35-64, 2018.

- vier, Amsterdam, 163–185, https://doi.org/10.1016/B978-0-444-88607-1.50016-4, 1992.
- Riis, F., Lundschien, B. A., Høy, T., Mørk, A., and Mørk, M. B. E.: Evolution of the Triassic shelf in the northern Barents Sea
- region, Polar Res., 27, 318–338, https://doi.org/10.1111/j.1751-8369.2008.00086.x, 2008.
- Rismyhr, B., Bjærke, T., Olaussen, S., Mulrooney, M. J., and Senger, K.: Facies, palynostratigraphy and sequence stratigraphy of the Wilhelmøya Subgroup (Upper Triassic–Middle Jurassic) in western central Spitsbergen, Svalbard, Nor. Geol. Tidsskr., 99,
- Rizzo, R. E., Inskip, N. F., Fazeli, H., Betlem, P., Bisdom, K., Kampman, N., and Busch, A.: Modelling geological CO<sub>2</sub> leakage: Integrating fracture permeability and fault zone outcrop analysis, Int. J. Greenh. Gas Control, 133, 104105, 2024.
- Roberts, A. J., Engelschion, V. S., and Hurum, J. H.: First threedimensional skull of the Middle Triassic mixosaurid ichthyosaur Phalarodon fraasi from Svalbard, Norway, Acta Palaeontol. Pol., 67, 51–62, 2022.
- 20 Rocha, B. C., Davies, J. H., Janasi, V. A., Schaltegger, U., Nardy, A. J., Greber, N. D., and Lucchetti, A. C. F.: Rapid eruption of silicic magmas from the Parana magmatic province (Brazil) did not trigger the Valanginian event, Geology, 48, 1174–1178, 2020.
- Rodriguez Blanco, L., Swart, P. K., Eberli, G. P., and Weger, R. J.: Negative δ<sup>13</sup>C carb values at the Jurassic-Cretaceous boundary Vaca Muerta Formation, Neuquén Basin, Argentinam, Palaeogeogr. Palaeoclimatol. Palaeoecol., 603, 111208, https://doi.org/10.1016/j.palaeo.2022.111208, 2022.
- Rodríguez-Tovar, F. J., Dorador, J., Zuchuat, V., Planke, S., and Hammer, Ø.: Response of macrobenthic trace maker community to the end-Permian mass extinction in Central Spitsbergen, Svalbard, Palaeogeogr. Palaeoclimatol. Palaeoecol., 581, https://doi.org/10.1016/j.palaeo.2021.110637, 2021.
- Roest, W. R. and Srivastava, S. P.: Sea-floor spreading in the Labrador Sea: A new reconstruction, Geology, 17, 1000–1003, https://doi.org/10.1130/0091-7613(1989)017<1000:Sfsitl>2.3.Co;2, 1989.
- Roghi, G.: Palynological investigations in the Carnian of the Cave del Predil area (Julian Alps, NE Italy), Rev. Palaeobot. Palynol., 132, 1–35, 2004.
- Rogov, M. A.: Ammonites infrazonal and stratigraphy and of the Kimmeridgian Volgian stages of Superrealm, T. Geol. Inst., 627, https://doi.org/10.54896/00023272\_2021\_627\_1, 2021.
- 45 Rogov, M. A., Ershova, V. B., Shchepetova, E. V., Zakharov, V. A., Pokrovsky, B. G., and Khudoley, A. K.: Earliest Cretaceous (late Berriasian) glendonites from Northeast Siberia revise the timing of initiation of transient Early Cretaceous cooling in the high latitudes, Cretac. Res., 71, 102–112, https://doi.org/10.1016/j.cretres.2016.11.011, 2017.
  - Rogov, M. A., Zakharov, V., and Kiselev, D.: Refined ammonite and bivalve biostratigraphy of the Agardhfjellet and lowermost Rurikfjellet formations (Bathonian–Ryazanian) of the Longyearbyen area, Spitsbergen., Neues Jahrbuch für
- Geologie und Paläontologie, Abhandlungen, 309, 169–198, https://doi.org/10.1127/njgpa/2023/1158, 2023.
  - Rosa, E. L. and Isbell, J. L.: Late paleozoic glaciation, Encyclopedia of Geology (Second Edition), Academic Press, 534-

- 545, ISBN 9780081029091, https://doi.org/10.1016/B978-0-08-102908-4.00063-1, 2021.
- Royer, D. L., Berner, R. A., Montañez, I. P., Tabor, N. J., and Beerling, D. J.: CO<sub>2</sub> as a primary driver of Phanerozoic climate, GSA Today, 14, 4–10, 2004.
- Salamon, M. A., Hanken, N., Gorzelak, P., Riise, H. E., and Ferré, B.: Crinoids from Svalbard in the aftermath of the end-Permian mass extinction, Pol. Polar Res., 36, 225–238, 2015.
- Sanei, H., Grasby, S. E., and Beauchamp, B.: Latest Permian mercury anomalies, Geology, 40, 63–66, 2012.
- Sanson Barrera, A.: Earliest Triassic climatic, environmental and floral evolution of East Greenland, (Doctoral dissertation, University of Zurich),, 55. https://doi.org/10.5167/uzh-204634, 2016.
- Schaaf, N. W., Osmundsen, P. T., Van der Lelij, R., Schönenberger, J. L., OK, R. T., and Senger, K.: Tectono-sedimentary evolution of the eastern Forlandsundet Graben, Svalbard, Nor. J. Geol., 75 100, 55, 3–4, https://doi.org/10.1785/njg100-4-4, 2021.
- Scheibner, C., Hartkopf-Fröder, C., Blomeier, D., and Forke, H.: The Mississippian (Lower Carboniferous) in northeast Spitsbergen (Svalbard) and a re-evaluation of the Billefjorden Group, Z. Dtsch. Ges. Geowiss., 163, 293, https://doi.org/10.1127/1860-1804/2012/0163-0293, 2012.
- Schlanger, S. O. and Jenkyns, H.: Cretaceous oceanic anoxic events: causes and consequences, Geol. Mijnb., 55, 3–4, 179–184, 1976.
- Schobben, M., Joachimski, M. M., Korn, D., Leda, L., and Korte, C.: Palaeotethys seawater temperature rise and an intensified hydrological cycle following the end-Permian mass extinction, Gondwana Res., 26, 675–683, 2014.
- Schobben, M., Foster, W. J., Sleveland, A. R., Zuchuat, V., Svensen, H. H., Planke, S., Bond, D. P., Marcelis, F., Newton, R. J., and Wignall, P. B.: A nutrient control on marine anoxia during the end-Permian mass extinction, Nat. Geosci., 13, 640–646, 2020.
- Schröder-Adams, C. J., Herrle, J. O., Embry, A. F., Haggart, J. W., Galloway, J. M., Pugh, A. T., and Harwood, D. M.: Aptian to Santonian foraminiferal biostratigraphy and paleoenvironmental change in the Sverdrup Basin as revealed at Glacier Fiord, Axel Heiberg Island, Canadian Arctic Archipelago, Palaeogeogr. Palaeoclimatol. Palaeoecol., 413, 81–100, 2014.
- Scotese, C. R. and Wright, N.: PALEOMAP Paleodigital Elevation Models (PaleoDEMs) for the Phanerozoic, PALEOMAP Project, https://www.earthbyte.org/ paleodem-resource-scotese-and-wright-2018 (last access:
- Scotese, C. R., Bambach, R. K., Barton, C., Van der Voo, R., and Ziegler, A. M.: Paleozoic base maps, J. Geol., 87, 217–277, https://doi.org/10.1086/628416, 1979.
- Scotese, C. R., Boucot, A. J., and McKerrow, W. S.: Gondwanan palaeogeography and palaeoclimatology, J. Afr. Earth Sci., 28, 99–114, 1999.
- Scotese, C. R., Song, H., Mills, B. J. W., and van der Meer, D. G.: Phanerozoic paleotemperatures: The earth's changing climate during the last 540 million years, Earth-Sci. Rev., 215, 103503, https://doi.org/10.1016/j.earscirev.2021.103503, 2021.
- Screen, J. A. and Simmonds, I.: The central role of diminishing sea ice in recent Arctic temperature amplification, Nature, 464, 1334–1337, https://doi.org/10.1038/nature09051, 2010.

115

- Seibold, E.: Geology and the environment keynote to EUG V Symposium 11, Eng. Geol., 29, 273–277, https://doi.org/10.1016/0013-7952(90)90062-6, 1990
- Sellwood, B. W. and Valdes, P. J.: Jurassic climates, Proceedings of the Geologists' Association, 119, 5–17, 2008.
- Senger, K., Planke, S., Polteau, S., Ogata, K., and Svensen, H.: Sill emplacement and contact metamorphism in a siliciclastic reservoir on Svalbard, Arctic Norway, Nor. J. Geol., 94, 155—169, 2014a.
- 10 Senger, K., Tveranger, J., Ogata, K., Braathen, A., and Planke, S.: Late Mesozoic magmatism in Svalbard: A review, Earth-Sci. Rev., 139, 123–144, 2014b.
- Senger, K., Brugmans, P., Grundvåg, S.-A., Jochmann, M.
  M., Nøttvedt, A., Olaussen, S., Skotte, A., and SmyrakSikora, A.: Petroleum, coal and research drilling onshore Svalbard: a historical perspective, Norw. J. Geol., 99, 3, https://doi.org/10.17850/njg99-3-1, 2019.
- Senger, K., Betlem, P., Birchall, T., Gonzaga Jr, L., Grundvåg, S.-A., Horota, R. K., Laake, A., Kuckero, L., Mørk, A., and Planke,
  S.: Digitising Svalbard's geology: the Festningen digital outcrop model, First Break, 40, 47–55, 2022.
- Senger, K., Betlem, P., Braathen, A., Olaussen, S., and Sand, G.: Longyearbyen CO<sub>2</sub> Lab project – from a vision of a CO2-neutral Svalbard to a geoscience data eldorado, Arct. Sci., 11, 1–26, https://doi.org/10.1139/as-2024-0019, 2024.
- Servais, T. and Harper, D. A.: The great Ordovician biodiversification event (GOBE): definition, concept and duration, Lethaia, 51, 151–164, 2018.
- Simms, M. J. and Ruffell, A. H.: Synchroneity of climatic change and extinctions in the Late Triassic, Geology, 17, 265–268, 1989.
- Śliwińska, K. K. and Head, M. J.: New species of the dinoflagellate cyst genus Svalbardella Manum, 1960, emend. from the Paleogene and Neogene of the northern high to middle latitudes, J. Micropalaeontol., 39, 139–154, 2020.
- 35 Śliwińska, K. K. and Heilmann-Clausen, C.: Early Oligocene cooling reflected by the dinoflagellate cyst Svalbardella cooksoniae, Palaeogeogr. Palaeoclimatol. Palaeoecol., 305, 138–149, 2011.
  - Śliwińska, K. K., Thomsen, E., Schouten, S., Schoon, P. L., and Heilmann-Clausen, C.: Climate-and gateway-driven cool-
- ing of Late Eocene to earliest Oligocene sea surface temperatures in the North Sea Basin, Sci. Rep., 9, 4458, https://doi.org/10.1038/s41598-019-41013-7, 2019.
- Śliwińska, K. K., Jelby, M. E., Grundvåg, S.-A., Nøhr-Hansen, H., Alsen, P., and Olaussen, S.: Dinocyst stratigraphy of the
- Valanginian–Aptian Rurikfjellet and Helvetiafjellet formations on Spitsbergen, Arctic Norway, Geol. Mag., 157, 1693–1714, https://doi.org/10.1017/S0016756819001249, 2020.
- Śliwińska, K. K., Coxall, H. K., Hutchinson, D. K., Liebrand, D., Schouten, S., and de Boer, A. M.: Sea surface temperature evo-
- lution of the North Atlantic Ocean across the Eocene–Oligocene transition, Clim. Past, 19, 123–140, https://doi.org/10.5194/cp-19-123-2023, 2023.
- Sluijs, A., Frieling, J., Inglis, G. N., Nierop, K. G. J., Peterse, F., Sangiorgi, F., and Schouten, S.: Late Paleocene–early Eocene
- Arctic Ocean sea surface temperatures: reassessing biomarker paleothermometry at Lomonosov Ridge, Clim. Past, 16, 2381—2400, https://doi.org/10.5194/cp-16-2381-2020, 2020.

- Smelror, M., Olaussen, S., Dumais, M. A., Grundvåg, S. A., and Abay, T. B.: Northern Svalbard Composite Tectono-Sedimentary Element, Geol. Soc. Lond. Mem., 57, M57-2023, 2024.
- Smyrak-Sikora, A. and Betlem, P.: Dataset and Interactive Plot for Smyrak-Sikora et al., 2025; Phanerozoic paleoenvironmental and paleoclimatic evolution in Svalbard, Zenodo [data set], https://doi.org/10.5281/zenodo.15405160, 2025.
- Smyrak-Sikora, A., Johannessen, E. P., Olaussen, S., Sandal, G., and Braathen, A.: Sedimentary architecture during Carboniferous rift initiation the arid Billefjorden Trough, Svalbard, J. Geol. Soc. Lond., 176, 225–252, https://doi.org/10.1144/jgs2018-100, 2018.
- Smyrak-Sikora, A., Nicolaisen, J. B., Braathen, A., Johannessen, E. P., Olaussen, S., and Stemmerik, L.: Impact of growth faults on mixed siliciclastic-carbonate-evaporite deposits during rift climax and reorganisation Billefjorden Trough, Svalbard, Norway, Basin Res., 33, 2643–2674, https://doi.org/10.1111/bre.12578, 2021.
- Smyrak-Sikora, A., Engelschiøn, V., Foster, W., Jelby, M. E., Jones, M., Mosociova, T., Śliwińska, K., Vickers, M. L., and Zuchuat, V.: Table: Review of Phanerozoic Paleoenvironmental and Paleoclimatic Evolution in Svalbard, Zenodo [data set], https://doi.org/10.5281/zenodo.14334261, 2025.
- Song, H., Wignall, P. B., Tong, J., Bond, D. P., Song, H., Lai, X., and Chen, Y.: Geochemical evidence from bio-apatite for multiple oceanic anoxic events during Permian—Triassic transition and the link with end-Permian extinction and recovery, Earth Planet. Sci. Lett., 353, 12–21, 2012.
- Song, H., Wignall, P. B., Song, H., Dai, X., and Chu, D.: Seawater temperature and dissolved oxygen over the past 500 million years, J. Earth Sci., 30, 236–243, 2019.
- Soreghan, G. S.: Déjà-Vu All Over Again: Deep Time (Climate) Is Here To Stay, PALAIOS, 19, 1–2, https://doi.org/10.1669/0883-1351(2004)019<0001:Daoadt>2.0.Co;2, 2004.
- Sorento, T., Olaussen, S., and Stemmerik, L.: Controls on deposition of shallow marine carbonates and evaporites lower Permian Gipshuken Formation, central Spitsbergen, Arctic Norway, Sedimentology, 67, 207–238, https://doi.org/10.1111/sed.12640, 95 2020.
- Soua, M.: Early Carnian anoxic event as recorded in the southern Tethyan margin, Tunisia: an overview, Int. Geol. Rev., 56, 1884– 1905, 2014.
- Speelman, E. N., van Kempen, M. M. L., Barke, J., Brinkhuis, 100
  H., Reichart, G. J., Smolders, A. J. P., Roelofs, J. G. M., Sangiorgi, F., de Leeuw, J. W., Lotter, A. F., and Sinninghe Damsté, J. S.: The Eocene Arctic Azolla bloom: environmental conditions, productivity and carbon drawdown, Geobiology, 7, 155–170, https://doi.org/10.1111/j.1472-4669.2009.00195.x, 2009.
- Spielhagen, R. F. and Tripati, A.: Evidence from Svalbard for near-freezing temperatures and climate oscillations in the Arctic during the Paleocene and Eocene, Palaeogeogr. Palaeoclimatol. Palaeoecol., 278, 48–56, https://doi.org/10.1016/j.palaeo.2009.04.012, 2009.
- Stanley Jr., G. D.: The evolution of modern corals and their early history, Earth-Sci. Rev., 60, 195–225, 2003.

115

Stanley, S. M.: Estimates of the magnitudes of major marine mass extinctions in earth history, P. Natl. Acad. Sci. USA, 113, E6325–E6334, https://doi.org/10.1073/pnas.161309411, 2016.

- Steel, R., Gjelberg, J., Helland-Hansen, W., Kleinspehn, K., Nøttvedt, A., and Rye-Larsen, M.: The Tertiary strike-slip basins and orogenic belt of Spitsbergen, Special Publications of SEPM, https://doi.org/10.2110/pec.85.37.0339, 1985.
- 5 Steel, R. J. and Worsley, D.: Svalbard's post-Caledonian strata—an atlas of sedimentational patterns and palaeogeographic evolution, in: Petroleum geology of the North European margin, edited by: Spencer, A. M., Springer, Dordrecht, 109–135, https://doi.org/10.1007/978-94-009-5626-1\_9, 1984.
- 10 Steel, R. J., Gjelberg, J., and Haarr, G.: Helvetiafjellet Formation (Barremian) at Festningen, Spitsbergen – a field guide, Nor. Polarinst. Årbok, 111–128, 1978.
- Steel, R. J., Dalland, A., Kalgraff, K., and Larsen, V.: The Central Tertiary Basin of Spitsbergen: sedimentary development of a sheared-margin basin, Geology of the North Atlantic Borderlands Memoir 7, CSPG Special Publications, 647–664, 1981.
- Stemmerik, L.: Late Palaeozoic evolution of the North Atlantic margin of Pangea, Palaeogeogr. Palaeoclimatol. Palaeoecol., 161, 95–126, https://doi.org/10.1016/s0031-0182(00)00119-x, 2000.
- 20 Stemmerik, L.: Influence of late Paleozoic Gondwana glaciations on the depositional evolution of the northern Pangean shelf, North Greenland, Svalbard, and the Barents Sea, Geol. Soc. Am. Spec. Pap., 441, https://doi.org/10.1016/s0031-0182(00)00119x, 2008.
- 25 Stemmerik, L. and Worsley, D.: 30 years on-Arctic Upper Palaeozoic stratigraphy, depositional evolution and hydrocarbon prospectivity, Nor. J. Geol., 85, 151–168 1850, 2005.
  - Stemmerik, L., Bendix-Almgreen, S. E., and Piasecki, S.: The Permian-Triassic boundary in central East Greenland: past and present views, Bull. Geol. Soc. Den., 48, 159–167, 2001.
  - Stewart, I.: Sustainable geoscience, Nat. Geosci., 9, 262, https://doi.org/10.1038/ngeo2678, 2016.
  - Stickley, C. E., Brinkhuis, H., Schellenberg, S. A., Sluijs, A., Röhl, U., Fuller, M., Grauert, M., Huber, M., Warnaar, J.,
- and Williams, G. L.: Timing and nature of the deepening of the Tasmanian Gateway, Paleoceanography, 19, 1857, https://doi.org/10.1029/2004PA001022, 2004. 1858
- Stordal, F., Svensen, H. H., Aarnes, I., and Roscher, M.: Global temperature response to century-scale degassing from the Siberian Traps Large igneous province, Palaeogeogr. Palaeoclimatol. Palaeoecol., 471, 96–107, https://doi.org/10.1016/j.palaeo.2017.01.045, 2017.
- Storey, M., Duncan, R. A., and Tegner, C.: Timing and duration of volcanism in the North Atlantic Igneous Province: Implica-
- tions for the geodynamics and links to the Iceland hotspot, Chem. Geol., 241, 264–281, 2007a.
  - Storey, M., Duncan, R. A., and Swisher III, C. C.: Paleocene-Eocene Thermal Maximum and the opening of the Northeast Atlantic, Science, 316, 587–589, 2007b.
- 50 Stouge, S., Christiansen, J. L., and Holmer, L. E.: Lower palaeozoic stratigraphy of Murchisonfjorden and Sparreneset, Nordaustlandet, Svalbard, Geogr. Ann. Ser. A-Phys. Geogr., 93, 209– 226, 2011.
- Stouge, S., Harper, D. A., Boyce, W. D., and Christiansen, I. K.
   L.: Development of the lower Cambrian–Middle Ordovician carbonate platform: North Atlantic Region, AAPG Memoir 597–626 [1859], 2012.
- Straume, E. O., Gaina, C., Medvedev, S., and Nisancioglu, K. H.: Global Cenozoic paleobathymetry with a focus on the North-

- ern Hemisphere oceanic gateways, Gondwana Res., 86, 126– 60 143, https://doi.org/10.1016/j.gr.2020.05.011, 2020.
- Straume, E. O., Nummelin, A., Gaina, C., and Nisancioglu, K. H.: Climate transition at the Eocene–Oligocene influenced by bathymetric changes to the Atlantic–Arctic oceanic gateways, P. Natl. Acad. Sci. USA, 119, e2115346119, https://doi.org/10.1073/pnas.2115346119, 2022.
- Suc, J.-P., Fauquette, S., Popescu, S.-M., and Robin, C.: Subtropical mangrove and evergreen forest reveal Paleogene terrestrial climate and physiography at the North Pole, Palaeogeogr. Palaeoclimatol. Palaeoecol., 551, 109755, 70 https://doi.org/10.1016/j.palaeo.2020.109755, 2020.
- Summerhayes, C. P.: Earth's climate evolution, John Wiley and Sons, 1860, 2015. 1861
- Summons, R. E., Welander, P. V., and Gold, D. A.: Lipid biomarkers: molecular tools for illuminating the history of microbial life, 75 Nat. Rev. Microbiol., 20, 174–185, 2022.
- Sun, Y., Joachimski, M. M., Wignall, P. B., Yan, C., Chen, Y., Jiang, H., Wang, L., and Lai, X.: Lethally hot temperatures during the Early Triassic greenhouse, Science, 338, 366–370, https://doi.org/10.1126/science.1224126, 2012.
- Sun, Y. D., Wignall, P. B., Joachimski, M. M., Bond, D. P., Grasby, S. E., Lai, X. L., and Sun, S.: Climate warming, euxinia and carbon isotope perturbations during the Carnian (Triassic) Crisis in South China, Earth Planet. Sci. Lett., 444, 88–100, 2016.
- Svensen, H., Planke, S., Malthe-Sørenssen, A., Jamtveit, B., Myklebust, R., Rasmussen Eidem, T., and Rey, S. S.: Release of methane from a volcanic basin as a mechanism for initial Eocene global warming, Nature, 429, 542–545, 2004.
- Svensen, H., Planke, S., Polozov, A. G., Schmidbauer, N., Corfu, F., Podladchikov, Y. Y., and Jamtveit, B.: Siberian gas venting and the end-Permian environmental crisis, Earth Planet. Sci. Lett., 277, 490–500, https://doi.org/10.1016/j.epsl.2008.11.015, 2009.
- Svensen, H. H., Frolov, S., Akhmanov, G. G., Polozov, A. G., Jerram, D. A., Shiganova, O. V., Melnikov, N. V., Iyer, K., and Planke, S.: Sills and gas generation in the Siberian Traps, Philos. Trans. R. Soc. A-Math. Phys. Eng. Sci., 376, 20170080, https://doi.org/10.1098/rsta.2017.0080, 2018.
- Svensen, H. H., Jerram, D. A., Polozov, A. G., Planke, S., Neal, C.
  R., Augland, L. E., and Emeleus, H. C.: Thinking about LIPs:
  A brief history of ideas in Large igneous province research, 100
  Tectonophysics, 760, 229–251, 2019.
- Swainson, I. P. and Hammond, R. P.: Ikaite, CaCO3•6H2O: Cold comfort for glendonites as paleothermometers, Am. Mineral., 86, 1530–1533, https://doi.org/10.2138/am-2001-11-1223, 2001.
- Tarduno, J., Sliter, W., Kroenke, L., Leckie, M., Mayer, H., Mahoney, J., Musgrave, R., Storey, M., and Winterer, E.: Rapid formation of Ontong Java Plateau by Aptian mantle plume volcanism, Science, 254, 399–403, 1991.
- Tejada, M., Mahoney, J., Neal, C., Duncan, R., and Petterson, M.: 110 Basement geochemistry and geochronology of Central Malaita, Solomon Islands, with implications for the origin and evolution of the Ontong Java Plateau, J. Petrol., 43, 449–484, 2002.
- Tejada, M. L. G., Suzuki, K., Kuroda, J., Coccioni, R., Mahoney, J. J., Ohkouchi, N., Sakamoto, T., and Tatsumi, Y.: Ontong Java 115 Plateau eruption as a trigger for the early Aptian oceanic anoxic event, Geology, 37, 855–858, 2009.

- Thordarson, T.: Accretionary-lapilli-bearing pyroclastic rocks at ODP Leg 192 Site 1184: a record of subaerial phreatomagmatic eruptions on the Ontong Java Plateau, Geol. Soc. Lond. Spec. Publ., 229, 275–306, 2004.
- <sup>5</sup> Throndsen, T.: Vitrinite reflectance studies of coals and dispersed organic matter in Tertiary deposits in the Adventdalen area, Svalbard, Polar Res., 2, 77–91, 1982.
- Torsvik, T. H. and Cocks, L. R. M.: The integration of palaeomagnetism, the geological record and mantle tomography in the location of ancient continents, Geol. Mag., 156, 242–260, 2019.
- Torsvik, T. H., Carlos, D., Mosar, J., Cocks, L. R. M., and Malme,
  T.: Global reconstructions and North Atlantic paleogeography
  440 Ma to recent, in: BATLAS–Mid Norway plate reconstruction atlas with global and Atlantic perspectives, edited by: Eide,
  E. A., Geol. Surv. Norw., Trondheim, 18–39, 1863, 2002.
- Torsvik, T. H., Van der Voo, R., Preeden, U., Mac Niocaill, C., Steinberger, B., Doubrovine, P. V., Van Hinsbergen, D. J., Domeier, M., Gaina, C., and Tohver, E.: Phanerozoic polar wander, palaeogeography and dynamics, Earth-Sci. Rev., 114, 325–368, 2012.
- Tozer, E. T.: A standard for Triassic Time, Geol. Surv. Can. Bull., 156, 1–103, 1967.
- Tozer, E. T. and Parker, J. R.: Notes on the Triassic biostratigraphy of Svalbard, Geol. Mag., 105, 526–542, 1968.
- 25 Tremolada, F., Bornemann, A., Bralower, T. J., Koeberl, C., and van de Schootbrugge, B.: Paleoceanographic changes across the Jurassic/Cretaceous boundary: The calcareous phytoplankton response, Earth Planet. Sci. Lett., 241, 361–371, https://doi.org/10.1016/j.epsl.2005.11.047, 2006.
- 30 Twitchett, R. J. and Barras, C. G.: Trace fossils in the aftermath of mass extinction events, Geol. Soc. Lond. Spec. Publ., 228, 95– 415, https://doi.org/10.1144/GSL.SP.2004.228.01.18, 2004.
- Twitchett, R. J., Looy, C. V., Morante, R., Visscher, H., and Wignall, P. B.: Rapid and synchronous collapse of marine and terrestrial ecosystems during the end-Permian biotic crisis, Geology, 29, 351–354, 2001.
- Uchman, A., Hanken, N.-M., Nielsen, J. K., Grundvåg, S.-A., and Piasecki, S.: Depositional environment, ichnological features and oxygenation of Permian to earliest Triassic marine sedi-
- ments in central Spitsbergen, Svalbard, Polar Res., 35, 24782, https://doi.org//10.3402/polar.v35.24782, 2016.
  - Uhl, D., Traiser, C., Griesser, U., and Denk, T.: Fossil leaves as palaeoclimate proxies in the Palaeogene of Spitsbergen (Svalbard), Acta Palaeobot., 47, 89, 2007.
- <sup>45</sup> Van Der Meer, D. G., Zeebe, R. E., van Hinsbergen, D. J., Sluijs, A., Spakman, W., and Torsvik, T. H.: Plate tectonic controls on atmospheric CO<sub>2</sub> levels since the Triassic, P. Natl. Acad. Sci. USA, 111, 4380–4385, 2014.
- Van der Meer, D. G., van Saparoea, A. V. D. B., Van Hinsbergen,
  D. J. J., Van de Weg, R. M. B., Godderis, Y., Le Hir, G., and Donnadieu, Y.: Reconstructing first-order changes in sea level during the Phanerozoic and Neoproterozoic using strontium isotopes, Gondwana Res., 44, 22–34, 2017.
- van de Schootbrugge, B., Föllmi, K. B., Bulot, L. G., and Burns, S. J.: Paleoceanographic changes during the early Cretaceous (Valanginian–Hauterivian): evidence from oxygen and carbon stable isotopes, Earth Planet. Sci. Lett., 181, 15–31, 2000.
- Veizer, J., Ala, D., Azmy, K., Bruckschen, P., Buhl, D., Bruhn, F., Carden, G. A. F., Diener, A., Ebneth, S., Godderis, Y.,

- Jasper, T., Korte, C., Pawellek, F., Podlaha, O. G., and Strauss, 60 H.: 87Sr/86Sr,  $\delta^{13}$ C and  $\delta^{18}$ O evolution of Phanerozoic seawater, Chem. Geol., 161, 59–88, https://doi.org/10.1016/s0009-2541(99)00081-9, 1999.
- Vérard, C. and Veizer, J.: On plate tectonics and ocean temperatures, Geology, 47, 881–885, 2019.
- Verba, M.: Kollektornye svoystva porod osadochnogo chekhla arkhipelaga Shpitsbergen [Sedimentary cover reservoir of Svalbard archipelago], Neftegaz. Geol. Teor. Prakt., 8, 1–45, 2013.
- Vickers, M. L., Price, G. D., Jerrett, R. M., and Watkinson, M.: Stratigraphic and geochemical expression of Barremian–Aptian 70 global climate change in Arctic Svalbard, Geosphere, 12, 1594–1605, https://doi.org/10.1130/ges01344.1, 2016.
- Vickers, M. L., Price, G. D., Jerrett, R. M., Sutton, P., Watkinson, M. P., and FitzPatrick, M.: The duration and magnitude of Cretaceous cool events: Evidence from the northern high latitudes, 75 GSA Bull., 131, 1979–1994, https://doi.org/10.1130/b35074.1, 2019a.
- Vickers, M. L., Bajnai, D., Price, G. D., Linckens, J., and Fiebig, J.: Southern high-latitude warmth during the Jurassic–Cretaceous: New evidence from clumped isotope thermometry, Geology, 47, 80 724–728, 2019b.
- Vickers, M. L., Fernandez, A., Hesselbo, S. P., Price, G. D., Bernasconi, S. M., Lode, S., Ullmann, C. V., Thibault, N., Hougaard, I. W., and Korte, C.: Unravelling Middle to Late Jurassic palaeoceanographic and palaeoclimatic signals in the Hebrides Basin using belemnite clumped isotope thermometry, Earth Planet. Sci. Lett., 546, 116401, https://doi.org/10.1016/j.epsl.2020.116401, 2020.
- Vickers, M. L., Bernasconi, S. M., Ullmann, C. V., Lode, S., Looser, N., Morales, L. G., Price, G. D., Wilby, P. R., Hougård, I. 90 W., Hesselbo, S. P., and Korte, C.: Marine temperatures underestimated for past greenhouse climate, Sci. Rep., 11, 19109, https://doi.org/10.1038/s41598-021-98528-1, 2021.
- Vickers, M. L., Jelby, M. E., Śliwińska, K. K., Percival, L. M., Wang, F., Sanei, H., Price, G. D., Ullmann, C. V., Grasby, S. E., and Reinhardt, L.: Volcanism and carbon cycle perturbations in the High Arctic during the Late Jurassic–Early Cretaceous, Palaeogeogr. Palaeoclimatol. Palaeoecol., 613, 111412, https://doi.org/10.1016/j.palaeo.2023.111412, 2023.
- Vigran, J. O.: Spores from Devonian deposits, Mimerdalen, Spits- 100 bergen, Norsk Polarinst. Skrifter, 132, 1–33, 1964.
- Vigran, J. O., Mangerud, G., Mørk, A., Worsley, D., and Hochuli, P. A.: Palynology and geology of the Triassic succession of Svalbard and the Barents Sea, Nor. Geol. Unders., 14, 1–270, https://doi.org/10.5167/uzh-99116, 2014.
- Vogt, T.: Geology of a Middle Devonian cannel coal from Spitsbergen, Nor. Geol. Tidsskr., 21, 1–12, 1941.
- Wappler, T. and Denk, T.: Herbivory in early Tertiary Arctic forests, Palaeogeogr. Palaeoclimatol. Palaeoecol., 310, 283-29-5, 2011.
- Ware, D., Jenks, J. F., Hautmann, M., and Bucher, H.: Dienerian 110 (Early Triassic) ammonoids from the Candelaria Hills (Nevada, USA) and their significance for palaeobiogeography and palaeoceanography, Swiss J. Geosci., 104, 161–181, 2011.
- Watson, R., Baste, I., Larigauderie, A., Leadley, P., Pascual, U., Baptiste, B., ... and Mooney, H. TSGS: Summary for policymakers of the global assessment report on biodiversity and ecosystem services of the Intergovernmental Science-Policy Platform on

- Biodiversity and Ecosystem Services, IPBES Secretariat: Bonn, Germany, 22–47 pp., 1866, 2019.
- Webby, B. D., Paris, F., Droser, M. L., and Percival, I. G.: The great Ordovician biodiversification event, Columbia University Press, 884, New York 1867, 2004. 884 pp
- Weber, M.: Paleoenvironments during the Paleogene in the High Arctic of Spitsbergen Evidence from Sedimentology and Palynology, Master thesis, Institute of Applied Geoscience, Technical University of Darmstadt University Centre in Svalbard, 100 pp., 1868, 2019.
- Weger, R. J., Eberli, G. P., Rodriguez Blanco, L., Tenaglia, M., and Swart, P. K.: Finding a VOICE in the Southern Hemisphere: A new record of global organic carbon?, Geol. Soc. Am. Bull., 135, 7–8, 2107—2120. https://doi.org/10.1130/B36405.1, 2022.
- Weissert, H. and Channell, J. E. T.: Tethyan carbonate carbon isotope stratigraphy across the Jurassic-Cretaceous boundary: An indicator of decelerated global carbon cycling?, Paleoceanography, 4, 483–494, https://doi.org/10.1029/PA004i004p00483, 1989
- Weissert, H. and Erba, E.: Volcanism, CO2 and palaeoclimate: a Late Jurassic–Early Cretaceous carbon and oxygen isotope record, J. Geol. Soc., 161, 695–702, https://doi.org/10.1144/0016-764903-087, 2004.
- Weissert, H., Lini, A., Föllmi, K. B., and Kuhn, O.: Correlation of Early Cretaceous carbon isotope stratigraphy and platform drowning events: a possible link?, Palaeogeogr. Palaeoclimatol. Palaeoecol., 137, 189–203, 1998.
- Wesenlund, F., Grundvåg, S.-A., Engelschiøn, V.S., Thießen, O., and Pedersen, J. H.: Linking facies variations, organic carbon richness and bulk bitumen content—A case study of the organic-rich Middle Triassic shales from eastern Svalbard, Mar. Petrol. Geol., 132, 105168, https://doi.org/10.1016/j.marpetgeo.2021.105168, 2021.
- Wesenlund, F., Grundvåg, S.-A., Engelschiøn, V. S., Thießen, O., and Pedersen, J. H.: Multi-elemental chemostratigraphy of Triassic mudstones in eastern Svalbard: Implications for source rock formation in front of the World's largest delta plain, The Depositional Record, 8, 718–753, https://doi.org/10.1002/dep2.182, 2022.
- Westerhold, T., Marwan, N., Drury, A. J., Liebrand, D., Agnini, C.,
   Anagnostou, E., Barnet, J. S., Bohaty, S. M., De Vleeschouwer,
   D., and Florindo, F.: An astronomically dated record of Earth's climate and its predictability over the last 66 million years, Science, 369, 1383–1387, https://doi.org/10.1126/science.aba6853,
   2020.
  - Wieczorek, R., Fantle, M. S., Kump, L. R., and Ravizza, G.: Geochemical evidence for volcanic activity prior to and enhanced terrestrial weathering during the Paleocene Eocene Thermal Maximum, Geochim. Cosmochim. Acta, 119, 391–410, https://doi.org/10.1016/j.gca.2013.06.005, 2013.
- Wierzbowski, H., Bajnai, D., Wacker, U., Rogov, M. A., Fiebig, J., and Tesakova, E. M.: Clumped isotope record of salinity variations in the Subboreal Province at the Middle–Late Jurassic transition, Global Planet. Change, 167, 172–189, 2018.
- 55 Wignall, P., Morante, R., and Newton, R.: The Permo-Triassic transition in Spitsbergen:  $\delta^{13}\text{Corg}$  chemostratigraphy, Fe and S geochemistry, facies, fauna and trace fossils, Geol. Mag., 135, 47–62, https://doi.org/10.1017/S0016756897008121, 1998.

- Wignall, P. B.: Large igneous provinces and mass extinctions, Earth-Sci. Rev., 53, 1–33, https://doi.org/10.1016/S0012-8252(00)00037-4, 2001.
- Wignall, P. B., Bond, D. P. G., Sun, Y., Grasby, S. E., Beauchamp, B., Joachimski, M. M., and Blomeier, D. P. G.: Ultra-shallow-marine anoxia in an Early Triassic shallow-marine clastic ramp (Spitsbergen) and the suppression of benthic radiation, Geol. Mag., 153, 316–331, https://doi.org/10.1017/s0016756815000588, 2016.
- Wiman, C.: Ichthyosaurier aus der Trias Spitzbergens, Bulletin of the Geological Institution of the University of Upsala, 10, 124– 148, 1910.
- Wiman, C.: Eine neue marine Reptilien-Ordnung aus der Trias Spitzbergens, Bulletin of the Geological Institute of the University of Uppsala, 22, 183–196, 1928.
- Worsley, D.: Sedimentological observations on the Grey Hoek Formation of northern Andrée Land, Spitsbergen, Nor. Polarinst. Årbok, 1970, 102–111, 1972.
- Worsley, D.: The post-Caledonian development of Svalbard and the western Barents Sea, Polar Res., 27, 298–317, https://doi.org/10.1111/j.1751-8369.2008.00085.x, 2008.
- Worsley, D., Agdestein, T., Gjelberg, J., Kirkemo, K., Mørk, A., 80 Nilsson, I., Olaussen, S., Steel, R. J., and Stemmerik, L.: The geological evolution of Bjørnøya, Arctic Norway: implications for the Barents shelf, Nor. J. Geol., 81, 195–234, 2001.
- Wu, Y., Chu, D., Tong, J., Song, H., Dal Corso, J., Wignall, P. B., Song, H., Du, Y., and Cui, Y.: Six-fold increase of atmospheric pCO<sub>2</sub> during the Permian–Triassic mass extinction, Nat. Commun., 12, 2137, https://doi.org/10.1038/s41467-021-22298-7, 2021.
- Zachos, J., Pagani, M., Sloan, L., Thomas, E., and Billups, K.: Trends, Rhythms, and Aberrations in Global 90 Climate 65 Ma to Present, Science, 292, 686–693, https://doi.org/10.1126/science.1059412, 2001.
- Žák, K., Košťák, M., Man, O., Zakharov, V. A., Rogov, M. A., Pruner, P., Rohovec, J., Dzyuba, O. S., and Mazuch, M.: Comparison of carbonate C and O stable isotope records across the Jurassic/Cretaceous boundary in the Tethyan and Boreal Realms, Palaeogeogr. Palaeoclimatol. Palaeoecol., 299, 83–96, https://doi.org/10.1016/j.palaeo.2010.10.038, 2011.
- Zakharov, V. A., Rogov, M. A., Dzyuba, O. S., Žák, K., Košťák, M., Pruner, P., Skupien, P., Chadima, M., Mazuch, M., and 100 Nikitenko, B. L.: Palaeoenvironments and palaeoceanography changes across the Jurassic/Cretaceous boundary in the Arctic realm: case study of the Nordvik section (north Siberia, Russia), Polar Res., 33, 19714, https://doi.org/10.3402/polar.v33.19714, 2014
- Zanin, Y. N., Zamirailova, A. G., and Eder, V. G.: Chalcophile elements in black shales of the Bazhenov Formation, West Siberian sea basin, Russ. Geol. Geophys., 57, 608–616, https://doi.org/10.1016/j.rgg.2015.03.018, 2016.
- Zeebe, R. E., Ridgwell, A., and Zachos, J. C.: Anthropogenic carbon release rate unprecedented during the past 66 million years, Nat. Geosci., 9, 325–329, https://doi.org/10.1038/ngeo2681, 2016.
- Zhang, H., Zhang, F., Chen, J.-B., Erwin, D. H., Syverson, D. D., Ni, P., Rampino, M., Chi, Z., Cai, Y.-F., Xiang, L., Li, W.-Q., Liu, S.-A., Wang, R.-C., Wang, X.-D., Feng, Z., Li, H.-M., Zhang, T., Cai, H.-M., Zheng, W., Cui, Y., Zhu, X.-K., Hou, Z.-Q., Wu, F.-

- Y., Xu, Y.-G., Planavsky, N., and Shen, S.-Z.: Felsic volcanism as a factor driving the end-Permian mass extinction, Sci. Adv., 7, eabh1390, https://doi.org/10.1126/sciadv.abh1390, 2021a.
- Zhang, L., Wang, C., Li, X., Cao, K., Song, Y., Hu, B., Lu, D., Wang, Q., Du, X., and Cao, S.: A new paleoclimate classification for deep time, Palaeogeogr. Palaeoclimatol. Palaeoecol., 443, 98–106, https://doi.org/10.1016/j.palaeo.2015.11.041, 2016.
- Zhang, Y., Ogg, J. G., Minguez, D., Hounslow, M. W., Olaussen, S., Gradstein, F. M., and Esmeray-Senlet, S.: Magnetostratigraphy of U-Pb-dated boreholes in Svalbard, Norway, implies that magnetochron M0r (a proposed Barremian-Aptian boundary marker) begins at 121.2 ± 0.4 Ma, Geology, 49, 733–737, https://doi.org/10.1130/g48591.1, 2021b.
- Zuchuat, V.: A Sedimentary Investigation of the Lower Triassic Formations and Their Underlying Permo-Carboniferous Units Across Spitsbergen, Svalbard. Institutt for geologi og bergteknikk, Norwegian University of Science and Technology, 165 pp., http://hdl.handle.net/11250/236289
- Zuchuat, V., Sleveland, A. R. N., Twitchett, R. J., Svensen, H. H., Turner, H., Augland, L. E., Jones, M. T., Hammer, Ø., Hauksson, B. T., Haflidason, H., Midtkandal, I., and Planke, S.: A new high-resolution stratigraphic and palaeoenvironmental record spanning the End-Permian Mass Extinction and its aftermath in central Spitsbergen, Svalbard, Palaeogeogr. Palaeoclimatol. Palaeoecol., 554, 109732, https://doi.org/10.1016/j.palaeo.2020.109732, 2020.

## Remarks from the language copy-editor

The university name was updated. Please confirm inserted city.

## Remarks from the typesetter

- Please note that figures 10 and 11 have not been updated. When they are different versions, they need to be checked and approved by the handling editor again. Please write a statement what went wrong and what has changed in these versions
- Please correct "Jakobsson et al., 2012". No exact match was found in the reference list.
- Please check your supplement again. Currently it only consists of Table S1.
- Please correct "Jens et al., 2015". No exact match was found in the reference list.
- 1998a and b?
- Please provide this reference.
- Please show exactly where you want the information about "De Geerdalen Fm (beach C)" to be inserted. It was not entirely clear from your comment.
- Please correct "Uchman and Hanken (2024)". No exact match was found in the reference list.
- Please correct "Gruszczynski et al., 1989". No exact match was found in the reference list.
- Please correct "Wignall et al., 2012". No exact match was found in the reference list.
- Please correct "Shen et al., 2005". No exact match was found in the reference list.
- Please check again request of 0. Where should it be inserted?
- Please correct "Lord et al. (2014)". No exact match was found in the reference list.
- Please correct "Smelror and Larssen (2016)". No exact match was found in the reference list.
- Please correct "Weitschat and Lehmann, 1978". No exact match was found in the reference list.
- Please correct "Hochuli and Vigran, 2010". No exact match was found in the reference list.
- Please correct "Brayard et al., 2009". No exact match was found in the reference list.
- Please correct "Twitchett and Wignall, 1996". No exact match was found in the reference list.
- Please correct "Rigo et al., 2012". No exact match was found in the reference list.
- Please correct "Gale et al., 2020". No exact match was found in the reference list.
- Please correct "Hesselbo et al., 2020". No exact match was found in the reference list.
- TS22 2021?
- Please correct "Lüthje et al., 2020". No exact match was found in the reference list.
- Please confirm deleted "Ma".
- Please note that units have been changed to exponential format throughout the text. Please check all instances.
- TS26 2015b?
- Please provide the reference for this DOI number.
- TS28 Please name all editors and persistent identifier.
- Please provide article number/page range and DOI number.
- TS30 Please name all authors.
- Please check this reference. A matching citation was not found.
- Please provide last access date
- Please provide last access date.
- Please provide persistent identifier (DOI number preferred, URL combined with last access date).
- Please provide persistent identifier (DOI number preferred, URL combined with last access date) and number of pages.
- Please check this reference. A matching citation was not found.
- Please provide persistent identifier (DOI number preferred, URL combined with last access date) and number of pages.
- Please provide persistent identifier (DOI number preferred, URL combined with last access date) and number of pages.
- Please provide persistent identifier (DOI number preferred, URL combined with last access date).
- TS40 Please provide your last access date.
- Please provide persistent identifier (DOI number preferred, URL combined with last access date) and number of pages.
- Please check this reference. A matching citation was not found.
- Please provide article number or page range.
- Please provide article number/page range and DOI number.
- Please provide persistent identifier (DOI number preferred, URL combined with last access date) and number of pages.
- Please provide persistent identifier (DOI number preferred, URL combined with last access date).

- Is it here "Maher Jr., H. D.", too?
- TS48 Please provide your last access date.
- Please provide persistent identifier (DOI number preferred, URL combined with last access date).
- Please provide your last access date.
- Please check editors name.
- Please provide persistent identifier (DOI number preferred, URL combined with last access date).
- Please provide article number/page range and DOI number.
- Please provide your last access date.
- Please provide your last access date.
- Please provide article number/page range and DOI number.
- Please provide article number or page range.
- Please check this reference. A matching citation was not found.
- Please provide persistent identifier (DOI number preferred, URL combined with last access date) and number of pages.
- Please provide persistent identifier (DOI number preferred, URL combined with last access date) and number of pages.
- Please check this reference. A matching citation was not found.
- Please check this reference. A matching citation was not found.
- Please provide persistent identifier (DOI number preferred, URL combined with last access date).
- Please check this reference. A matching citation was not found.
- TS65 Please name all authors.
- Please provide persistent identifier (DOI number preferred, URL combined with last access date).
- Please provide persistent identifier (DOI number preferred, URL combined with last access date) and number of pages.
- Please provide persistent identifier (DOI number preferred, URL combined with last access date).
- Please provide persistent identifier (DOI number preferred, URL combined with last access date).